VINÍCIUS AUGUSTO DE OLIVEIRA

IMPACTOS ANTRÓPICOS NA HIDROLOGIA E NO POTENCIAL DE GERAÇÃO HIDROELÉTRICA NO ALTO RIO GRANDE - MG

LAVRAS – MG
2016

VINÍCIUS AUGUSTO DE OLIVEIRA

IMPACTOS ANTRÓPICOS NA HIDROLOGIA E NO POTENCIAL DE GERAÇÃO HIDROELÉTRICA NO ALTO RIO GRANDE - MG

Tese apresentada à Universidade Federal de Lavras, como parte das exigências do Programa de Pós-Graduação em Recursos Hídricos em Sistemas Agrícolas, área de concentração em Recursos Hídricos e Saneamento Ambiental, para a obtenção do título de Doutor.

Prof. Dr. Carlos Rogério de Mello
Orientador
Prof. Dr. Marcelo Ribeiro Viola
Coorientador

LAVRAS – MG
2016

Ficha catalográfica elaborada pelo Sistema de Geração de Ficha Catalográfica da Biblioteca Universitária da UFLA, com dados informados pelo(a) próprio(a) autor(a).

Oliveira, Vinícius Augusto de.
Impactos antrópicos na hidrologia e no potencial de geração hidroelétrica no Alto Rio Grande - MG : / Vinícius Augusto de Oliveira. - 2016.
144 p. : il.

Orientador(a): Carlos Rogério de Mello.
Coorientador(a): Marcelo Ribeiro Viola.
Tese (doutorado) - Universidade Federal de Lavras, 2016.
Bibliografia.

1. Impactos hidrológicos. 2. Mudanças climáticas. 3. Mudanças no uso do solo. I. Mello, Carlos Rogério de. II. Viola, Marcelo Ribeiro. III. Título.

VINÍCIUS AUGUSTO DE OLIVEIRA

IMPACTOS HIDROLÓGICOS DECORRENTES DE MUDANÇAS CLIMÁTICAS E DE USO DO SOLO NA REGIÃO HIDROGRÁFICA DO ALTO RIO GRANDE

Tese apresentada à Universidade Federal de Lavras, como parte das exigências do Programa de Pós-Graduação em Recursos Hídricos em Sistemas Agrícolas, área de concentração em Recursos Hídricos e Saneamento Ambiental, para a obtenção do título de Doutor.

Em 08 de dezembro de 2016.

Dra. Silvia de Nazará Monteiro Yanagi UFLA
Dr. Antônio Marciano da Silva UNIFAL
Dr. Samuel Beskow UFPEL

Prof. Dr. Carlos Rogério de Mello
Orientador
Prof. Dr. Marcelo Ribeiro Viola
Coorientador

LAVRAS – MG
2016

Aos meus pais, João e Vani, por todo o incentivo, apoio e amor dedicado a mim por toda minha vida,

DEDICO

Agradecimentos

A Deus, por me dar saúde e força para vencer mais uma importante etapa na minha vida.

À Universidade Federal de Lavras e ao Programa de Pós-Graduação em Recursos Hídricos em Sistemas Agrícolas pela oportunidade.

À CAPES, pela concessão das bolsas de doutorado e doutorado sanduíche no exterior (Processo 99999.09530/2014-02).

À Texas A&M University e ao professor Raghavan Srinivasan, pela oportunidade, ensinamentos e sugestões para a produção desse trabalho.

À Dra. Sin San Chou, pesquisadora do CPTEC/INPE, por ter disponibilizado os resultados das simulações dos modelos climáticos utilizados nesse trabalho.

Ao projeto "Projeções das mudanças climáticas para estudos de impactos sobre a disponibilidade hídrica no país com implicações na segurança alimentar e energética", financiado por CNPq/ANA e coordenado pelo CPTEC/INPE.

À FAPEMIG, pelo financiamento do projeto "Simulação dos impactos de mudanças climáticas sobre o potencial de geração de energia elétrica no sul de Minas Gerais" (processo PPM-00415-16)

Aos meus pais, João e Vani e minha irmã Polyanna, por serem fonte de inspiração e dedicação, amor e carinho, mesmo nos momentos mais difíceis.

À minha namorada, Ariela, pela dedicação, apoio, incentivo, amor e carinho. Por sempre acreditar que eu era capaz de superar os desafios encontrados nessa jornada.

Ao meu orientador, professor Carlos Rogério de Mello, pelos ensinamentos, sugestões, convivência e pela confiança depositada em mim para a conclusão desse trabalho.

Ao coorientador, professor Marcelo Viola, por toda a ajuda, companheirismo, ensinamentos e sugestões para a realização desse trabalho.

Aos membros da banca, professores Samuel Beskow, Antônio Marciano da Silva e Silvia Yanagi, pela disponibilidade e presteza.

Aos amigos do núcleo didático-científico de Engenharia de Água e Solo da UFLA, pela convivência, troca de experiências e companheirismo, em especial aos amigos Renato, Alisson, Marcelo Linon, Lívia e Geovane.

Aos meus queridos amigos, pela amizade e companheirismo, sempre presentes, mesmo que distantes.

A todos, que de alguma forma contribuíram, direta ou indiretamente, para a realização de mais uma importante etapa da minha vida.

MUITO OBRIGADO!

RESUMO GERAL

O Brasil é um país extremamente dependente de seus recursos hídricos, principalmente no que se refere ao setor energético, em que a geração hidráulica é responsável por produzir cerca de 70% de toda a energia elétrica do país. Assim, alterações no regime hidrológico decorrentes de mudanças de solo e do clima, podem comprometer a capacidade de geração de energia elétrica, bem como reduzir a capacidade de abastecimento. Neste contexto, o objetivo desse estudo foi avaliar os impactos decorrentes de mudanças no uso do solo e do clima na região hidrográfica do Alto Rio Grande, por meio do modelo hidrológico SWAT, bem como simular os impactos no potencial de geração de energia elétrica nas usinas hidrelétricas de Camargos, Itutinga e Funil. Os resultados mostraram que o modelo hidrológico SWAT foi capaz de reproduzir adequadamente os processos hidrológicos das seções de controle analisadas. As simulações de impactos hidrológicos decorrentes de mudanças no uso do solo por meio de cinco cenários tendenciais indicaram que a disponibilidade dos recursos hídricos da região poderá sofrer alterações nesses cenários. Os cenários S_1 e S_2, que abordam o desmatamento da floresta nativa e plantio de pastagens, indicaram um aumento no deflúvio, com no escoamento superficial direto devido à diminuição da capacidade de infiltração e de retenção de água no solo, o que pode levar à diminuição da capacidade de recarga de águas subterrâneas. Por outro lado, os cenários de reflorestamento (S_3 e S_4) indicaram uma redução no deflúvio e no escoamento superficial direto, devido a melhores condições de infiltração e maior capacidade de retenção de água pelo solo. A conversão de pastagens para agricultura (S_5) indicou um aumento no deflúvio e no escoamento superficial direto. Os resultados relacionados aos impactos hidrológicos de mudanças climáticas indicam redução da vazão média mensal durante todo o período analisado, para ambos os modelos (Eta-HadGEM2-ES e Eta-MIROC5) e forçantes de concentração (RCP 4.5 e RCP 8.5), tendo como projeções mais críticas aquelas baseadas no modelo Eta-HadGEM2-ES. Os resultados indicam que as usinas hidrelétricas de Camargos, Itutinga e Funil poderão sofrer sérias consequências no que diz respeito ao potencial de geração de energia elétrica, deixando de operar em 28%, 69% e 50% do tempo, respectivamente, entre 2071 e 2099, pois o potencial mínimo de geração não seria atingido.

Palavras-chave: Simulação hidrológica. Mudanças climáticas. Mudanças de uso do solo.

GENERAL ABSTRACT

Brazil is extremely dependent on its water resources, especially the energy sector, which hydropower is responsible for producing about 70% of all electric energy in the country. Thus, changes in the hydrological regime due to changes in land-use and climate can compromise the capacity of electric energy generation, as well as reduce the water availability. In this context, the objective of this study was to evaluate the hydrological impacts due to changes in land-use and climate in the headwater region of the Alto Rio Grande using the hydrological model SWAT, as well as to simulate the impacts on the potential of electric energy generation in Camargos, Itutinga and Funil hydropower plants. The results showed that SWAT was able to adequately reproduce the hydrological processes of the analyzed outlets. Simulations of hydrological impacts due to changes in land-use through five trend scenarios have indicated that the availability of the water resources in the region may change. The scenarios S_1 and S_2, which represents the deforestation of the native forest into pastures, indicated an increase in the runoff, with consequent increase in the surface runoff due to the reduction of the infiltration and soil water holding capacities, which can lead to a reduction of groundwater recharge capacity. On the other hand, reforestation scenarios (S_3 and S_4) indicated a reduction in the runoff and surface runoff due to better infiltration conditions and greater soil retention capacity. The conversion of pasture into agriculture (S_5) indicated an increase in the runoff and surface runoff. The results related to the hydrological impacts of climate change indicate a reduction in the average monthly flow rate during the analyzed period, for both models (Eta-HadGEM2-ES and Eta-MIROC5) and Representative Concentration Pathways (RCP 4.5 and RCP 8.5), with the most critical projections based on the Eta-HadGEM2-ES model. The results indicate that Camargos, Itutinga and Funil hydropower plants could suffer serious consequences in terms of potential electric energy generation, failing to operate in 28%, 69% and 50% of the time, respectively, during the period between 2071 and 2099, because the minimum generation capacity would not be reached.

Keywords: Hydrological simulation. Climate change. Land-use change.

SUMÁRIO

PRIMEIRA PARTE

1 INTRODUÇÃO

A água é um recurso natural indispensável para a sobrevivência dos seres vivos, sendo um fator preponderante e cada vez mais limitante para o desenvolvimento da sociedade, especialmente no Brasil, que é extremamente dependente de seus recursos hídricos, principalmente no que se refere ao setor energético. Segundo relatório do Balanço Energético Nacional de 2013 da Agencia Nacional de Energia Elétrica (ANEEL), a geração hidráulica é responsável por produzir cerca de 70% de toda a energia elétrica do país.

Por sua vez, a intervenção antrópica sobre o uso e ocupação do solo e os efeitos das mudanças climáticas são os principais responsáveis pelas alterações no regime hidrológico de uma determinada região. Neste tocante, entender e modelar as complexas inter-relações entre a dinâmica da água, a paisagem e o clima apresentam importância fundamental no âmbito do planejamento e conservação ambiental.

O monitoramento de bacias hidrográficas constitui-se em uma importante ferramenta de suporte à avaliação da dinâmica da água, permitindo analisar as "respostas" positivas ou negativas dos recursos hídricos às diferentes práticas de manejo e gestão adotadas. Contudo, para se obter um monitoramento adequado, são necessários elevados investimentos tanto em equipamentos quanto em pessoal, para se implementar uma estrutura capaz de cobrir todas as regiões de interesse, bem como longo tempo de monitoramento, o que resulta em uma escassez de dados observados.

Para suprir as deficiências acima citadas, os modelos hidrológicos têm sido amplamente explorados. Com a interação entre os modelos hidrológicos e os Sistemas de Informações Geográficas (SIGs), além das técnicas de sensoriamento remoto, a simulação hidrológica tem se consolidado no âmbito científico, como uma alternativa viável para análise e

entendimento do comportamento hidrológico sob as pressões antrópicas ou naturais.

Neste contexto, a simulação hidrológica tem sido utilizada na avaliação de impactos hidrológicos, especialmente aqueles associados às mudanças no uso e ocupação do solo e às mudanças climáticas. As alterações no uso do solo, principalmente o desmatamento de florestas nativas, têm causado grandes problemas ambientais como: escassez de água devido à deficiente recarga de aquíferos, perdas de solo e transporte de sedimentos, levando à deterioração da qualidade do solo e da água, entre outros.

As alterações climáticas podem afetar o regime pluvial e a evapotranspiração, o que pode alterar o regime hidrológico de maneira definitiva, sobretudo no tocante aos eventos extremos, tais como: aumento na ocorrência de cheias, estresse hídrico de espécies vegetais, períodos de estiagem prolongados, entre outros.

No âmbito da modelagem hidrológica, os modelos hidrológicos do tipo chuva-vazão têm sido calibrados e aplicados com êxito em estudos de avaliações de impactos hidrológicos decorrentes de mudanças no uso do solo e de mudanças climáticas. Para essa finalidade, o modelo hidrológico *Soil and Water Assessment Tool (SWAT)* tem sido amplamente aplicado no Brasil e no mundo.

Neste contexto, este estudo foi realizado com os objetivos de: (i) calibrar e validar o modelo hidrológico SWAT para a simulação de vazões na região hidrográfica de cabeceira do Alto Rio Grande, delimitada a partir das seções de controle de Macaia e das usinas hidrelétricas de Camargos, Itutinga e Funil; (ii) simular os impactos hidrológicos decorrentes de mudanças de uso do solo por meio de cenários tendenciais na região; (iii) simular os impactos hidrológicos decorrentes de mudanças climáticas associadas às forçantes de concentração representativa RCP 4.5 e RCP 8.5, simuladas pelos modelos regionais Eta-HadGEM2-ES e Eta-MIROC5 e (iv) simular os impactos no potencial de produção de energia elétrica decorrentes

de mudanças climáticas nas usinas hidrelétricas de Camargos, Itutinga e Funil.

Na “Primeira parte”, apresenta-se uma revisão de literatura sobre modelagem hidrológica, bem como suas aplicações em estudos de avaliação de impactos decorrentes de mudanças de uso do solo e do clima. No “Artigo 1” são apresentadas as simulações de impactos hidrológicos decorrentes de mudanças no uso do solo na região de cabeceira do Alto rio Grande, delimitada a partir da seção de controle de Macaia. No “Artigo 2” são apresentadas as simulações de impactos hidrológicos decorrentes de mudanças climáticas, bem como os impactos na potencial de geração de energia elétrica das usinas hidrelétricas de Camargos, Itutinga e Funil.

2 REFERENCIAL TEÓRICO

2.1 O ciclo hidrológico

O ciclo hidrológico corresponde à dinâmica da água no meio ambiente, compreendendo seus diferentes estados físicos (líquido, vapor e sólido) que se verifica nos ambientes terrestres, impulsionado principalmente pela energia solar. Outros fatores que impulsionam o ciclo hidrológico são a força dos ventos, que são responsáveis pelo transporte do vapor d'água para os continentes e a força da gravidade, responsável pelos fenômenos da precipitação, infiltração e deslocamento de massas de água (MELLO; SILVA, 2013; TUNDISI, 2003).

O intercâmbio entre as circulações de água na superfície terrestre e na atmosfera ocorrem tanto no sentido superfície-atmosfera, em que o fluxo de água se dá fundamentalmente na forma de vapor em decorrência dos fenômenos de evaporação e transpiração, como no sentido atmosfera-superfície, em que a transferência de água ocorre mais significativamente na forma de chuva em bacias hidrográficas tropicais (TUCCI, 2007).

A análise e compreensão dos fatores que regem o ciclo hidrológico são de importância fundamental para a caracterização do comportamento dinâmico da água na paisagem, pois estes se constituem na base para subsidiar o planejamento, a gestão e o desenvolvimento de ações de exploração e conservação dos recursos hídricos. Os principais componentes do ciclo hidrológico estão representados na Figura 1.

Figura 1 – Representação dos principais componentes do ciclo hidrológico

Fonte: Mello e Silva (2013)

A precipitação é considerada o principal componente de entrada na fase terrestre do ciclo hidrológico. Parte da água precipitada pode ser interceptada pela cobertura do solo e pelos corpos hídricos. A água interceptada pela cobertura vegetal pode ser devolvida à atmosfera na forma de vapor d'água, pela evaporação direta e transpiração da cobertura vegetal.

O volume que atravessa a cobertura vegetal e atinge a superfície do solo, é dividido em duas parcelas: uma se infiltra e se redistribui no perfil do solo, e, a depender das condições de umidade, pode percolar (LP), promovendo a recarga do aquífero freático.

Outra parcela, gerada quando a superfície do solo se encontra saturada, ou quando a capacidade de infiltração do solo é inferior à taxa de precipitação, escoa superficialmente, originando o escoamento superficial.

O deflúvio pode ser dividido em três constituintes: escoamento superficial direto, que representa a parcela que escoa diretamente sobre a superfície do solo, o escoamento subterrâneo ou de base, que representa a contribuição do aquífero livre ao escoamento, e escoamento subsuperficial, que representa o escoamento pela camada superficial insaturada do solo.

Pode haver ainda, em situações de estresse hídrico das camadas superiores do solo, uma contribuição secundária ao ciclo, oriunda de um fluxo ascendente originário a partir do lençol freático, denominado de ascensão capilar (LC), frequentemente observada em regiões de descarga do aquífero, como em matas ciliares.

Concluindo o ciclo, a água armazenada na matriz do solo e posteriormente absorvida pelas plantas, retorna à atmosfera na forma de vapor d'água por meio da transpiração, juntamente com a água que é evaporada das superfícies (solo e dossel), constituindo no componente denominado evapotranspiração.

Neste contexto, faz-se necessário caracterizar o ciclo hidrológico com o meio natural e antrópico em uma determinada unidade territorial de interesse, a qual é chamada bacia hidrográfica.

As bacias hidrográficas são áreas delimitadas espacialmente por divisores de água, os quais são definidos por pontos elevados do terreno, que determinam a direção do escoamento da água da chuva. As bacias hidrográficas são constituídas de uma rede de drenagem interligada, cujo escoamento converge para uma seção comum, denominada de seção de controle ou exutório da bacia, onde se juntam a outros corpos d'água tais como rios, lagos, reservatórios, estuários e oceanos (DEBARRY, 2004; MELLO; SILVA, 2013).

A fim de mensurar e interpretar o ciclo hidrológico em uma bacia hidrográfica, tem-se como ferramenta o balanço hídrico, que consiste de uma

análise de entrada e saída de tais componentes adotando-se uma camada de solo como um volume de controle durante um determinado intervalo de tempo. Por meio do balanço hídrico é possível analisar variações temporais no armazenamento de água no solo e avaliar a condição de estresse hídrico da região em estudo, indicando potencialidades de exploração de recursos hídricos na bacia hidrográfica.

2.2 Modelagem hidrológica

Devido às complexas relações entre os componentes do ciclo hidrológico, a utilização de modelos é essencial para a análise e interpretação dos fenômenos envolvidos. Segundo Sorooshian et al. (2008), os modelos hidrológicos são uma representação simplificada de sistema real a ser estudado. Assim, um modelo hidrológico pode ser entendido como uma representação dos fenômenos associados ao ciclo hidrológico nas bacias hidrográficas, o qual simula os processos naturais em função de estímulos físicos e climáticos.

2.2.1 Classificação de modelos hidrológicos

Os modelos podem ser classificados sob diferentes aspectos, associados à sua estrutura, objetivos, discretização do tempo e espaço, entre outros, sendo aqui considerados os mais importantes.

Quanto à forma de representação espacial, os modelos podem ser concentrados ou distribuídos. Um modelo é dito concentrado quando este não leva em conta a variabilidade espacial, assumindo valores médios para a bacia hidrográfica, utilizando somente o tempo como variável independente (HARTMANN; BALES; SOROOSHIAN, 1999; TUCCI, 2005).

Quanto à discretização do tempo, um modelo é dito contínuo quando os fenômenos são contínuos no tempo, caso contrário, discretos. A escolha do intervalo de tempo (passo) no qual o modelo será executado depende

basicamente do fenômeno estudado, da disponibilidade de dados e da precisão desejada nos resultados (RENNÓ, 2003).

Segundo Shaw (1994), os modelos hidrológicos podem ser classificados em dois grupos: determinísticos e estocásticos. Os modelos determinísticos procuram simular os processos físicos envolvidos na transformação da precipitação em escoamento superficial, enquanto que os modelos estocásticos utilizam a probabilidade a fim de gerar séries hidrológicas de variáveis como precipitação, evaporação e vazão.

Os modelos hidrológicos também podem ser classificados em empírico, físico ou semiconceitual. Em modelos empíricos, são utilizados modelos de probabilidade para realizar o ajuste de dados observados aos simulados, não considerando os parâmetros físicos envolvidos no processo. Já em modelos físicos, são empregadas equações diferenciais na descrição dos processos, utilizando parâmetros determinados com base física (VIOLA, 2011).

Nos modelos semiconceituais, embora sejam aplicadas formulações que visam a descrição física dos processos, são empregados parâmetros calibráveis, os quais, embora possam ser associados a algumas características geomorfológicas, mantêm um certo empirismo (DURÃES, 2010).

A escolha do modelo que melhor se adeque à aplicação que se deseja, depende basicamente da disponibilidade e da qualidade dos dados de entrada. Conceitualmente, os modelos físicos distribuídos são os que melhor representam os processos físicos dentro de uma bacia hidrográfica e são inerentemente superiores a um modelo concentrado. Por outro lado, requerem uma grande quantidade de informação com alto nível de detalhamento sobre a área a ser estudada, o que torna esse tipo de modelo mais robusto.

2.2.2 Calibração, validação e análise de sensibilidade de modelos hidrológicos

Conceitualmente, na simulação hidrológica, ao se ajustar um modelo a uma determinada bacia hidrográfica, busca-se os valores dos parâmetros que melhor representem o comportamento físico da mesma.

Segundo Collischonn e Tucci (2003), o ajuste de parâmetros de um modelo hidrológico é uma etapa que envolve maior esforço para o usuário devido à necessidade de maior entendimento do comportamento do modelo e dos parâmetros, e aos problemas com a qualidade e a representatividade dos dados hidrológicos.

Segundo Arnold et al. (2012) e Daggupati et al. (2015), o primeiro passo no processo de ajuste de um modelo a uma determinada bacia hidrográfica consiste na seleção de parâmetros a serem calibrados. Esta seleção pode ser feita pela determinação dos parâmetros mais sensíveis do modelo a ser adotado, processo conhecido como análise de sensibilidade, que pode ser entendida como o processo de determinação da variação da mudança na saída do modelo em relação às mudanças na entrada do modelo (parâmetros) (MORIASI et al., 2007).

Segundo Veith et al. (2010), a análise de sensibilidade é importante para estabelecer variações viáveis dos valores de parâmetros para posterior calibração, distinguindo parâmetros que possuem impactos regionais e/ou interações com aqueles que possuem impacto universal.

Outros métodos utilizados para a determinação de parâmetros são por experiência do usuário a um determinado modelo, conhecimento da área de estudo e revisão de literatura (DAGGUPATI et al., 2015).

O segundo passo para a utilização de modelos hidrológicos em bacias hidrográficas é a calibração. A calibração é um esforço para refinar os valores dos parâmetros de um modelo para um determinado conjunto de condições locais, reduzindo, assim, a incerteza da previsão. A calibração do modelo é feita selecionando cuidadosamente os valores para os parâmetros

de entrada do modelo (dentro de suas respectivas faixas de incerteza), comparando previsões do modelo (saída) para um determinado conjunto de condições assumidas com os dados observados para as mesmas condições (ARNOLD et al., 2012).

De maneira geral, a calibração pode ser realizada manualmente ou por métodos automáticos. A calibração manual é muito subjetiva, demorada e depende muito da experiência do usuário do modelo, especialmente quando o modelo apresenta um grande número de parâmetros. Porém, esse processo permite que o usuário agregue seu conhecimento da área de estudo e sua experiência ao modelo. Por outro lado, na calibração automática são empregados métodos matemáticos de otimização, sendo o mais frequente a minimização de uma função objetivo que mede o desvio entre as séries de vazão observada e simulada (BRAVO; COLLISCHONN; TUCCI, 2009; TUCCI; ORDONEZ; SIMÕES, 1982). Este método consiste de um algoritmo que calcula diversas combinações de parâmetros, comparando-se os valores calculados até que o valor ótimo da função seja atingido (VIOLA, 2011). Assim, os métodos automáticos de calibração, procuram reduzir o tempo de ajuste do modelo. Porém, como o método consiste em um ajuste matemático, a solução pode convergir para valores irreais, fora de sua faixa de variação física (TUCCI, 2005).

Diversos algoritmos de otimização têm sido utilizados para a calibração automática de modelos hidrológicos, os quais destacam-se: o *Sequential Uncertainty Fitting* - SUFI-2 (ABBASPOUR; JOHNSON; VAN GENUCHTEN, 2004; ABBASPOUR et al., 2007); *Generalized Likelihood Uncertainty Estimation* - GLUE (BEVEN; BINLEY, 1992); *Parameter Solution* - ParaSol (VAN GRIENSVEN; MEIXNER, 2003); *Markov Chain Monte Carlo* – MCMC (KUCZERA; PARENT, 1998); e *Particle swarm optimization* – PSO (KENNEDY; EBERHART, 1995).

O terceiro e último passo na simulação hidrológica é a validação, que consiste em executar o modelo utilizando os parâmetros que foram medidos ou determinados durante o processo de calibração, e comparar as

previsões geradas pelo modelo aos dados observados, não considerados na calibração. Os processos de calibração e validação geralmente são realizados separando os dados observados disponíveis em duas partes: uma para calibração e outra para validação (ARNOLD et al., 2012).

Entre os métodos de validação de modelos hidrológicos destacam-se as técnicas de avaliações gráficas, de desempenho e a validação científica. A qualidade do ajuste pode ser analisada por meio de critérios qualitativos e quantitativos. O critério qualitativo baseia-se na comparação gráfica entre os dados observados e simulados, enquanto o critério quantitativo baseia-se em coeficientes estatísticos. A validação científica baseia-se na quantificação de fontes de incertezas associadas à simulação hidrológica, além dos critérios qualitativos e quantitativos (BIONDI et al., 2012).

Os principais coeficientes utilizados para avaliação de desempenho de modelos hidrológicos são: coeficiente de Nash-Sutcliffe (C_{NS}) (NASH; SUTCLIFFE, 1970); coeficiente de determinação (R^2) (LEGATES; MCCABE JÚNIOR, 1999); e P_{bias}.

2.3 Alguns modelos hidrológicos

Historicamente, o desenvolvimento de computadores e de novas tecnologias entre as décadas de 1950 e 1960 possibilitaram o desenvolvimento de modelos de transformação Precipitação-Vazão, destacando-se os modelos SSARR (ROCKWOOD, 1961) e STANDFORD IV (CRAWFORD; LINSLEY, 1966).

Com a evolução tecnológica e, principalmente com o desenvolvimento dos Sistemas de Informações Geográficas (SIG) e técnicas de sensoriamento remoto, os modelos hidrológicos foram aprimorados, possibilitando boa aproximação dos fenômenos simulados.

Atualmente, existem diversos modelos hidrológicos que são aplicados em diversas situações, estruturados física ou conceitualmente, discretizados espacialmente como concentrados ou distribuídos, desde níveis

de sub-bacias até regiões hidrologicamente homogêneas. Desses modelos, destacam-se: HBV (BERGSTRÖM; 1992); IPH-II (TUCCI; ORDONEZ; SIMÕES, 1982); SWAT (ARNOLD; ALLEN; BERNHARDT, 1993); TOPMODEL (BEVEN et al., 1994); DHSVM (WIGMOSTA; VAIL; LETTENMAIER, 1994); MGB-IPH (COLLISCHONN; TUCCI, 2001); e LASH (BESKOW; MELLO; NORTON, 2011; MELLO et al., 2008).

O SWAT (*Soil and Water Assessment Tool*) é um modelo de simulação de base hidrológica desenvolvido pelo *Agricultural Research Service* (ARS) em Temple no Texas, Estados Unidos da América. O SWAT foi desenvolvido com a finalidade de prever os impactos hidrológicos de práticas de manejo do solo, sedimentos e compostos químicos na produção agrícola em grandes bacias hidrográficas complexas com deferentes tipos de solo, uso e ocupação e condições de manejo do solo durante longos períodos de tempo (NEITSCH et al., 2005).

O modelo SWAT é um modelo de base física e conceitual, que permite a análise de diferentes processos em bacias hidrográficas por meio de parâmetros espacialmente distribuídos em nível de sub-bacias com discretização temporal contínua operando com passo de tempo diário (ARNOLD et al., 1998).

O SWAT incorpora recursos de vários modelos desenvolvidos pela ARS, tendo sua base derivada do modelo SWRRB, desenvolvido para simular o comportamento do escoamento superficial a nível de sub-bacias. O SWRRB, por sua vez, agregava os modelos CREAMS (componente de análise de precipitação diária), GLEAMS (componente de propagação de nutrientes e pesticidas) e EPIC (componente para simulação do crescimento de culturas) (GASSMAN et al., 2007; NEITSCH et al., 2005).

Os modelos QUAL2E e ROTO também contribuíram para o desenvolvimento do SWAT, fornecendo o componente de cinética de fluxo e estrutura de propagação, respectivamente.

O modelo adota como informação base o Modelo Digital de Elevação (MDE) e, a partir do qual, são obtidas informações de área de

contribuição, rede de drenagem e sub-bacias com seus respectivos parâmetros. Como informações geoespaciais, o modelo ainda requer dados de classe e uso do solo (NEITSCH et al., 2005).

No modelo SWAT, a bacia hidrográfica é dividida em múltiplas sub-bacias conectadas pela rede de drenagem e, posteriormente, divididas em Unidades de Resposta Hidrológica (URHs). As URHs são uma combinação única de classe de solo, uso do solo e relevo, sendo consideradas unidades hidrologicamente homogêneas. O escoamento calculado de cada URH é somado e propagado para obter o escoamento total da sub-bacia, o que pode aumentar a precisão das predições e fornecer uma melhor descrição física do balanço hídrico na bacia hidrográfica (ARNOLD et al., 1998, 2010; GASSMAN et al., 2007).

O SWAT tem como componentes principais: hidrologia, clima, solo, erosão, crescimento vegetal, nutrientes, pesticidas e manejo do solo (NEITSCH et al., 2005). O componente **hidrologia** é responsável pelo cálculo do balanço hídrico diário considerando a interação entre os fenômenos que regem o balanço de água no solo (infiltração, percolação, ascensão capilar e fluxo subsuperficial), escoamento superficial, escoamento subterrâneo e evapotranspiração. O componente **clima** gerencia dados de precipitação, temperatura, radiação solar e umidade relativa, gerando dados climáticos faltantes a partir de algoritmos implementados no modelo. Uma descrição detalhada dos componentes **hidrologia** e **clima** é apresentada no Anexo A.

O componente **solo** é responsável por armazenar e gerenciar informações relativas aos parâmetros físicos (textura, albedo, profundidade da camada do solo) e hídricos (condutividade hidráulica do solo, capacidade de armazenamento, entre outros).

O componente ArcSWAT permite a interface entre um Sistema de Informação Geográfica (SIG) e o modelo a fim de facilitar sua aplicação. Com a finalidade de assegurar uma simulação bem sucedida, a interface

requer informações relativas ao uso e ocupação do solo, tipo de solo, clima, manejo de uso da água, entre outros (WINCHELL et al., 2013).

2.4 Desempenho de modelos hidrológicos

Os modelos hidrológicos têm sido utilizados em diversas aplicações, tais como: manejo integrado de bacias hidrográficas, análise de impactos hidrológicos decorrentes de mudanças do uso e ocupação do solo, mudanças climáticas, erosão, poluição, entre outros, apresentando uma ampla literatura técnico-científica, corroborando a eficácia de modelos para tais finalidades.

Beskow, Norton e Mello (2013) aplicaram o modelo LASH na bacia do ribeirão Jaguara (32 km^2) para estimar as vazões máximas, mínimas e médias considerando os seguintes cenários de uso e ocupação do solo: atual (1), substituição de pastagens por eucalipto (2) e substituição de eucalipto por pastagens (3). De acordo com os autores, o modelo apresentou um bom desempenho com respeito ao cenário 1, apresentando C_{NS} de 0,81, 0,82 e 0,98 na simulação de vazões máximas, mínimas e médias, respectivamente. Na simulação do cenário 2, os resultados apresentaram uma redução das vazões mínimas, médias e máximas de 7,39%, 13,84% e 20,38%, respectivamente. Por outro lado, o cenário 3 apresentou um aumento de 0,23%, 0,44% e 1,19% para as vazões mínimas, médias e máximas, respectivamente.

Viola et al. (2013) simularam o comportamento hidrológico de quatro bacias de cabeceira (rios Aiuruoca [2.095 km^2], Grande [2.080 km^2], Sapucaí [7.325 km^2] e Verde [4.178 km^2]) na bacia hidrográfica do rio Grande, sul de Minas Gerais, utilizando o modelo LASH. Segundo os autores, o modelo apresentou-se adequado na simulação dos processos hidrológicos nas referidas bacias, apresentando valores de C_{NS} maiores que 0,70, tanto na fase de calibração quanto na de validação.

Durães, Mello e Naghettini (2011) aplicaram o modelo SWAT para avaliar o comportamento hidrológico da bacia do rio Paraopeba (10.200

km^2), no estado de Minas Gerais, sob diferentes usos e ocupação do solo. Os autores constataram que o modelo apresentou grande sensibilidade de parâmetros relacionados ao escoamento base. Além disso, o modelo apresentou valores de C_{NS} maiores que 0,75, sendo assim adequado para representar a área de estudo. O modelo SWAT também forneceu resultados satisfatórios na simulação do comportamento hidrológico sob diferentes cenários de uso e ocupação do solo.

Aplicando o modelo SWAT na simulação hidrológica da bacia do lago Jebba (12.992 km^2), Nigéria, Adeogun et al. (2014) observaram que o modelo mostrou-se eficiente na predição da vazão média diária, apresentando coeficientes de Nash e Sutcliffe e R^2 maiores que 0,7 para as fases de calibração e validação.

George e James (2013) aplicaram o SWAT para calibração e validação da vazão média diária na bacia hidrográfica de Kerala (1.272 km^2), Índia, utilizando múltiplas estações. Os autores observaram um bom desempenho do modelo nas fases de calibração e validação, obtendo C_{NS} maiores que 0,75.

Chiang et al. (2014) avaliaram o desempenho do modelo SWAT adotando diferentes estratégias de calibração (calibração em um único e em múltiplos locais) na simulação da vazão e cargas de sedimentos em suspensão e nitrogênio total no rio Kaskaskia, no estado de Illinois, Estados Unidos da América.

Rossi et al. (2009) avaliando o desempenho do modelo SWAT na simulação das vazões médias diárias e mensais em múltiplas estações na bacia do baixo Mekong, no continente Asiático, concluíram que o modelo apresentou-se adequado para a simulação hidrológica das bacias hidrográficas analisadas. Segundo os autores, as fases de calibração e validação das variáveis analisadas apresentaram C_{NS} variando entre 0,8 e 1,0.

2.5 Mudanças Climáticas

Mudança climática refere-se à mudança no estado do clima que pode ser identificada por mudanças na média e/ou da variabilidade de suas propriedades, persistindo por longos períodos. A mudança climática pode ser causada por processos internos e/ou forçantes externas, sendo esta, a causa que apresenta um maior interesse científico (INTERGOVERNMENTAL PANEL ON CLIMATE CHANGE – IPCC, 2007).

As influências externas podem ocorrer naturalmente, como mudanças na radiação solar ou na atividade vulcânica, ou como resultado de ações antrópicas, como alterações no albedo da superfície terrestre, na composição da atmosfera devido à emissão de gases provenientes das atividades industriais, entre outras. Para o entendimento e comparação da influência das forçantes naturais e antropogênicas sobre o aquecimento ou resfriamento do clima global, adota-se o conceito de foçamento radiativo, expresso em watts por metro quadrado (W m^{-2}) (IPCC, 2007).

De acordo com IPCC (2007), a estimativa do efeito líquido das atividades humanas, em média, desde 1750 até 2005, foi de aquecimento, com um forçamento radiativo da ordem de 1,6 [0,6 a 2,4] W m^{-2}. Outros fatores analisados foram o forçamento indireto do albedo das nuvens (0,35 [0,25 a 0,65] W m^{-2}); gases do efeito estufa (-0,5 [-0,9 a -0,1] W m^{-2}); aerossóis (-0,7 [-1,8 a -0,3] W m^{-2}); entre outros.

De acordo com o IPCC (2001), o principal responsável pelo aquecimento global é a intensificação do efeito estufa. Esse fenômeno consiste na absorção e na posterior reemissão da energia de onda longa emitida pela superfície terrestre, pelos “gases de efeito estufa”, sendo um fenômeno natural e necessário à vida no planeta.

Os gases do efeito estufa afetam o clima, alterando a radiação solar incidente e dispersando a radiação infravermelha (termal), que são parte do balanço de energia da Terra. A alteração da quantidade ou das propriedades dos gases presentes na atmosfera podem levar a um aquecimento ou resfriamento do sistema climático (IPCC, 2007).

2.5.1 Modelos de Circulação Global (MCG) e Regional (MCR)

Os Modelos de Circulação Global (MCG) são ferramentas utilizadas para projetar futuras mudanças do clima, como consequência de futuros cenários de forçamento climático, como emissão de gases de efeito estufa e aerossóis. Os modelos globais de clima projetam para o futuro, ainda com algum grau de incerteza, possíveis mudanças em extremos climáticos, como ondas de calor, ondas de frio, chuvas intensas e enchentes, secas; e mais intensos e/ou frequentes, furações e ciclones tropicais e extratropicais (MARENGO, 2007).

Alguns dos MCGs disponíveis são: *Hadley Centre for Climate Prediction and Research* (Had), da Inglaterra; *Australia's Commonwealth Scientific and Industrial Research Organization*, da Austrália (CSIRO-Mk2); *Canadian Center for Climate Modeling and Analysis*, do Canadá (CCCMA); *National Oceanic and Atmospheric Administration - NOAA-Geophysical Fluids Dynamic Laboratory*, dos Estados Unidos (GFDL); e *Model for Interdisciplinary Research on Climate*, do Japão (MIROC).

Segundo Chou et al. (2014a), os Modelos de Circulação Global (MCG) são as principais ferramentas para o estudo de variabilidade e mudança do clima. No entanto, estes modelos apresentam resoluções grosseiras, o que limita a simulação climática dos processos de mesoescala e na representação da topografia, uso do solo e a distribuição oceano/continente.

Para se alcançar uma melhor resolução espacial e, consequentemente, uma simulação climática mais eficiente, são adotadas técnicas de regionalização, conhecidas como *downscaling*, sendo: refinamento de parte da grade (*grid*) da resolução do modelo global; acoplamento de Modelos Climáticos Regionais (MCRs) aos MCGs; e a regionalização estatística das simulações dos MCGs. As projeções climáticas derivadas dos MCRs podem ser consideradas úteis para o estudo de impactos

devido aos padrões naturais subcontinentais e da magnitude das mudanças (CHOU et al., 2011, 2014a).

Neste contexto, diversos estudos utilizando técnicas de regionalização de MCGs na América do Sul têm sido realizados a fim de avaliar os potenciais impactos sobre o clima e sobre os recursos naturais, destacando-se Chou et al. (2011, 2012), Marengo et al. (2011) e Pesquero et al. (2009).

Chou et al. (2014a, 2014b) avaliaram o impacto de mudanças climáticas sobre o clima da América do Sul por meio de técnicas de regionalização (*downscaling*) de dois MCGs utilizando o modelo regional Eta. O modelo HadGEM2-ES é um modelo de circulação do sistema terrestre desenvolvido pelo Hadley Centre (COLLINS et al., 2011; MARTIN et al., 2011) com resolução especial de 1,875 graus em longitude e 1,275 graus em latitude. O modelo MIROC5 (WATANABE et al., 2010) é um modelo acoplado oceano-atmosfera japonês com resolução espacial de aproximadamente 150 km na horizontal e 40 km na vertical.

O modelo regional Eta foi adaptado pelo Instituto Nacional de Pesquisas Espaciais – Centro de Previsão de Tempo e Estudos Climáticos (INPE/CPTEC) para simular integrações climáticas de longo prazo sobre as Américas Central e do Sul. Os modelos Eta-HadGEM2-ES e Eta-MIROC5, resultantes do acoplamento entre os modelos descritos anteriormente, foram simulados baseados em dois diferentes Cenários Representativos de Concentração (*Representative Concentration Pathways* – RCP).

2.5.2 Cenários Representativos de Concentração

Os cenários de emissão representam uma visão possível do desenvolvimento futuro de emissões de substâncias que têm um efeito radiativo potencial (gases de efeito estufa, aerossóis) combinado com crescimento populacional, aos desenvolvimentos tecnológico, econômico e social, entre outros (IPCC, 2001; VAN VUUREN et al., 2011).

Em 1988, o Painel Intergovernamental sobre Mudanças Climáticas (IPCC) foi criado pela Organização Meteorológica Mundial (OMM) e pelo Programa das Nações Unidas para o Meio Ambiente (PNUMA) com o objetivo de apoiar com trabalhos científicos as avaliações do clima e os cenários de mudanças climáticas para o futuro.

Em 2000, em seu Relatório Especial sobre Cenários de Emissão (SRES), o IPCC desenvolveu diferentes famílias de cenários futuros de mudanças climáticas, baseado na emissão de gases de efeito estufa com projeções até para 2100. Porém, segundo van Vuuen et al. (2011), houve a necessidade de desenvolver novos cenários que apresentassem um maior nível de detalhamento e que explorassem explicitamente o impacto de diferentes estratégias climáticas governamentais antes não abordados pelos cenários previamente existentes. Neste contexto, novos cenários foram desenvolvidos pela comunidade científica e aprovados pelo IPCC para compor o Quinto Relatório de Avaliação (AR5), divulgado em 2013 (IPCC, 2013).

Assim, criaram-se os Cenários Representativos de Concentração (*Representative Concentration Pathways* – RCP), os quais se baseiam nos forçantes radiativos antropogênicos ao final do século 21. Quatro diferentes cenários foram desenvolvidos: RCP 8.5, RCP 6.0, RCP 4.5 e RCP 2.6, os quais correspondem aos forçantes radiativos de 8,5 W m^{-2}, 6 W m^{-2}, 4,5 W m^{-2} e 2,6 W m^{-2}. Essas estimativas são baseadas na concentração de gases de efeito estufa e outros agentes (CHUO et al., 2014a; VAN VUUREN et al., 2011).

O RCP 2.6 representa um cenário de mitigação com nível forçante muito baixo, o que implica em redução substancial da concentração de gases de efeito estufa na atmosfera até o fim do século 21. Os RCPs 4.5 e 6.0 representam cenários médios de estabilização e o RCP 8.5 representa uma grande concentração de gases de efeito estufa na atmosfera em 2100 (VAN VUUREN et al., 2011).

2.6 Impactos hidrológicos decorrentes de mudanças climáticas

Algumas das principais consequências das mudanças climáticas nos recursos hídricos são o aumento na variabilidade da precipitação, maior ocorrência e magnitude de eventos extremos, como secas prolongadas, cheias e mudança na frequência de vazões, causando assim uma alteração na disponibilidade de recursos hídricos (BELL et al., 2007; HAGUMA et al., 2014).

Assim, a fim de caracterizar esse impacto, a simulação de tendências climáticas de longo prazo pode ser realizada por Modelos Climáticos de Circulação Global (MCG) em escala global e traduzidos para a escala local por modelos climáticos regionais, também chamados de modelos de *downscaling* (AMBRIZZI et al., 2007). Os impactos hidrológicos devido às mudanças climáticas, usualmente são estimados por meio da definição de dados de entrada de cenários de mudanças climáticas para um modelo hidrológico a partir da saída de um Modelo Climático de Circulação Global (MCG) ou de um Modelo Climático Regional (MCR).

De acordo com o IPCC (2013), a análise adequada desses impactos depende de três principais fatores a serem desenvolvidos: a) construção de cenários adequados para avaliação dos impactos hidrológicos; b) desenvolvimento e utilização de modelos hidrológicos realistas; e c) melhor compreensão das relações entre o clima e o sistema hidrológico.

Apesar da possibilidade de diferentes modelos hidrológicos calcularem diferentes valores de vazão para determinado dado de entrada, as maiores incertezas no efeito do clima sobre as vazões, resultam de incertezas dos cenários de mudanças climáticas, contanto que se use um modelo hidrológico seguro (PRUDHOMME; DAVIES, 2009).

A utilização de modelos hidrológicos para a análise de impactos no regime hidrológico decorrentes de mudanças climáticas apresenta vasta literatura técnico-científica.

Ouyang et al. (2015) avaliaram o impacto de mudanças climáticas nas vazões da bacia hidrográfica de Huangnizhuang, na China, utilizando seis diferentes MCGs sob influência dos cenários RCPs 2.6, 4.5 e 8.5 acoplados ao modelo hidrológico SWAT. Os resultados deste estudo projetam, de forma geral, um aumento na precipitação entre a metade e o final do século 21 variando de -2,4% a 9%. Entretanto, projeções indicam decréscimo das vazões, variando de -6,9 a 0,8%, principalmente devido ao acréscimo da evapotranspiração na área estudada.

Huang, Krysanova e Hattermann (2014) avaliaram o impacto de mudanças climáticas nas vazões máximas e mínimas na Alemanha durante o período de 2061 a 2100 utilizando um conjunto de 15 MCRs, sob influência do cenário SRES A1B, acoplados ao modelo hidrológico SWIM. O estudo indica que, durante o período analisado, a maioria dos rios na Alemanha poderá sofrer inundações e secas mais frequentes, destacando-se projeções de aumento da vazão na bacia do rio Elbe e de decréscimo na bacia hidrográfica do rio Rhine.

Xu et al. (2013), utilizando o modelo SWAT, avaliaram os potenciais impactos de mudanças climáticas sobre a precipitação, evapotranspiração potencial e vazão na bacia do rio Qiantang, China, para o período de 2011 a 2100 (2011 a 2040; 2041 a 2071; 2071 a 2100), sobre influência de três cenários SRES A1B, A2 e B1, simuladas pelo modelo AOGCM.

Os resultados deste estudo indicaram que a vazão sofrerá uma diminuição em todos os cenários de emissão e em todos os estágios de tempo, indicando menor quantidade de água disponível para aquela região. Além disso, simulações mensais indicaram que as maiores reduções nas vazões ocorrerão no período do inverno e os maiores aumentos no verão, aumentando a possibilidade de ocorrência de desastres nessa região.

Bauwens, Sohier e Degré (2011) avaliaram os impactos hidrológicos associados às mudanças climáticas em duas bacias hidrográficas na região de Wallonia, Bélgica, acoplando o modelo hidrológico EPICgrid aos cenários

desenvolvidos pelo projeto CCI-HYDR, baseado em cenários SRES e criado especialmente para representar as características de circulação atmosférica da região da Bélgica.

Os autores constataram uma diminuição na evapotranspiração da vegetação de 10% a 17% até o fim do século XXI. Além disso, o estudo aponta uma diminuição da vazão mínima de sete dias consecutivos da ordem de 19% a 24% para um período de retorno de dois anos e, entre 20% a 35%, para um período de retorno de 50 anos, indicando uma estiagem severa que poderá ocasionar grandes problemas na disponibilidade de água.

Tshimanga e Hughes (2012) avaliaram o efeito das mudanças climáticas associadas ao cenário SRES A2 sobre o regime hidrológico da bacia do rio Congo, África. Os autores acoplaram três modelos climáticos regionais (MCR's) ao modelo hidrológico GW-PITMAN, dando enfoque na precipitação, interceptação, evapotranspiração potencial, armazenamento de água no solo e recarga de aquíferos. Os resultados mostraram que, em geral, houve uma diminuição de 10% na vazão da bacia em estudo. Além disso, a evapotranspiração foi o componente que mais apresentou mudanças, com valores atingindo 10,3% de aumento para os três MCR's analisados.

Marengo et al. (2011) avaliaram as possíveis mudanças climáticas futuras associadas ao cenário SRES A1B, simuladas pelo modelo Eta-CPTEC/HadCM3 considerando três grandes bacias hidrográficas brasileiras (rios Amazonas, Paraná e São Francisco). Os resultados sinalizaram uma diminuição da precipitação até 2100, com valores da ordem de -1 mm dia^{-1} [0,7 a -1,2 mm dia^{-1}] na bacia do rio Amazonas, -0,2 mm dia^{-1} [+0,5 a -0,5 mm dia^{-1}] na bacia do rio Paraná e -1 mm dia^{-1} [-0,5 a -1,5 mm dia^{-1}] na bacia do rio São Francisco. Em relação à temperatura, as projeções indicaram, para 2100, um acréscimo de até 5ºC [4 a 6ºC] para a bacia Amazônica, 4,5ºC [3,5 a 6ºC] na bacia hidrográfica do rio Paraná, e 4ºC [3 a 4ºC] para a bacia do rio São Francisco.

Ho, Thompson e Brierley (2016) investigaram os possíveis impactos decorrentes de mudanças climáticas na bacia hidrográfica dos rios

Tocantins-Araguaia no final do século 21 (2071-2100), utilizando um conjunto de 41 MCGs sob influência do Cenário Representativo de Concentração RCP 4.5 acoplados ao modelo hidrológico STELLA. Os autores relatam que a maioria dos modelos climáticos indica um decréscimo na vazão anual média apesar de alguns apresentarem aumento. Uma grande proporção das simulações indica uma expressiva redução nas vazões, especialmente durante a transição entre o período seco e chuvoso. Ainda, mais de 75% dos modelos analisados sugerem uma redução nas vazões mínimas, o que poderia prejudicar o planejamento atual e futuro da rede de produção de energia na bacia.

Viola et al. (2015), utilizando o modelo hidrológico LASH, simularam os possíveis impactos hidrológicos associados ao cenário SRES A1B projetado pelo MCR Eta-CPTEC/HadCM3 nos períodos de 2011 a 2040, 2041 a 2070 e de 2071 a 2098, nas bacias hidrográficas dos rios Aiuruoca, Grande, Sapucaí e Verde, no sul de Minas Gerais. Os resultados indicaram possível redução do escoamento anual para o período entre 2011 e 2040 nas bacias analisadas. Por outro lado, para os demais períodos, os resultados sinalizaram aumento no escoamento médio anual em todas as bacias, alcançando valores de até 166,12 mm ano^{-1}.

Alvarenga et al. (2016) avaliaram os impactos das mudanças climáticas na hidrologia na bacia de cabeceira Lavrinha, localizada na serra da Mantiqueira, no sul de Minas Gerais. Os autores utilizaram o modelo hidrológico DHSVM forçado pelo MCR Eta-HadGEM2- ES sob influência do cenário RCP 8.5. Os resultados mostraram uma redução na vazão mensal entre 20 e 77% ao longo do século 21 (2011 a 2099), correspondendo a reduções drásticas no escoamento e, consequentemente, na capacidade de produção de água da região.

2.6.1 Impactos na produção de energia elétrica decorrentes de mudanças climáticas

A geração de energia elétrica por meio de usinas hidrelétricas depende diretamente da disponibilidade dos recursos hídricos, e, portanto, do ciclo hidrológico. Atualmente, aproximadamente 70% de toda energia elétrica no Brasil é produzida por meio de usinas hidrelétricas, o que torna o país extremamente dependente do regime hidrológico, sendo assim vulnerável à variabilidade dos fatores climáticos (EMPRESA DE PESQUISA ENERGÉTICA - EPE, 2016).

Segundo Schaeffer et al. (2012), a abordagem metodológica mais comumente usada para análise de impactos de mudanças climáticas na produção de energia consiste em estimar o escoamento por meio de modelos climáticos (MCGs ou MCRs) acoplados aos modelos hidrológicos a fim de se estimar os possíveis impactos futuros na produção de energia.

Segundo Majone et al. (2016), de maneira geral, a análise de impactos no potencial de geração hidrelétrica, definida como a energia capaz de ser produzida por uma usina hidrelétrica, proporciona uma sólida medida indicativa de possíveis tendências na produção de energia relacionadas às mudanças climáticas.

Neste contexto, diversos estudos têm adotado esta metodologia a fim de avaliar os impactos de mudanças climáticas no potencial de produção de energia ao redor do mundo. van Vliet et al. (2016) investigaram os impactos de mudanças climáticas no potencial de produção de energia elétrica e termelétrica em escala global utilizando cinco diferentes MCGs sob influência dos cenários RCP 2.6 e RCP 8.5. De acordo com o estudo, a maioria das usinas hidrelétricas (61% considerando o RCP 2.6 e 74% considerando o RCP 8.5) está localizada em regiões onde são projetadas reduções significantes no escoamento, resultando em uma redução global média na capacidade útil de produção.

Estas tendências de redução são atenuadas pelas tendências de aumento nas vazões no Canadá, norte europeu, África Central, Índia e no nordeste chinês. Reduções na capacidade de produção global variaram de 1,7% a 0,4% sob influência do RCP 2,6 e de 1,9% a 6,1% sob influência do

RCP 8.5 entre o período de 2020 e 2080. Reduções mensais na capacidade de produção foram de 8,9%, 9,6% e 8,3% para o RCP 2.6 e 9,2%, 17% e 24% para o RCP 8.5 para as décadas de 2020, 2050 e 2080, respectivamente, com 5 e 22% (RCP 2.6 e RCP 8.5) das usinas hidrelétricas apresentando reduções no potencial de geração maiores que 30% para a década de 2050.

Lehner, Czisch e Vassolo (2005) utilizaram três MCGs para avaliação de impactos no potencial de produção hidrelétrica na Europa. Os autores indicaram uma tendência de redução no potencial de produção anual em mais de 25% no sul e em partes do centro-leste europeu, especialmente Espanha, Turquia, Bulgária e Ucrânia. Por outro lado, projeções estimaram uma tendência de aumento em mais de 25% no norte europeu, principalmente na Noruega, Finlândia, Suécia e Rússia.

Minville et al. (2009) avaliaram os impactos no potencial de produção hidrelétrica na bacia do rio Peribonka, no Canadá. Os resultados apresentaram uma diminuição na produção anual de 1,8% no período de 2010 a 2039, seguido de um aumento de 9,3% e 18% durante os períodos 2040-2069 e 2070-2099, respectivamente.

Lobanova et al. (2016) estudaram os impactos no potencial produção de energia elétrica em três usinas hidrelétricas localizadas na bacia hidrográfica do rio Targus, entre Espanha e Portugal, utilizando diferentes projeções do MCR ISI-MIP sob influência dos cenários RCP 4.5 e RCP 8.5 entre os períodos 2021-2050 e 2071-2100. Os resultados deste estudo apresentaram reduções no potencial de produção variando de 10% a 50% sob influência do RCP 4.5, ao passo que, sob influência do RCP 8.5 as reduções variaram entre 40% e 60% para os períodos 2021-2050 e 2071-2100, respectivamente.

Mohor et al. (2015) avaliaram os impactos de mudanças climáticas no potencial de produção na hidrelétrica de Teles Pires, localizada na bacia hidrográfica de Tapajós, na região Amazônica, utilizando oito MCGs acoplados ao modelo hidrológico MDH-INPE. O estudo indica que a projeção mais crítica, sugere que a Usina hidrelétrica de Teles Pires poderá

não operar em 59% do tempo durante o período de 2041 a 2070, pois os requisitos mínimos de operação não deverão ser alcançados.

2.7 Impactos hidrológicos decorrentes de mudanças no uso do solo

O regime hidrológico de uma bacia hidrográfica é resultado da complexa interação entre solos, vegetação, relevo e clima. Consequentemente, qualquer alteração no uso e ocupação do solo pode causar alteração no balanço hídrico da bacia hidrográfica, podendo gerar impactos positivos ou negativos para seu regime hidrológico. Neste contexto, a avaliação dos impactos nos recursos hídricos produzidos por mudanças de uso do solo, consiste em uma das aplicações mais relevantes para o planejamento ambiental da bacia hidrográfica (VIOLA; MELLO, 2009).

De acordo com Bruijnzeel (1988), o escoamento de uma bacia é influenciado principalmente por três fenômenos: a capacidade de infiltração, a evapotranspiração associada a cada tipo de uso do solo e a interceptação da precipitação pela cobertura vegetal. Além disso, a profundidade do sistema radicular também tem papel importante no comportamento hidrológico, pois define o reservatório de água disponível para a evapotranspiração e, normalmente, é a referência para o balanço hídrico de modelos (VIOLA, 2011).

Os impactos decorrentes de uso do solo em termos hidrológicos afetam o escoamento superficial, a vazão máxima de cheia, os fluxos de base, a recarga subterrânea, a umidade do solo, o volume de perda de solo e o transporte de sedimentos (PERAZZOLI; PINHEIRO; KAUFMANN, 2013).

Segundo Bruijnzeel (1988) e Scherer e Pike (2003), a remoção de florestas afeta diretamente na capacidade de infiltração do solo, interceptação, evapotranspiração e na profundidade de sistema radicular. Em coberturas vegetais florestais são notadas características que tendem a

maximizar o fluxo vertical de água, com destaque para: a) albedo reduzido, o que resulta em maior energia líquida disponibilizada para evapotranspiração; b) sistema radicular profundo, indicando maior capacidade de retirada de água do solo e c) elevado índice de área foliar, proporcionando maiores taxas de interceptação (VIOLA, 2011). Ao se retirar a cobertura vegetal, há tendência de diminuição do fluxo vertical, e consequentemente, há aumento do fluxo horizontal.

De acordo com Scherer e Pike (2003), a redução da evapotranspiração e interceptação associada ao desmatamento de florestas são os principais mecanismos de mudanças das vazões mínimas, que são regidas pelo comportamento de recarga dos aquíferos. Neste tocante, as florestas tendem a apresentar sistema radicular profundo, com maior possibilidade de absorção de água, podendo influir sobre a recarga.

Diferentes métodos têm sido usados para avaliar os impactos hidrológicos decorrentes de mudanças de uso do solo. A análise desses impactos pode ser determinada experimentalmente; porém, métodos experimentais para a investigação de processos hidrológicos são onerosos e demandam tempo. Consequentemente, o uso de modelos hidrológicos tem sido cada vez mais comum para essa finalidade (YEN et al., 2014).

Viola et al. (2014) avaliaram os impactos de mudanças do uso do solo no regime hidrológico em quatro bacias na região de cabeceira da bacia do rio Grande, em Minas Gerais, utilizando o modelo hidrológico LASH e cinco diferentes cenários futuros de uso do solo. Os autores constataram que os cenários de desmatamento reduziriam o deflúvio total das bacias entre 9 mm ano^{-1} e 23,5 mm ano^{-1}. Por outro lado, considerando os cenários de reflorestamento, o escoamento aumentaria entre 7,36 mm ano^{-1} e 37,74 mm ano^{-1}.

Bieger, Hörmann e Fohrer (2015) avaliaram o impacto de mudanças no uso do solo na produção de sedimentos e no balanço hídrico na bacia hidrográfica do rio Xiangxi, na China. Os autores consideraram cenários de reflorestamento baseados em programas de conservação nos quais

agricultores são incentivados a substituir terras agrícolas por florestas ou pastagens em locais com declividade maiores que 25º. Os resultados sugerem uma redução de 5,9%, 47,7%, 0,7% e 41,9% no escoamento superficial direto, perda de solo, vazão e descarga de sedimentos, respectivamente. Porém, o efeito positivo do reflorestamento poderá ser atenuado pelos efeitos negativos de uma intensificação de uso do solo em outras partes da bacia.

Can et al. (2015) avaliaram os impactos hidrológicos devido à mudança da cobertura vegetal na bacia do rio Fuhe, na China. Os resultados mostraram um decréscimo no escoamento superficial direto, enquanto a recarga do lençol subterrâneo e a evapotranspiração mostraram aumento à medida que áreas de floresta, agricultura e/ou pastagens aumentaram e arrozais e áreas urbanas diminuíram. Os autores concluíram que a urbanização na bacia do rio Fuhe é o fator que mais contribuiu para as mudanças no escoamento superficial direto, deflúvio e evapotranspiração.

3 CONSIDERAÇÕES GERAIS

Este trabalho consistiu na simulação de impactos hidrológicos decorrentes de mudanças climáticas e do uso do solo na região de cabeceira do rio Grande com a finalidade de oferecer subsídios para uma melhor gestão de recursos hídricos na região. Para tal, diferentes cenários tendenciais de uso do solo foram desenvolvidos, com base em diretrizes propostas por órgãos governamentais.

Para a simulação climática, dois modelos climáticos regionais, Eta-HadGEM2-ES e Eta-MIROC5, simulados sob influência de duas forçantes de concentração, RCP 4.5 e RCP 8.5 foram utilizados. Subsequentemente, foram avaliados os impactos decorrentes dessas mudanças climáticas no potencial de geração de energia elétrica nas usinas hidrelétricas instaladas no Alto Rio Grande: Camargos, Itutinga e Funil.

É importante ressaltar que este trabalho traz uma abordagem inédita com relação à avaliação de impactos hidrológicos decorrentes de mudanças climáticas na produção de energia na região, com a finalidade de investigar e propor melhorias metodológicas para pesquisas futuras.

REFERÊNCIAS

ABBASPOUR, K. C. et al. Modelling hydrology and water quality in the pre-alpine/alpine Thur watershed using SWAT. **Journal of Hydrology,** Amsterdam, v. 333, n. 2/4, p. 413–430, 2007.

ABBASPOUR, K. C.; JOHNSON, C. A.; VAN GENUCHTEN, M. T. Estimating uncertain flow and transport parameters using a sequential uncertainty fitting procedure. **Vadose Zone Journal,** Madison**,** v. 3, n. 4. p. 1340–1352, 2004.

ADEOGUN, A. G. et al. Validation of swat model for prediction of water yield and water balance : case study of Upstream Catchment of Jebba Dam in Nigeria. I**nternational Journal of Physical, Nuclear Science and Engineering**, Bradford, v. 8, n. 2, p. 1-7, 2014.

ALVARENGA, L. A. et al. Assessment of land cover change on the hydrology of a Brazilian head- water watershed using the Distributed Hydrology-Soil-Vegetation Model. **Catena,** Amsterdam, v. 143, p. 7–17, 2016.

AMBRIZZI, T. et al. **Cenários regionalizados de clima no Brasil para o século XXI:** projeções de clima usando três modelos regionais. Brasília: MMA, 2007. 108 p.

ARNOLD, J. G.; ALLEN, P. M.; BERNHARDT, G. A comprehensive surface-groundwater flow model. **Journal of Hydrology**, Amsterdam, v. 142, n. 1/4, p. 47-69, 1993.

ARNOLD, J. G. et al. Assessment of different representations of spatial variability on SWAT model performance. **Transactions of the ASABE**, St. Joseph, v. 53, n. 5, p. 1433-1443, 2010.

ARNOLD, J. G. et al. Large area hydrologic modeling and assessment part I: model development. **Journal of the American Water Resources Association**, Herndon, v. 34, n. 1, p. 73-89, 1998.

ARNOLD, J G. et al. SWAT: model use, calibration and validation. **Transactions of the ASABE**, St. Joseph, v. 55, n. 4, p. 1491-1508, 2012.

BAUWENS, A.; SOHIER, C.; DEGRÉ, A. Hydrological response to climate change in the Lesse and the Vesdre catchments: contribution of a physically based model (Wallonia, Belgium). **Hydrology and Earth System Sciences**, Saskatoon, v. 15, n. 6, p. 1745-1756, 2011.

BELL, V. A. et al. Use of a grid-based hydrological model and regional climate model outputs to assess changing flood risk. **International Journal of Climatology**, Chichester, v. 27, n. 12, p. 1657–1671, 2007.

BERGSTRÖM, S. The HBV model: its structure and applications. **Hydrology**, Norrköping, n. 4, p. 1-35, 1992.

BESKOW, S.; MELLO, C. R.; NORTON, L. D. Development, sensitivity and uncertainty analysis of LASH model. **Scientia Agricola**, Piracicaba, v. 68, n. 3, p. 265-274, 2011.

BESKOW, S.; NORTON, L. D.; MELLO, C. R. Hydrological prediction in a Tropical Watershed Dominated by Oxisols Using a distributed Hydrological Model. **Water Resources Management**, Reidel, v. 27, n. 2, p. 341-363, 2013.

BEVEN, K. J.; BINLEY, A. The future of distributed models - model calibration and uncertainty prediction. **Hydrological Processes**, Chichester, v. 6, n. 3, p. 279-298, 1992.

BEVEN, K. J. et al. Topmodel. In: SINGH, V. P. (Ed.). **Computer model of watershed hydrology**. Fort Collins: Water Resource, 1994. p. 1130.

BIEGER, K.; HÖRMANN, G.; FOHRER, N. The impact of land use change in the Xiangxi Catchment (China) on water balance and sediment transport. **Regional Environmental Change**, New York, v. 15, n. 3, p. 485-498, 2015.

BIONDI, D. et al. Validation of hydrological models: conceptual basis , methodological approaches and a proposal for a code of practice. **Physics and Chemistry of the Earth**, Oxford, v. 42/44, n. 1, p. 70-76, 2012.

BRAVO, J. M.; COLLISCHONN, W.; TUCCI, C. E, M. Verificação da eficiência e eficácia de um algoritmo evolucionário multi-objetivo na calibração automática do modelo hidrológico IPH II. **Revista Brasileira de Recursos Hídricos**, Porto Alegre, v. 14, n. 3, p. 37-50, 2009.

BRUIJNZEEL, L. A. (De)forestation and dry season flow in the tropics: a closer look. **Journal of Tropical Forest Science**, Kuala Lumpur, v. 1, n. 3, p. 229-243, 1988.

CAN, T. et al. Using SWAT model to assess impacts of different land use scenarios on water budget of Fuhe River , China. **International Journal of Agricultural and Biological Engineering**, Beijing, v. 8, n. 3, p. 1-15, 2015.

CHIANG, L. et al. Assessing SWAT's performance in the Kaskaskia River watershed as influenced by the number of calibration stations used. **Hydrological Processes**, Chichester, v. 687, p. 676-687, 2014.

CHOU, S. C. et al. Assessment of Climate Change over South America under RCP 4.5 and 8.5 Downscaling Scenarios. **American Journal of Climate Change**, Irvine, v. 3, n. 5, p. 512-525, 2014a.

CHOU, S. C. et al. Downscaling of South America present climate driven by 4-member HadCM3 runs. **Climate Dynamics**, Berlin, v. 38, n. 3/4, p. 635-653, 2011.

CHOU, S. C. et al. Downscaling of South America present climate driven by 4-Member HadCM3 Runs. **Climate Dynamics**, Berlin, v. 38, n. 3, p. 635-653, 2012.

CHOU, S. C. et al. Evaluation of the Eta Simulations Nested in Three Global Climate Models. **American Journal of Climate Change**, Irvine, v. 3, n. 5, p. 512-525, 2014b.

COLLINS, W. J. et al. Development and evaluation of an Earth-System model – HadGEM2. **Geoscientific Model Development**, Munich, v. 4, p. 1051–1075, 2011.

COLLISCHONN, W.; TUCCI, C. E. M. Ajuste multiobjetivo dos parâmetros de um modelo hidrológico. **Revista Brasileira de Recursos Hídricos**, Porto Alegre, v. 8, n. 3, p. 27-39, 2003.

COLLISCHONN, W.; TUCCI, C. E. M. Simulação hidrológica de grandes bacias. **Revista Brasileira de Recursos Hídricos**, Porto Alegre, v. 6, n. 2, 2001. Disponível em: <https:// www.abrh.org.br/SGCv3/index.php?PUB=1&ID=42&SUMARIO=625>. Acesso em: 22 dez. 2016.

CRAWFORD, M.; LINSLEY, R. **Digital simulation in hydrology:** Stanford watershed model IV. Stanford: Stanford University, 1966.

DAGGUPATI, P. et al. A recommended calibration and validation strateggy for hydrologic and water quality models. **Transactions of the ASABE**, St. Joseph, v. 58, n. 6, p. 1705-1719, 2015.

DE BARRY, P. A. **Watersheds:** process, assessment and management. Hoboken: J. Wiley and Sons, 2004. 700 p.

DURÃES, M. F. **Caracterização e avaliação do estresse hidrológico da bacia do rio Paraopeba, por meio de simulação chuva-vazão de cenários atuais e prospectivos de ocupação e uso do solo utilizando um modelo hidrológico distribuído**. 2010. 147 p. Dissertação (Mestrado em Saneamento, Meio Ambiente e Recursos Hídricos) - Universidade Federal de Minas Gerais, Belo Horizonte, 2010.

DURÃES, M. F.; MELLO, C. R.; NAGHETTINI, M. Applicability of the SWAT model for hydrologic simulation in Paraopeba river basin, MG. **Cerne**, Lavras, v. 17, n. 4, p. 481-488, 2011.

EMPRESA DE PESQUISA ENERGÉTICA. **Balanço energético nacional 2016:** relatório síntese - ano base 2015. Brasília: MME, 2016. Disponível em: <https://ben.epe.gov.br/

downloads/S%C3%ADntese%20do%20Relat%C3%B3rio%20Final_2016_Web.pdf>. Acesso em: 30 ago. 2016.

GASSMAN, P. W. et al. the soil and water assessment tool : historical development, applications, and future research directions. **Transactions of the ASAE**, St. Joseph, v. 50, n. 4, p. 1211–1250, 2007.

GEORGE, C.; JAMES, E. J. Simulation of streamflow using soil and water assessment tool (SWAT) in Meenachil river basin of Kerala, India. **Scholars Journal of Engineering and Technology**, Tangier, v. 1, n. 2, p. 68-77, 2013.

HAGUMA, D. et al. Optimal hydropower generation under climate change conditions for a Northern Water Resources System. **Water Resources Management**, Reidel, v. 28, n. 13, p. 4631-4644, 2014.

HARTMANN, H. C.; BALES, R.; SOROOSHIAN, S. **Weather, climate and hydrologic forecasting for the Southwest U.S.** Tucson: ISPE/CLIMA, 1999. 173 p.

HO, J. T.; THOMPSON, J. R.; BRIERLEY, C. Projections of hydrology in the Tocantins-Araguaia Basin, Brazil: uncertainty assessment using the CMIP5 ensemble. **Hydrological Sciences Journal,** Oxford, v. 61, n. 3, p. 1-17, 2016.

HUANG, S.; KRYSANOVA, V.; HATTERMANN, F. Projections of climate change impacts on floods and droughts in Germany using an ensemble of climate change scenarios. **Regional Environmental Change**, New York, v. 15, n. 3, p. 461–473, 2014.

INTERGOVERNMENTAL PANEL ON CLIMATE CHANGE. **Climate change 2013**: the physical science basis. Cambridge: Cambridge University, 2013. Disponível em: <http:// www.ipcc.ch/report/ar5/wg1/>. Acesso em: 8 fev. 2016.

INTERGOVERNMENTAL PANEL ON CLIMATE CHANGE. **Emissions scenarios for the IPCC**: an update. Cambridge: Cambridge University, 2007. Disponível em: <http://www. ipcc.ch/ipccreports/1992%20IPCC%20Supplement/IPCC_Suppl_Report_19

92_wg_I/ipcc_ wg_I_1992_suppl_report_section_a3.pdf>. Acesso em: 10 out. 2016.

INTERGOVERNMENTAL PANEL ON CLIMATE CHANGE. **Summary for policymakers, in climate change 2001:** the scientific basis. Cambridge: Cambridge University, 2001. Disponível em: <http://www.ipcc.ch/pub/reports.htm>. Acesso em: 15 out. 2016.

KENNEDY, J.; EBERHART, R. **Particle swarm optimization**. 1995. Disponível em: <http://ieeexplore.ieee.org/document/488968/?reload=true>. Acesso em: 15 dez. 2016

KUCZERA, G.; PARENT, E. Monte Carlo assessment of parameter uncertainty in conceptual catchment models: the Metropolis algorithm. **Journal of Hydrology**, Amsterdam, v. 211, n. 1-4, p. 69-85, 1998.

LEGATES, D. R.; MCCABE JÚNIOR, G. J. Evaluating the use of "goodness-of-fit" measures in hydrologic and hydroclimatic model validation. **Water Resources Research**, Ann Abor, v. 35, n. 1, p. 233-241, 1999.

LEHNER, B.; CZISCH, G.; VASSOLO, S. The impact of global change on the hydropower potential of Europe: a model-based analysis. **Energy Policy,** Surrey, v. 33, n. 7, p. 839-855, 2005.

LOBANOVA, A. et al. Impacts of changing climate on the hydrology and hydropower production of the Tagus River basin. **Hydrological Processes**, Chichester, 2016.

MAJONE, B. et al. Impact of climate change and water use policies on hydropower potential in the south-eastern Alpine region. **Science of the Total Environment**, Amsterdam, v. 543(B), p. 965-980, 2016.

MARENGO, J. A. et al. Development of regional future climate change scenarios in South America using the Eta CPTEC/HadCM3 climate change projections: climatology and regional analyses for the Amazon, São Francisco and the Paraná River basins. **Climate Dynamics**, Berlin, v. 38, n. 9-10, p. 1829-1848, 2011.

MARENGO, J. A. **Caracterização do clima no Século XX e cenários climáticos no Brasil e na América do Sul para o Século XXI derivados dos modelos globais de clima do IPCC.** Brasília: MMA, 2007. 184 p.

MARTIN, G. M. et al. The HadGEM2 family of Met Office Unified Model climate configurations. **Geoscientific Model Development**, Munich, v. 4, n. 3, p. 723–757, 2011.

MELLO, C. R. Development and application of a simple hydrologic model simulation for a Brazilian headwater basin. **Catena,** Amsterdam, v. 75, n. 3, p. 235-247, 2008.

MELLO, C. R.; SILVA, A. M. **Hidrologia:** princípios e aplicações em sistemas agrícolas. Lavras: UFLA, 2013. 455 p.

MINVILLE, M. et al. Adaptation to climate change in the management of a Canadian water-resources system exploited for hydropower. **Water Resources Management**, Reidel, v. 23, n. 14, p. 2965-2986, 2009.

MOHOR, G. S. et al. Exploratory analyses for the assessment of climate change impacts on the energy production in an Amazon run-of-river hydropower plant. **Journal of Hydrology**, Amsterdam, v. 4, p. 41-59, 2015.

MORIASI, D. N. et al. Model evaluation guidelines for systematic quantification of accuracy in watershed simulations. **Transactions of the ASABE**, St. Joseph, v. 50, n. 3, p. 885-900, 2007.

NASH, J. E.; SUTCLIFFE, J. V. River flow forecasting through conceptual models: a discussion of principles. **Journal of Hydrology**, Amsterdam, v. 10, p. 282-290, 1970.

NEITSCH, S. L. et al. **Soil and water assessment tool theoretical documentation**. Temple: Blackland Research Center, 2005.

OUYANG, F. et al. Impacts of climate change under CMIP5 RCP scenarios on streamflow in the Huangnizhuang catchment. **Stochastic Environmental Research and Risk Assessment,** Berlin, v. 29, n. 7, p. 1781–1795, 2015.

PERAZZOLI, M.; PINHEIRO, A.; KAUFMANN, V. Efeitos de cenários de uso do solo sobre o regime hidríco e produção de sedimentos na bacia do ribeirão Concórdia - SC. **Revista Árvore**, Viçosa, MG, v. 37, n. 5, p. 859-869, 2013.

PESQUERO, J. F. et al. Climate downscaling over South America for 1961–1970 using the Eta Model. **Theoretical and Applied Climatology,** Wien, v. 99, n. 1-2, p. 75–93, 2009.

PRUDHOMME, C.; DAVIES, H. Assessing uncertainties in climate change impact analyses on the river flow regimes in the UK. Part 2: future climate. **Climatic Change**, Dordrecht, v. 93, n. 1-2, p. 197-222, 2009.

RENNÓ, C. D. **Construção de um sistema de análise e simulação hidrológica: aplicação a bacias hidrográficas**. 2003. 148 p. Tese (Doutorado em Sensoriamento Remoto) – Instituto Nacional de Pesquisas Espaciais, São José dos Campos, 2003.

ROCKWOOD, D. Columbia Basin streamflow routing by computer. **Transactions of the ASCE**, New York, v. 126, n. 4, p. 32-45, 1961.

ROSSI, C. G. et al. Hydrologic evaluation of the lower Mekong river basin with the soil and water assessment tool model. **International Agricultural Engineering Journal**, Beijing, v. 18, n. 1-2, p. 1-13, 2009.

SCHAEFFER, R. et al. Energy sector vulnerability to climate change: a review. **Energy,** Oxford, v. 38, 1, p. 1-12, 2012.

SCHERER, R.; PIKE, R. G. **Management activities on streamflow in the Okanagam Basin**: outcomes of a literature review and a workshop. British Columbia: Forrex, 2003. 46 p.

SLOAN, P. G.; MOORE, I. D. Modeling subsurface stormflow on steeply sloping forested watersheds. **Water Resources Research**, Ann Abor, v. 20, n. 12, p. 1815-1822, 1984.

SHAW, E. M. **Hydrology in practice**. 3rd ed. London: Chapman and Hall, 2004. 569 p.

SOROOSHIAN, S. et al. **Hydrological modelling and the water cycle**. Springer: Heidelberg, 2008. 291 p.

TSHIMANGA, R. M.; HUGHES, D. A. Climate change and impacts on the hydrology of the Congo Basin: the case of the northern sub-basins of the Oubangui and Sangha Rivers. **Physics and Chemistry of the Earth,** Oxford, v. 50/52, p. 72-83, 2012.

TUCCI, C. E. M. **Hidrologia**: ciência e aplicação. 4. ed. Porto Alegre: UFRGS/ABRH, 2007. 943 p.

TUCCI, C. E. M. **Modelos hidrológicos**. 2. ed. Porto Alegre: UFRGS/ABRH, 2005. 678 p.

TUNDISI, J. G. **Água no século XXI**: enfrentando a escassez. São Carlos: RiMa, 2003. 248 p.

VAN GRIENSVEN, A.; BAUWENS, W. Multi-objective auto-calibration for semi-distributed water quality models. **Water Resources Research**, Washington, v. 39, n. 12, p. 1348, Dec. 2003.

VAN VUUREN, D. P. et al. The representative concentration pathways: an overview. **Climatic Change**, Dordrecht, v. 109, n. 5, p. 5-31, 2011.

VEITH, T. L. et al. Parameter sensitivity and uncertainty in SWAT: a comparison across five USDA-ARS watersheds. **Transactions of the ASABE**, St. Joseph, v. 53, n. 5, p. 1477-1486, 2010.

VIOLA, M. R. et al. Applicability of the LASH Model for Hydrological Simulation of the Grande River Basin, Brazil. **Journal of Hydrologic Engineering**, Reston, v. 18, p. 1639-1652, 2013.

VIOLA, M. R. et al. Assessing climate change impacts on Upper Grande River Basin hydrology, Southeast Brazil. **International Journal of Climatology**, Chichester, v. 35, n. 6, p. 1054–1068, 2015.

VIOLA, M. R. et al. Impacts of Land-use Changes on the Hydrology of the Grande River Basin Headwaters, Southeastern Brazil. **Water Resources Management**, Reidel, v. 28, n. 13, p. 4537-4550, 2014.

VIOLA, M. R.; MELLO, C. R. Modelagem hidrológica na bacia hidrográfica do Rio Aiuruoca , Hydrologic modeling in the Aiuruoca river basin , Minas Gerais State. **Revista Brasileira de Engenharia Agrícola e Ambiental**, Campina Grande, v. 13, n. 5, p. 581-590, 2009.

VIOLA, M. R. **Simulação hidrológica na cabeceira da bacia hidrográfica do Rio Grande de cenários de usos do solo e mudanças climáticas A1B.** 2011. 287 p. Tese (Doutorado em Recursos Hídricos em Sistemas Agrícolas) – Universidade Federal de Lavras, Lavras, 2011.

WATANABE, M. et al. Improved climate simulation by MIROC5: mean states, variability, and climate sensitivity. **Journal of Climate,** Boston, v. 23, p. 6312-6335, 2010.

WIGMOSTA, M. S.; VAIL, L. W.; LETTENMAIER, D. P. A distributed hydrology-vegetation model for complex terrain. **Water Resources Research**, Washington, v. 30, n. 6, p. 1665-1679, 1994.

WINCHELL, M. et al. **ArcSWAT interface for SWAT2012:** user's guide. Temple: USDA/ARS, 2013.

XU, Y. et al. Impact of climate change on hydrology of upper reaches of Qiantang River Basin, East China. **Journal of Hydrology**, Amsterdam, v. 483, n. 1/2, p. 51-60, 2013.

YEN, H. et al. A framework for propagation of uncertainty contributed by parameterization, input data , model structure , and calibration / validation data in watershed modeling. **Environmental Modelling & Software**, Oxford, v. 54, n. 1, p. 211-221, 2014.

SEGUNDA PARTE - ARTIGOS

ARTIGO 1 – HYDROLOGICAL IMPACTS FROM LAND-USE CHANGE SCENARIOS IN THE UPPER GRANDE RIVER BASIN, BRAZIL

Artigo submetido ao periódico Environmental Modeling and Assessment – ISSN: 1573-2967, sendo apresentado segundo normas de publicação do mesmo.

[1]*Vinícius Augusto de Oliveira, [1]Carlos Rogério de Mello, [1]Marcelo Ribeiro Viola, [2]Raghavan Srinivasan

[1] Department of Engineering, Federal University of Lavras, 37200-000, Lavras, MG, Brazil

[2] Department of Ecosystem Science and Management, Texas A&M University, 77840, College Station, TX, United States of America

ABSTRACT: Land-use changes are considered one of the most important factors that affect the water resources. The objective of this study was to investigate the potential impacts of land-use changes on the hydrological behavior of the Upper Grande River Basin, southern Minas Gerais state, Brazil, based on different land-use scenarios using SWAT model. For this purpose, five land-use scenarios were developed following official environmental planning reports: S_1 and S_2 – conversion of forest into pasture of 20 and 50%, respectively; S_3 and S_4 – conversion of pasture into forest of 20 and 50%, respectively; and S_5 – conversion of pasture into croplands of 20%. The results have showed that, in general, the deforestation scenarios (S_1 and S_2) presented an increase in runoff and in surface runoff, whereas the reforestation scenarios (S_3 and S_4) have showed the opposite. Impacts from crop plantation scenario (S_5) indicate increase in both runoff and surface runoff. These results show that the land-use changes can generate positive impacts, such as reduction of surface runoff and increase in the baseflow, as well as negative ones, like increase in soil erosion and flood risks.

KEYWORDS: Hydrological modeling, SWAT model, Land-use changes, deforestation

1. INTRODUCTION

Brazil is strongly dependent of the surface water resources for economy and, therefore, very susceptible to the weather variability and changes in the hydrological behavior. The country relies in its water resources to generate electric energy, where almost 78% of all energy is produced by hydropower plants [15]. Also, its demographic and socioeconomic development has led to a strong and growing demand for the production of food, fiber, wood, and raw material needed for various uses [39].

The Grande River Basin is one of the most important Brazilian hydrologic regions regarding water availability and electric energy production. Its headwater region is located in the southern Minas Gerais state, in which three large reservoirs are installed. Thus, streamflow yields in this region is extremely important, since it directly supplies three hydropower plants reservoirs (Camargos, Itutinga and Funil) and plays an important role for hydrology regulating for other downstream reservoirs, highlighting Furnas hydropower plant [40].

Land-use, hydrology and hydropower facilities are directly linked. Land-use changes have been considered one of the most important factors that affect water budget within a given watershed. It is well-established that a

change of land-use may lead to changes in water balance components, which can cause both positive and negative impacts [9, 10].

In general, a reduction in forested areas trends to increase the runoff, and, due to a reduction in the soil-water infiltration capacity, an increase in the surface runoff is expected, which can accelerate the erosive processes, reducing the water availability and affecting the water quality [4, 9, 11, 13]. In addition, it can be inferred that the negative impacts over urban areas by flooding and landslide can change the landscape and increase the risks for the human beings.

On the other hand, the grassland shift into forest contributes with a reduction of the surface runoff due to increase of both infiltration rates and soil-water holding capacity due to increase of organic matter and preferential flows formed in the soil profile [32]. Consequently, a reduction of soil water erosion and sediment load transportation is expected as well as a reduction of floods risks and water shortages. Also, an increase of forested areas reduces the runoff, mainly due to an increase in water consumption by the trees and decrease in the peak flows events over the hydrological year [10, 13, 39].

Hence, understanding and interpreting the mechanisms between land-use and hydrology are essential to improve both water and land-use management. In this regard, paired catchment experiments have been used in studies such as [10] and [34]. Although it is considered a reliable method, experimental methods for the investigation of hydrological processes are generally expensive and time consuming. Therefore, assessing the impacts of land-use changes using hydrological models can be a reliable scientific alternative despite of the limitations and uncertainties of the models to represent the dynamic of the hydrological processes, especially the infiltration-runoff and groundwater recharge [24].

Hydrological models, such as the Soil and Water Assessment Tool (SWAT), have been successfully used for the assessment of land-use impacts on water quantity and quality in many studies worldwide such as [8, 26, 33, 35, 44], among others. Also, this assessment has been performed in some catchments in Brazil. [31] assessed the land-use change impacts on the streamflow of Galo creek watershed (943 km^2), in Espirito Santo state, southeast Brazil, in which three land-use scenarios were analyzed: the preservation scenario (C1), in which the entire permanent preservation areas of the region are forested; an optimistic scenario (C2), in which considers the watershed to be almost entirely covered by native vegetation; and a pessimistic scenario (C3), in which the

watershed would be almost entirely covered by pasture. The authors found that a mean reduction of 10 % of the native forest cover would cause a mean annual increase of approximately 11.5 mm in total runoff.

[30] used three different land-use change scenarios to analyze its impacts on the hydrology of the Pomba river basin, southeast Brazil. The authors considered a preservation scenario (S1) in which the entire permanent preservation areas of the region are forested, a reforestation scenario (S2), in which 10% of pastures were converted into eucalyptus plantation and an agricultural expansion scenario (S3), in which 10% of pastures were converted in perennial and annual crops. The results showed a mean annual reduction in runoff from 13.6, 4.0, and 6.5 mm for scenarios S1, S2, and S3, respectively.

[33] compared the original land-use of Pará river basin (12,300 km^2), located in Minas Gerais state, with the current land-use. Originally, the basin was predominantly occupied by Atlantic forests and Cerrado biome, while in the current scenario 50% of the Atlantic Forest and 25% of the Cerrado biome are replaced by land-uses such as pasture, eucalyptus plantation and perennial crops. The authors found that the conversion of the native vegetation to the previously cited land-uses promoted an increase of 10% on streamflow of the Pará river basin.

However, the uncertainties related to model structure, parameterization and land-use scenarios are rarely presented and/or discussed in any of the studies cited above. Thus, the objective of this research was to assess the potential impacts of land-use changes on the hydrological behavior of the Grande River Basin headwaters under different land-use scenarios using SWAT, providing information to enhance water planning and management in this basin as it is one of the most important Brazilian hydrologic region regarding hydroelectricity production. Also, important insights on data, model uncertainties and parameterization are discussed.

2. MATERIAL AND METHODS

2.1 Study area

The assessment of impacts of land-use on hydrology was conducted in the southern Minas Gerais state, Brazil. The basin was delineated from Macaia gauge station, in the Grande River Basin headwaters, located at the latitude 21° 8’ 41” S and the longitude 44° 54’ 50” W, presenting a drainage area of 15409.2 km^2. The elevation

within the basin varies from 752 to 2644 m. The location of the Grande River Basin delimited from Macaia gauge station (GRB-M) is shown in Fig. 1.

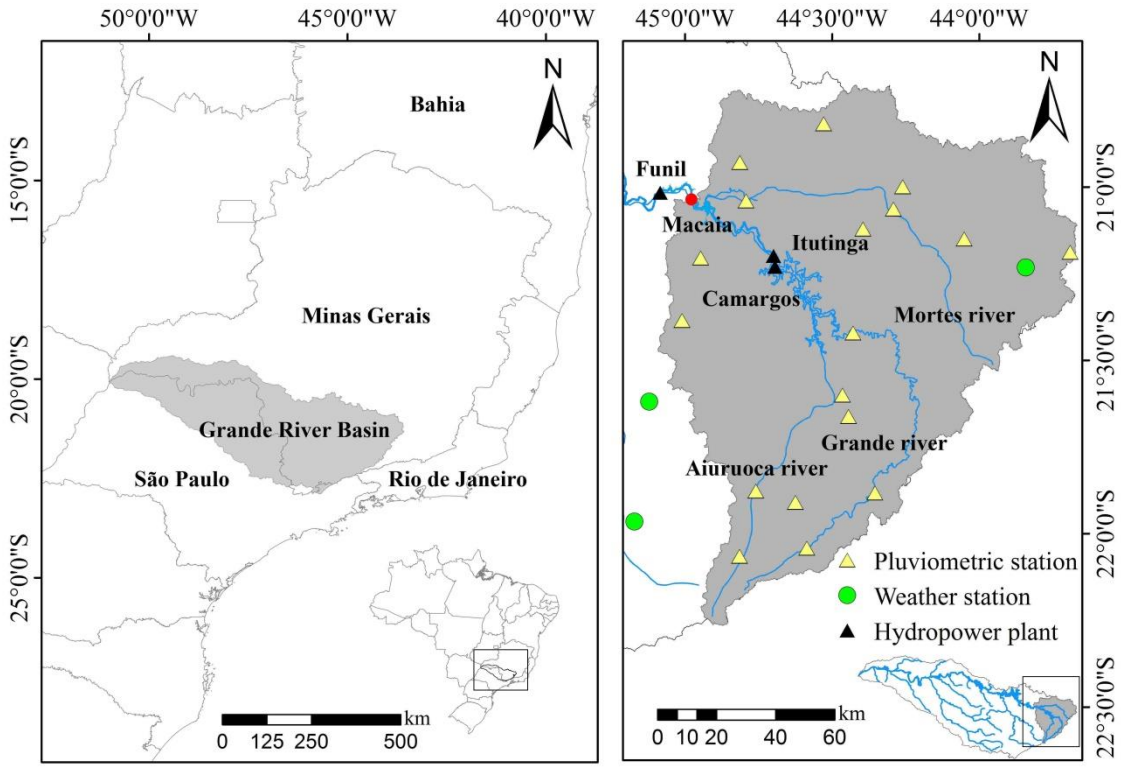

Fig. 1 Geographical location of the Grande River Basin in Brazilian territory and the Upper Grande River Basin (GRB-M)

The topography of the basin is undulated, with 57.2% of the area presenting slopes greater than 15%. Mean annual temperature of the region is about 19 ºC with minimum and maximum temperatures varying from 2°C to 34ºC. The climate of the region is classified as Cwa and Cwb. The former is predominant in most of the basin, and the latter in the south/southeast of the basin where is located the Mantiqueira Range, which strongly influences the temperatures and the amount of precipitation in its neighboring areas. These climate types present two seasons well characterized by mild and rainy summers and cool and dry winters. The mean annual rainfall is about 1500 mm, which varies from 1100 mm to 2100 mm [23, 29, 40].

2.2 SWAT inputs requirements and database

Daily maximum and minimum temperatures, solar radiation, relative humidity and wind speed were obtained from weather stations of the Brazilian National Institute of Meteorology (INMET) for Lavras, São Lourenço and Barbacena (Fig. 1). In addition, daily rainfall (16 gauges) and streamflow data series were obtained from the Brazilian National Water Agency (ANA-Hidroweb). Meteorological data sets were both obtained on a daily basis from 1992 to 2001 from which five years were used for calibration (1994-1998) and three years for validation (1999-2001). The period from 1992 to 1993 was used as a warm-up period, as recommended by [14].

The Aster Digital Elevation Model (DEM), with spatial resolution of 30 m, was used to process the topographical procedures such as generation of the drainage network and the delineation of the sub-basins of the GRB-M. The current land-use and soil maps are illustrated in figures 2a and 2b, respectively. Current land-use map was derived from Landsat 8 images from 2013 with the aid of supervised classification through the maximum likelihood classifier. Pasture is the predominant land-use, followed by forests and agriculture, covering 70.6%, 15.8% and 10.4% of the area, respectively.

The soil map was obtained from the Minas Gerais State Environmental Foundation [16] in a scale of 1:650,000. The soil types present within the GRB-M are Latosol (Oxisol), Argisol, Cambisol, Fluvic Neosol and Litholic Neosol with predominance of Cambisols (47.9%) followed by Latosols (32.6%), Litholic Neosols (9.53%), Argisols (9.2%) and Fluvic Neosols (0.7%).

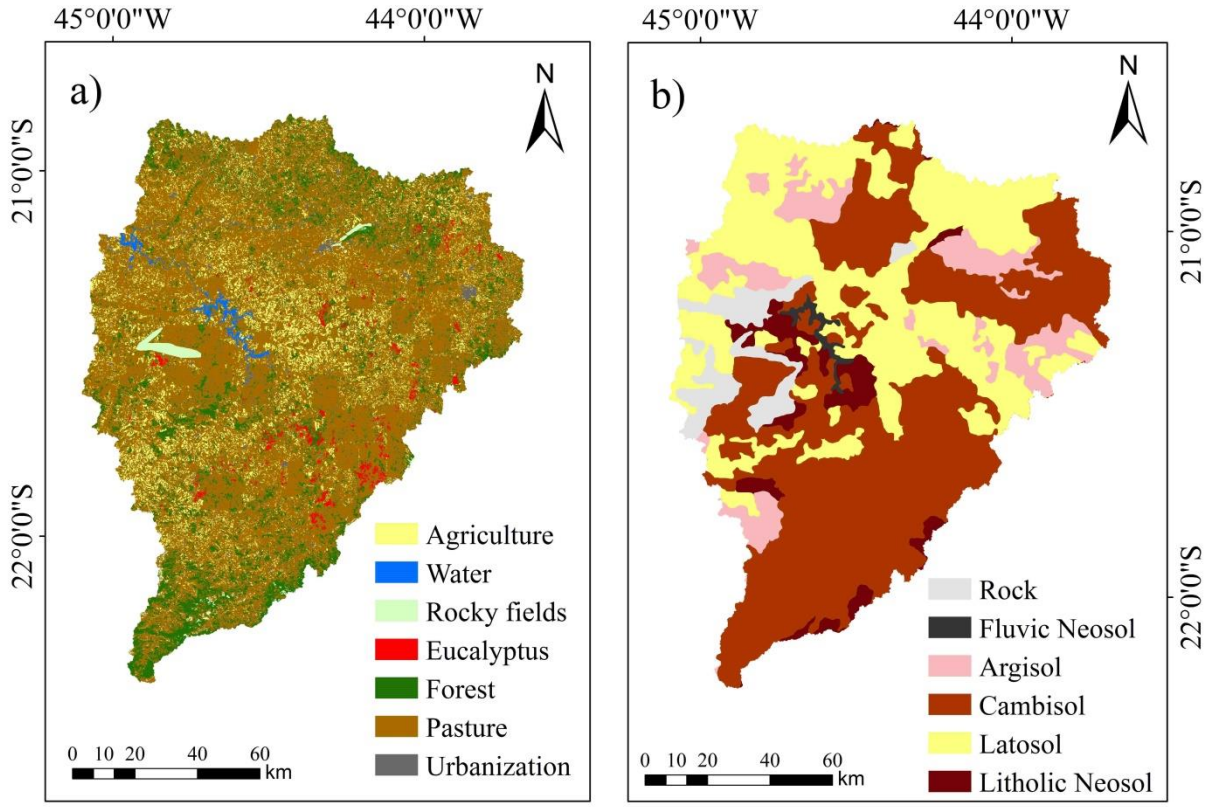

Fig. 2 Current land-use (a) and soil (b) maps of GRB-M

2.3 The SWAT model

The Soil and Water Assessment Tool (SWAT) is a large-scale model which was developed to predict the impact of land-use and management practices on water, sediment and agricultural chemical generated in large complex watersheds, land-use and management conditions over long periods of time [28]. It is a continuous-time, long-term, distributed-parameter, physically based hydrological model that divides the watershed into sub-basins connected by a stream network. Each sub-basin is further delineated into hydrological response units (HRUs) which consist of a unique combination of land cover, slope and soil type and are non-spatially distributed [6, 36].

SWAT simulations are based on water balance and are achieved through hydrological routines that calculate the water cycle components such as surface and subsurface flows, evapotranspiration, infiltration, percolation and soil moisture. Equation 1 describes the water balance adopted by the SWAT model.

$$SW_t = SW_0 + \sum_{i=1}^{t}\left(P_{day} - Q_{surf} - E_a - w_{seep} - Q_{gw}\right) \quad (1)$$

Where SW_t is the final soil water content (mm), SW_0 is the initial soil water content on day i (mm), t is the time (days), P_{day} is the amount of precipitation on day i (mm H_2O), Q_{surf} is the amount of surface runoff on day i (mm), E_a is the amount of evapotranspiration on day i (mm), w_{seep} is the amount of water entering the vadose zone from the soil profile on day i (mm), and Q_{gw} is the base flow on day i (mm).

The model requires topography, soil, land-use and weather data as input to estimate the runoff, surface and subsurface flows, base flow, sediment, and nutrient and pesticides loadings carried out the watershed's outlet. For this study, only the components regarding the runoff process will be analyzed. A detailed description of the SWAT model is given by [6, 28, 37].

2.4 Calibration, validation and model performance evaluation

The calibration and uncertainty analyses for SWAT are carried out in SWAT-CUP, which is a stand-alone program that links to SWAT's output text file sets and integrates different optimization algorithms. Among them, the Sequential Uncertainty Fitting (SUFI-2) algorithm stands out due to its capability to account for all sources of uncertainty on the parameter ranges such as uncertainty in driving variables (e.g., rainfall), conceptual model, parameters, and measured data [2].

This algorithm seeks to capture most of the measured data within the 95% prediction uncertainty (95PPU) calculated at the 2.5% and 97.5% levels of the cumulative distribution of an output variable obtained through Latin hypercube sampling. The degree in which all uncertainties are accounted for is quantified by a measure referred as p-factor, which is the percentage of measured data bracketed by the 95% prediction uncertainty band (95PPU). Yet, another statistic to account the uncertainties is the r-factor, which corresponds to the average thickness of the 95PPU band divided by the standard deviation of the measured data. For streamflow, simulations with good prediction of uncertainties are those with p-factor greater than 0.7 (> 70%) and r-factor around 1 [1, 2].

Automatic calibration through SUFI-2 was performed using daily streamflow time series from Macaia gauge station, at Grande River, for the period from 1994 to 1998, with a warm-up period from 1992 to 1993. The validation was performed updating the SWAT previously calibrated for the period from 1999 to 2001.

To evaluate the goodness of fit of the calibration and validation periods, the Nash-Sutcliffe Efficiency (NSE) [27] and the percent bias (PBIAS) were applied and are represented as follows:

$$NSE = 1 - \left[\frac{\sum_{i=1}^{n} (Q_{obs_i} - Q_{sim_i})^2}{\sum_{i=1}^{n} (Q_{obs_i} - Q_{mean_i})^2} \right] \quad (2)$$

$$PBIAS = \left[\frac{\sum_{i=1}^{n} (Q_{obs_i} - Q_{sim_i})}{\sum_{i=1}^{n} (Q_{obs_i})} \right] \times 100 \quad (3)$$

Where, Q_{obs}, Q_{sim} and Q_{mean} are the observed, simulated and mean streamflow, respectively.

Regarding NSE, this study adopted the recommendation proposed by [17], who suggest that simulations with NSE equal or greater than 0.4 are qualified as "satisfactory" considering the daily time step. The model performance regarding PBIAS was evaluated based on the recommendations of [38] for simulations on a daily time step: |PBIAS|< 10% as "very good"; 10% < |PBIAS| < 15% as "good"; 15% < |PBIAS| < 25% as "fair"; and |PBIAS| > 25% as "unsatisfactory".

2.5 Land-use scenarios

This study investigated the impacts of land-use changes given by the interactions through five different scenarios. These scenarios were developed based on directives suggested by environmental agencies responsible for the water resources management in Minas Gerais state. These directives aim to provide management practices for a sustainable use of the natural resources considering the current and future socioeconomic features and environmental conditions of the region.

For this purpose, results and analyses published in studies like the Forest Inventory of Minas Gerais state [12], the Ecological-Economic Zoning of Minas Gerais State [22] and the Water Resources Directives of the Upper Grande River Basin [18] were taken into account. This methodology was previously adopted by [39] assessing the

impacts of land-use changes on hydrology in four sub-basins of GRB headwaters, and by [7] for another watershed that drains directly to Camargos Hydropower Plant Reservoir.

According to the assessment performed by [12], the deforestation of the native vegetation within GRB-M has increased. This assessment suggests a deforestation rate of about 0.024% per year between 2005 and 2007. Corroborating this study, [19] states that the Upper Grande River Basin is expected to suffer alterations in the land-use/land cover and soil management, which will lead to a reduction on soil-water infiltration rates, and, consequently, reducing the groundwater recharge potential.

Southern Minas Gerais is traditionally recognized for its dairy production and, therefore, grazing is a frequent activity. According to [39], this activity has been expanded towards the Mantiqueira Range region, converting the native vegetation into extensive pastures (with low protection of soil surface). This conversion reduces the effective root zone of the vegetation, and, therefore, reduces the infiltration rates and soil-water holding capacity (SWC). In addition, it reduces both rainfall interception by the canopy and the evapotranspiration. On the other hand, it increases the runoff and decreases the groundwater recharge and, consequently, the water availability. Thus, the interaction of these factors is a complex matter as all these effects need to be considered adequately by the hydrologic model. In this regard, two deforestation scenarios were considered: S_1 that considers 20% of the native vegetation in the entire basin was converted into pasture; and S_2 that considers 50%.

In addition to these scenarios, two others were structured motivated by ongoing government environmental programs such as the “Water Producer Program”, which provides a payment for ecological services and is headed by the Brazilian National Water Agency (ANA). This program aims to reduce the soil erosion and sediment deposition in the water bodies, providing better quality and increasing the quantity as well as natural flows regularization in the catchments mostly located in the Mantiqueira Range region by means of conservation practices, highlighting the reforestation of springs [5].

According to [20], this program has generated satisfactory results in watersheds within the municipality of Extrema, Minas Gerais state, being considered as a good strategy to ensure the practice of both sustainable agriculture and forest management that directly influence the conservation and the integrated management of water resources and forest. In this context, S_3 and S_4 scenarios considered the conversion of pastures into forests in the whole basin area by 20% and 50%, respectively.

At last, according to [19], the agricultural activities in this region is expected to be intensified in the next 30 years, thus, expanding the cropland areas and, consequently, increasing the water demand for irrigation. In this case, scenario S_5 was developed considering the conversion of pastures into cropland areas by 20%.

The land-use changes were performed through the SWAT module "Land-Use Update". The "Land-Use Update" automatically adjusts the fractions of HRUs updating the current use for the new use based on the percentage given by the modeler. Consequently, the vegetative parameters, like Leaf Area Index (LAI), aerodynamic and stomatal conductance and others related to evapotranspiration are automatically changed.

The impacts of the land-use changes on the basins' hydrology were quantified by comparing the simulations obtained from the land-use scenarios against the simulations obtained from the baseline (validation period). The calibrated parameters, meteorological data, soil map and landscape characteristics of the baseline simulation remained the same for the future scenarios to provide a consistent basis for comparison between the baseline and land-use change scenarios [11]. Also, according to [8] and [18], when assessing impacts of land-use scenarios, all scenarios for a watershed are subjected to the same input data uncertainty, therefore, it can be assumed that the relative differences in the results can be attributed to the applied scenario changes.

Table 1 summarizes the land-use scenarios presenting the new percentages of forests and agricultural areas after changes from the current scenario (baseline). The changes were made considering the entire area of each land-use class.

Table 1 Land-use changes scenarios considering the area and the percentages of forests (S_1, S_2, S_3 and S_4) and agriculture (S_5) in relation to the current land-use

Scenario	Description	Δ Area (km^2)	%	Total class área (km^2)	Δ %
S_1	20% - Deforestation	-486.9	12.6	1947.7	-3.1
S_2	50% - Deforestation	-1217.3	7.9	1217.3	-7.9
S_3	20% - Reforestation	2175.8	29.9	4610.5	14.1
S_4	50% - Reforestation	5439.4	51.1	7874.1	35.3
S_5	20% - Crop Plantation	2175.8	12.5	3525.7	22.9

3 RESULTS AND DISCUSSION

3.1 Model calibration and validation

The SWAT model was previously calibrated and validated before being applied to assess the impacts of land-use scenarios. To calibrate it to GRB-M on a daily time step, a set of 20 parameters regarding surface and subsurface runoff behavior were chosen. The range of the parameters, their description and their respective calibrated values are represented in Table 2.

Table 2 Parameters used to calibrate SWAT for GRB-M and their respective initial ranges and final calibrated values. The prefixes "v", "r" and "a" correspond to the operations "replace", "relative" and "add", respectively

Parameter	Parameter description	Initial range		Final value
		Min	Max	
v_ESCO	Soil evaporation compensation coefficient	0.5	0.95	0.812
r_CN2	Initial SCS runoff curve number for moisture condition II	-0.1	0.1	-0.011
v_ALPHA_BF	The baseflow recession constant	0.005	0.015	0.009
a_GW_DELAY (days)	Groundwater delay time	-30	60	-9.75
a_GWQMN (mm)	Threshold depth of water in the shallow aquifer required for return flow to occur	-1000	1000	906
v_CANMX (mm)	Maximum canopy storage	0	30	14.67
v_CH_K2 (mm h^{-1})	Effective hydraulic conductivity in main channel	0	10	8.849
v_CH_N2	Manning's "n" value for the main channel	-0.01	0.2	0.15
v_EPCO	Plant uptake compensation factor	0.01	1	0.951
v_GW_REVAP	Groundwater "revap" coefficient	0.02	0.2	0.043
a_REVAPMN (mm)	Threshold depth of water in the shallow aquifer for "revap" or percolation to the deep aquifer to occur	-1000	1000	610
r_SOL_AWC (mm mm^{-1})	Soil available water capacity	-0.05	0.05	-0.024

r_SOL_K (mm h^{-1})	Saturated hydraulic conductivity	-0.05	0.05	-0.029
v_SURLAG (days)	Surface runoff lag coefficient	0.01	24	1.713
v_CH_N1	Manning's "n" value for tributary channels	0.01	0.2	0.199
v_CH_K1 (mm h^{-1})	Effective hydraulic conductivity in tributary channels	0	5	1.705
v_SLSOIL (m)	Slope length for lateral subsurface flow	0	150	13.823
v_LAT_TTIME (days)	Lateral flow travel time	0	150	11.25
r_HRU_SLP (m/m)	Average slope steepness	-0.25	0.25	-0.093
r_SLSUBBSN	Average slope length	-0.25	0.25	0.142

The model performance statistics showed that SWAT was able to adequately predict the daily streamflow in GRB-M, presenting a NSE of 0.72 and PBIAS of 2% for the calibration period and 0.63 and 10%, respectively, for the validation period. Therefore, the results can be framed as “satisfactory” and “very good”, respectively, based on the recommendations previously described. In relation to the uncertainty prediction, the p-factor and r-factor were 0.93 and 1.01, respectively, for the calibration period, while in the validation, these results were 0.79 and 1.93, respectively, presenting greater degree of uncertainty during validation. The hydrographs of the simulated and observed streamflow are shown in Fig. 3.

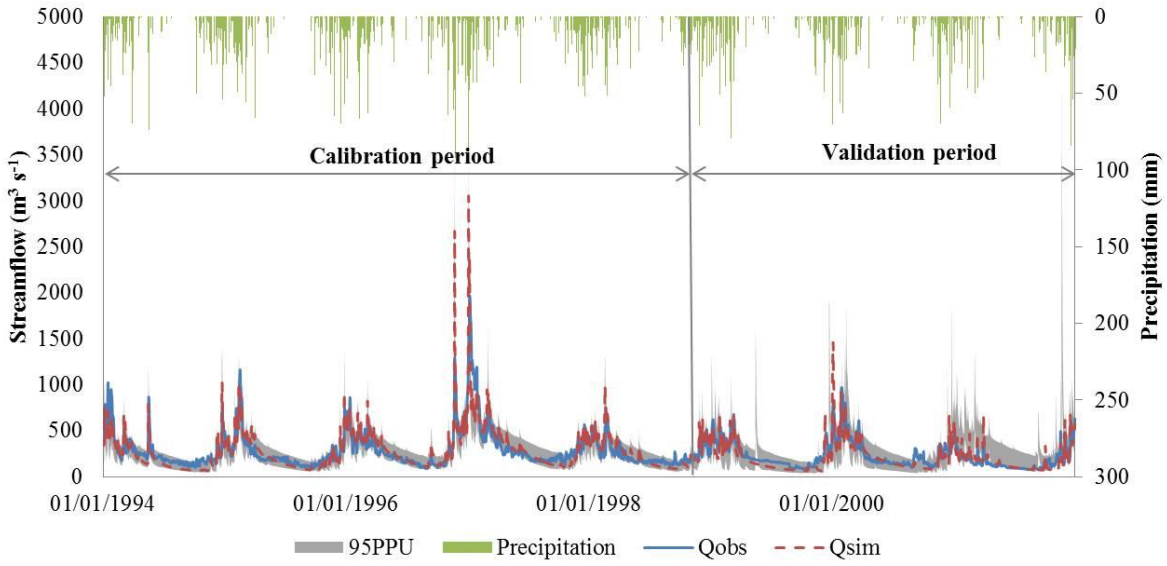

Fig. 3 Observed and simulated daily streamflow during the calibration and validation periods by SWAT and respective 95PPU band for GRB-M

Taking Fig. 3 as reference, it is possible to observe that both calibration and validation periods presented a good agreement with the observed data, especially for the prediction of the lowest flows. On the other hand, there was some slight overestimation on the peak flows, especially in the summer of 1996-1997.

According to [25], the NSE is very sensitive to extreme high flows, and, therefore, an overestimation of the peak flows can influence the NSE statistics. PBIAS statistic measures the average bias of the simulated data, thus, positive values indicate underestimation and negative values, overestimation of the observed data. The results showed that the simulated streamflow has presented the same trend for both calibration and validation periods, with a slight better performance during calibration.

3.2 Impacts of projected land-use change scenarios on the hydrology of GRB-M

In order to assess the impacts of land-use changes on hydrology, the average streamflow data set was divided into summer and winter seasonal flows. This assessment is essential since it indicates the variations of the streamflow during the winter and summer periods, when the low and peak flows, respectively, are pronounced.

Table 3 shows the variations on the mean summer and winter streamflows compared to the baseline (1999-2001). It also shows the mean observed streamflow for the period 1999-2001. The average summer streamflow was calculated for the period between December and March, whereas the winter ones were calculated from June to September.

Table 3 Annual mean, summer and winter mean streamflow variations caused by the land-use scenarios in relation to the baseline, considering the 1999-2001 period

Streamflow	Observation	$Q_{baseline}$	S_1	S_2	S_3	S_4	S_5
($m^3 s^{-1}$)	($m^3 s^{-1}$)	($m^3 s^{-1}$)	ΔQ ($m^3 s^{-1}$)				
Q_{mean}	220.8	198.4	0.5	1.2	-1.7	-3.9	3.2
Q_{summer}	293.8	264.2	1.5	3.9	-5.5	-12.1	10.4
Q_{winter}	148	133	-0.2	-0.6	0.5	1.8	-0.5
Q_{max}	757.1	938.3	1.6	1.9	-4.1	-11.4	69.4
Q_{min}	88.1	69	-0.02	-0.1	-0.12	0.13	-0.22

The results showed that the mean streamflow increased under the deforestation scenarios of 0.5 and 1.2 $m^3 s^{-1}$ for S_1 and S_2, respectively, and decreased in the reforestation scenarios of -1.7 and -3.9 $m^3 s^{-1}$ for S_3 and S_4, respectively. The S_5 showed an increase in the mean streamflow of 3.2 $m^3 s^{-1}$, which might be a response to an increase in the surface runoff.

For the deforestation scenarios, the results show a reduction of the mean winter flows of -0.2 and -0.6 $m^3 s^{-1}$ for S_1 and S_2, respectively, and an increase in the mean summer flows of 1.5 and 3.9 $m^3 s^{-1}$. These results indicate a reduction in the low flows during the winter and an increase of the peak flows during the summer, which is corroborated by the increase in the maximum streamflow of 1.6 and 1.9 $m^3 s^{-1}$ for S_1 and S_2 scenarios, respectively.

In general, the removal of the native vegetation leads to an increase in the peak flows. When forests are removed, the infiltration and SWC are both reduced, which leads to an increase in the surface runoff, and therefore, increasing the peak flows and the total runoff, as properly stated by [10].

The reforestation would increase the mean winter flows of 0.5 and 1.8 $m^3 s^{-1}$ for S_3 and S_4 scenarios, respectively, thus, indicating increases of the low flows and in the ground water recharge. On the other hand, reductions of the summer flows of -5.5 and -12.1 $m^3 s^{-1}$ and in the maximum streamflows of -4.1 and -11.4 $m^3 s^{-1}$, were also observed, respectively, indicating an attenuation of the peak flows from December to March.

The reforestation of grasslands leads to a regulation of the low flows and a reduction of the peak flows, since it increases the infiltration capacity and the effective root zone, thus, increasing SWC. It also increases the rainfall interception and the evapotranspiration due to an increase of the land cover area. In addition, the soil erosion risks are reduced, since the reforestation provides protection for the soil.

The impact on streamflow due to an increase on cropland is represented by S_5 scenario. The summer flows and the maximum streamflow showed an increase of 10.4 and 69.4 $m^3 s^{-1}$, respectively, whereas the winter flows showed a reduction of -0.5 $m^3 s^{-1}$. In general, the conversion of grasslands into croplands increases the SWC due to an increase in the effective root zone. However, an increase on the surface runoff is expected since the vegetation cover is reduced, especially in croplands under standard tillage systems [10].

Table 4 shows the deviations of the mean annual runoff (R), baseflow (BF), surface runoff (SR), evapotranspiration (ET) and precipitation (P) and the hydrological indicators (BF/R; SR/R) under land-use scenarios in relation to the baseline.

Table 4 Hydrological indicators and water balance components and their deviation from the baseline simulation

Components	Observed	Baseline	S_1	S_2	S_3	S_4	S_5
	(mm)	(mm)	Δ (mm)				
R	428.7	403.9	1.4	1.9	-0.9	-2.8	5.1
BF	324.6	279	-0.6	-4.6	4.3	6.9	1.7
BF/R	0.76	0.69	0.69	0.68	0.7	0.71	0.69
SR	104.1	124.9	1.9	7	-5.2	-9.7	3.4
SR/R	0.24	0.31	0.31	0.32	0.30	0.29	0.31
ET	-	763.4	-1.1	-2.9	4.5	11.3	-3.8

P	1402.1	-	-	-	-	-	-

The signal of the water balance results of the simulated scenarios show an agreement with experimental and simulation results presented by [8, 10, 11, 13, 34, 39], among others. However, as discussed by [30], with respect to the changes in water quantity there has been no consensus. It is noted an increase in the mean annual runoff under the deforestation scenarios S_1 and S_2 of 1.4 and 1.9 mm, respectively. These scenarios also showed a decrease in the base flow of -0.6 and -4.6 mm and an increase in the surface runoff of 1.9 and 7 mm, respectively, corroborating with the assumptions previously discussed.

Alternatively, regarding the reforestation scenarios, the water balance shows the same behavior as the one assessed previously. These scenarios indicate an increase in the baseflow of 4.3 and 6.9 mm and a decrease in the runoff of -0.9 and -2.8 mm for S_3 and S_4, respectively. However, the results obtained in this study with respect to the annual runoff were below the ones cited above, which report that an increase of 10% in forested areas may lead to a decrease in the annual runoff of 10 mm. The contribution of the baseflow in relation to the runoff would increase from 69%, under baseline conditions, to 71 and 72% under S_3 and S_4, respectively. Beyond this, these scenarios showed a reduction of the surface runoff of -5.2 and -9.7 mm, respectively, for S_3 and S_4.

This finding can be explained by an increase in the effective root zone, since forests have deeper roots than grasslands, which leads to an increase of SWC, therefore decreasing the surface runoff. Furthermore, the water consumption by the trees increases, which also contributes for this reduction. This situation generates a positive impact over the region by increasing the ground water contribution and attenuating the peak flows, making the basin more capable to sustain the baseflow due to greater capacity for natural regularization of the streamflows.

In accordance with the assessments presented in Table 3, the simulation under S_5 scenario showed an expected behavior regarding the groundwater and surface runoff contributions. These results show an increase on the baseflow and surface runoff of 1.7 and 3.4 mm, respectively.

Similar to the results based on the simulations of S_1 and S_2 scenarios, the S_5 scenario would generate a negative impact within the GRB-M, increasing flood risks and soil erosion. On the other hand, the expansion of agriculture would have positive impacts regarding food production, food security and socioeconomic development in the regional scale.

3.3 Uncertainties and limitations of land-use change simulations

Given the model performance statistics in this study, SWAT could be successfully applied to investigate the impacts of land-use changes on the hydrology of GRB-M. However, uncertainties and limitations, on the data, model and scenarios should be considered.

According to [42], the main sources of uncertainties in this kind of simulations are associated with the model parameters related to approximations and from model structures. The uncertainties related to the first source were contemplated during the calibration period, which presented an acceptable performance.

The uncertainties in hydrological model structures are related to the assumption and simplifications. Regarding SWAT, the model uses a number of empirical and quasi-physical equations that were developed based on climate conditions in the U. S., such as the Curve Number Method (SCS-CN). Although the calibration and validation were successful, the application of this method in tropical climates, like in Brazil, might have some degree of uncertainty [21].

Also, there are uncertainties related to the land-use scenarios, which were built under simplifications and assumptions based on regional trends reported in directives made by environmental agencies without using land-use models that can project changes considering factors such as population growth, socioeconomic aspects, land-use policy, among others.

To illustrate these uncertainties, a comparison between this study and three others performed in the same region was carried out. The trends on the variations of the runoff presented in this study are in accordance with [4, 7, 39]. [7] investigated the impacts of land-use changes on the hydrology of a small watershed (32 km^2) within the GRB-M using the LASH hydrological model. The authors compared the current scenario with two regional trends scenarios: conversion of pasture into eucalyptus plantation and conversion of eucalyptus into pasture. The authors found that the conversion of pastures to eucalyptus lead to a reduction of runoff varying from 36.72 to 43.09%, whereas the deforestation of eucalyptus lead to an increase of 1.16 to 4.97%.

Also using LASH, [39] assessed the land-use impacts on two headwaters of Upper Grande river basin considering five different scenarios: S_1, S_2 as conversion of pasture into eucalyptus by 30 and 70%, respectively; S_3 as conversion of pasture into eucalyptus in sub-basin where eucalyptus plantation is predominant; and S_4 and S_5 as

conversion of the native vegetation into pasture by 30 and 70%, respectively. The authors found an increase in runoff varying from 7.36 to 26.4%, for the deforestation scenarios, while decreases from 7.6 and 23.3% were observed in the reforestation scenarios. Regarding surface runoff, the authors found reductions from 12.9 and 27.1% for the reforestation scenarios and increases from 10.6 to 31.2% for the deforestation scenarios.

[4] investigated the land-use change impacts in a small watershed located in the Mantiqueira range (in GRB-M headwaters). The authors used the DHSVM hydrological model and four land-use scenarios: 100% of the area occupied by Atlantic Forest; 100% of the area occupied by pastures; conversion of existing Atlantic Forest to pasture above 1300 m of altitude; and conversion of existing Atlantic Forest to pasture below 1300 m of altitude. The authors found that the deforestation of the Atlantic Forest would increase the surface and total runoff by 33 and 22%, respectively, which generated an increase of 17 and 25% in the daily highest and lowest streamflows.

The present study presented an increase in runoff of just 0.35 and 0.47% and in surface runoff of 1.5 and 5.6% under S_1 and S_2 scenarios, respectively, and decreases in runoff of -0.22 and -0.69% and surface runoff of -4.2 and 7.8%, under S_3 and S_4 scenarios, respectively.

This difference can also be explained by the difference in scale between the three studies. [8] and [43] justified that behavior because of the compensating effects in complex watersheds with a variety of land-use types and impacts of land-use changes on hydrology are relatively small at large scales, while they are much more pronounced at smaller scales.

In a similar study, [30] assessed the land-use change impacts on streamflow of Pomba river basin (8,600 km^2) using three different scenarios. Two of which represented a shift in 10% of pastures into forest (S2) and 10% of pastures into crop plantation (S3). The authors found a reduction on the annual runoff of 4 mm under the reforestation scenario (S2), while in the present study the reforestation scenarios S_3 and S_4 presented reductions of 0.9 and -2.8 mm, respectively. Considering the agricultural expansion scenario, this study showed an increase in the annual runoff of 5.1 mm, while [Pereira et al. 2016] found a reduction of 6.5 mm, although [Bruizinjeeel] and [3] suggests that the conversion of pastures into agricultural areas may lead to an increase in the total runoff due to a reduction in the infiltration capacity.

To illustrate these scale differences, two small sub-basins were selected within GRB-M. The first one (SB1) is the smallest sub-basin with the highest percentage of forest, whereas the second one (SB2) is the smallest sub-

basin with the highest percentage of pasture. The location of the sub-basins is presented in Fig. 4. The deforestation scenarios were then compared to the baseline of SB1, while the reforestation scenarios were compared to the baseline of SB2.

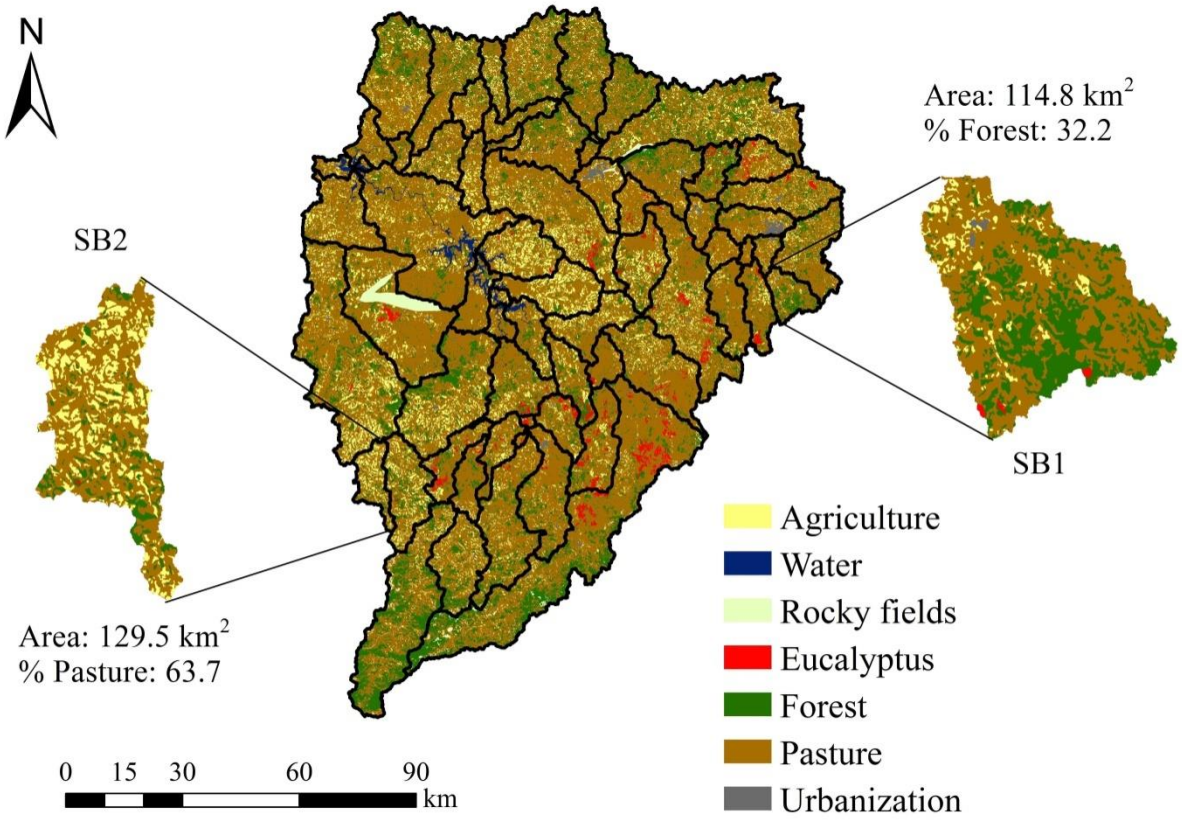

Fig. 4. Location, area and percentages of forest and pasture of SB1 and SB2

Table 5 presents the mean annual runoff, baseflow and surface runoff of SB1 and SB2.

Table 5 Mean annual runoff, baseflow and surface runoff simulated to SB1 and SB2. The values between parentheses represent the percent changes (%) of the water balance components of the land-use change scenarios in relation to the baseline.

Components	SB1	SB2

	Baseline (mm)	S_1 (Δ mm)	S_2 (Δ mm)	Baseline (mm)	S_3 (Δ mm)	S_4 (Δ mm)
R	568.5	9.4 (1.7)	13.1 (2.3)	494.7	-91.5 (-18.5)	-96.5 (-19.5)
BF	378.7	-3.7 (-0.98)	-19.1 (-5)	208.5	-75.9 (-36)	-50.1 (-24)
SR	189.8	13 (6.8)	32.2 (17)	286.2	-15.6 (-5.5)	-30.9 (-10.8)

According to the experimental results presented by [34], a reduction of 10% in deciduous forest may lead to an increase in runoff by 17-19 mm. In the present study, regarding the SB1, the deforestation scenarios (S_1 and S_2) showed an increase in runoff of 9.4 and 13.1 mm, which represents 1.7 and 2.3%, respectively. It also showed an increase in the surface runoff of 13 and 32.2 mm (6.8 and 17%). The ratio between the baseflow and runoff (BF/R) decreases from 67% to 65% and 62% for S_1 and S_2, respectively, whereas the ratio between surface runoff and runoff increased from 33% to 35 and 38%, respectively.

In SB2, it was obtained a decrease in runoff of -91.5 and -96.5 mm, representing a reduction of -18.5 and -19.5%, for S_3 and S_4, respectively. The surface runoff also decreases in -15.6 and -30.9 mm, which represents a reduction of -5.5 and -10.8%. These results related to changes in runoff converge with [39], which reported a decrease in the runoff from -7.57 and -17.63% under reforestation scenarios. Although it was expected an increase in the groundwater contribution, the hydrological behavior of SB2 showed otherwise, with a decrease from 36% under S_3. However, an increase of 40% in relation to S_3 was observed under S_4 scenario.

The differences between the magnitude of changes between SB1 and SB2 can be explained by the differences in location, soil, topography, weather and vegetation. The forest only contributes with 32.2% of the SB1 area, whereas the pasture contributes with 63.7%, being a predominant use in SB2. After deforestation of 20 and 50% in SB1, the forests cover only 25.8 and 19.2% of the area, respectively, while after reforestation of 20 and 50% in SB2, the pastures cover 51 and 38.2%, respectively. This might influence the magnitude of increases and decreases of the runoff in these sub-basins, since the contribution of pastures in SB2 is bigger than the contribution of forests in SB1.

In addition, 96.7% of the SB1 area presents Latosols and Argisols as soil type, which are deeper and present better infiltration, SWC and is more susceptible to preferential flows than Cambisols (Inceptsols), which covers only 3.3% of the area [41]. This characteristic of SB1 might attenuate the magnitude of increases in the runoff and surface

runoff. In SB2, 68.5% of the area is covered with deep soils (Latosols and Argisols) and 41.5% is covered with shallow soils (Cambisols and Litholic Neosols). Furthermore, the mean annual precipitation in SB1 region is about 1350 mm, whereas in SB2 is about 1600 during the simulated period.

4. CONCLUSIONS

According to the results presented in this research, SWAT model was able to predict adequately the hydrological processes in GRB-M, located at the upper Grande River Basin, in Minas Gerais state, southeast Brazil. Therefore, despite all uncertainties involved, SWAT was also able to reproduce the changes on streamflow based on different land-use scenarios. All statistics of model performance met the guidelines presented in hydrological modeling studies, enabling the daily time step simulations presented in this study to be classified as "satisfactory" and "very good".

The trends of changes on the streamflow simulations presented in this study are in agreement with a number of simulation and experimental results of hydrological impacts due to changes in land-use. In general, the deforestation scenarios (S_1 and S_2) would tend to present an increase in the runoff and decrease in the baseflow. Consequently, this condition lead to an increase in the maximum streamflows and in surface runoff, being a negative scenario in hydrological terms. These land-use scenarios might generate negative impacts within GRB-M not only in the hydrological cycle - reducing the water availability and increasing soil erosion and flood risks - but in socioeconomic development, given its importance in agricultural production and hydropower generation in the regional scale.

Regarding the reforestation scenarios (S_3 and S_4), the results showed a decrease in runoff and an increase in the baseflow, which lead to a decrease in the surface runoff. These results indicate an increase in water availability, maintaining the potential for groundwater recharge and the regularization of streamflow.

In addition, the conversion of pasture into croplands represented by the S_5 scenario indicates an increase in both runoff and surface runoff, which can generate both negative and positive impacts. The former would increase soil erosion and floods, whereas the latter would increase the agricultural production within GRB-M.

In general, these changes can be attributed mainly due to an increase or decrease in the effective root zone system combined with an increase or decrease of soil protection (i.e. land cover). At last, the results showed that the

interaction between the land-use and the hydrological cycle are complex and strongly correlated. Thus, development of methods linked to the reduction of uncertainties in hydrological simulations would enable a better understanding of land-use change impacts, providing a better support in water resources management.

5. REFERENCES

1. Abbaspour, K.C., Johnson, C.A., Van Genuchten, M.T. (2004). Estimating Uncertain Flow and Transport Parameters Using a Sequential Uncertainty Fitting Procedure. *Vadose Zone Journal*. 3(4), 1340–1352.
2. Abbaspour, K.C., Yang, J., Maximov, I., Siber, R., Bogner, K., Mieleitner, J., et al. (2007). Modelling hydrology and water quality in the pre-alpine/alpine Thur watershed using SWAT. *Journal of Hydrology*. 333(2-4), 413–430.
3. Aich, V., Liersch, S., Vetter, T., Fournet, S., Andersson, J.C.M, Calmanti, S., van Weert, F.H.A., Hattermann, F.F., Paton, E.N. (2016). Flood projections within the Niger River Basin under future land use and climate change. Science of the Total Environment, 562,666-677.
4. Alvarenga, L.A., Mello, C.R., Colombo, A., Cuartas, L.A., Bowling, L.C. (2016). Assessment of land cover change on the hydrology of a Brazilian head- water watershed using the Distributed Hydrology-Soil-Vegetation Model. *Catena*, 143, 7–17.
5. Agência Nacional de Águas (ANA). 2012. Programa produtor de água. http://produtordeagua.ana.gov.br/. Acessed 10 October 2016.
6. Arnold, J.G., Srinivasan, R., Muttiah, R.S., Williams, J.R. (1998). Large area hydrologic modeling and assessment part I: model development. *Journal of the American water Resources Association*, 34(1), 73–89.
7. Beskow, S.; Norton, L.D., Mello, C.R. (2013). Hydrological Prediction in a Tropical Watershed Dominated by Oxisols Using a Distributed Hydrological Model. *Water Resources Management*, 27(1), 341-363.
8. Bieger, K., Hörmann, G., Fohrer, N. (2015). The impact of land use change in the Xiangxi Catchment (China) on water balance and sediment transport. *Regional Environmental Change*, 15(3), 485–498.

9. Brown, A.E., Zhang, L., Mcmahon, T.A., Western, A.W., Vertessy, R.A. (2005). A review of paired catchment studies for determining changes in water yield resulting from alterations in vegetation. *Journal of Hydrology*, 310(1-4), 28–61.
10. Bruijnzeel, L.A. (1990). *Hydrology of moist tropical forests and effects of conversion: a state of knowledge review.* Amsterdam, The Netherlands: UNESCO.
11. Can, T., Xiaoling, C., Jianzhong, L., Gassman, P., Sabine, S., Pé, S. (2015). Using SWAT model to assess impacts of different land use scenarios on water budget of Fuhe River , China. *International Journal of Agricultural and Biological Engineering*, 8(3), 1–15.
12. Carvalho, L.M.T., Scolforo, J.R.S. (2008). Inventário Florestal de Minas Gerais - Monitoramento da Flora Nativa 2005–2007. Lavras, Brazil: Editora UFLA.
13. Carvalho-Santos, C., Nunes, J.P., Monteiro, A.T., Hein, L., Honrado, J.P., 2016. Assessing the effects of land cover and future climate conditions on the provision of hydrological services in a medium-sized watershed of Portugal. *Hydrological Processess*, 30(5), 720–738.
14. Daggupati, P., Pai, N., Ale, S., Douglas-Mankin, K R., Zeckoski, R W., Jeong, J. et al. (2016). A recommended calibration and validation strateggy for hydrologic and water quality models. *Transactions of ASABE*. 58(6), 1705-1719.
15. Empresa de Pesquisa Energética (EPE). (2016). Balanço Energético Nacional 2016: Relatório síntese - Ano base 2015. Ministério de Minas e Energia: Brasília, Brasil. https://ben.epe.gov.br/downloads/S%C3%ADntese%20do%20Relat%C3%B3rio%20Final_2016_Web.pdf. Acessed 30 August 2016.
16. Fernandes Filho, E.I., Curi, N. Mapa de solos do estado de Minas Gerais. (2010). Belo Horizonte, MG: Fundação Estadual Do Meio Ambiente (FEAM).
17. Green, C.H., Tomer, M.D., Luzio, M. Di, Arnold, J.G. (2006). Hydrologic evaluation of the Soil And Water Assessment Tool for a large tile-drained watershed in Iowa. *Transactions of ASABE*, 49(2), 413–422.
18. Hessel, R., Messing, I., Liding, C., Ritsema, C., Stolte, J. (2003). Soil erosion simulations of land use scenarios for a small Loess Plateau catchment. *Catena*, 54, 289–302.
19. Instituto Mineiro de Gestão das Águas/Consórcio ECOPLAN-LUME-SKILL (IGAM). (2012). *Plano*

Diretor de Recursos Hídricos e Enquadramento de Corpos de Água da Bacia Hidrografia do Alto Rio Grande. Belo Horizonte, Brazil: IGAM.

20. Jardim, M.H., Bursztyn, M.A. (2015). Pagamento por serviços ambientais na gestão de recursos hídricos : o caso de Extrema (MG). Engenharia Sanitária e Ambiental, 20(3), 353–360.
21. Khoi, D.N., Thom, V.T. (2015). Parameter uncertainty analysis for simulating streamflow in a river catchment of Vietnam. *Global Ecology and Conservation*, 4(2), 538-548.
22. Mello, C.R., Silva, A.M., Coelho, G.,Marques, J.J.G.S.M., Campos, C.M.M. (2008). Recursos Hídricos. In: Scolforo, J.R.S., Carvalho, L.M.T., Oliveira, A.D. (Eds.), *Zoneamento ecológico-econômico do Estado de Minas Gerais: componentes geofísicos e biótico*. pp. 103–135. Lavras: Editora UFLA.
23. Mello, C.R., Norton, L.D., Curi, N., Yanagi, S.N.M. (2012). Sea Surface Temperature (SST) and rainfall erosivity in the Upper Grande River Basin, Southeast Brazil. *Ciência & Agrotecnologia*, 36(1), 53–59.
24. Mello, C.R., Norton, L.D., Pinto, L.C., Beskow, S., Curi, N. (20116). Agricultural watershed modeling: a review for hydrology and soil erosion processes. *Ciência & Agrotecnologia*, 40(1), 7-25.
25. Moriasi, D.N., Arnold, J.G., Van Liew, M.W., Bingner, R.L., Harmel, R.D., Veith, T.L. (2007). Model evaluation guidelines for systematic quantification of accuracy in watershed simulations. *Transactions of ASABE*, 50(3), 885–900.
26. Mwangi, H.M., Julich, S., Patil, S.D., Mcdonald, M.A., Feger, K. (2016). Modelling the impact of agroforestry on hydrology of Mara River Basin in East Africa, Hydrological Processess, 30(18), 3139–3155.
27. Nash, J.E., Sutcliffe, J. V. (1970). River flow forecasting through conceptual models: a discussion of principles. *Journal of Hydrology*, 10(3), 282–290.
28. Neitsch, S.L., Arnold, J.G., Kiniry, J.R., Williams, J.R. (2005). *Soil and Water Assessment Tool theoretical documentation*. Temple, Texas.
29. Oliveira, V.A., Mello, C.R., Durães, M.F., Silva, A.M. (2014). Soil erosion vulnerability in the Verde River Basin, Southern Minas Gerais. *Ciência & Agrotecnologia*, 38(3), 262–269.
30. Pereira, D.R., Martinez, M.A., Silva, D.D., Pruski, F.F. (2016). Hydrological simulation in a basin of typical tropical climate and soil using the SWAT Model Part II : Simulation of hydrological variables and soil use

scenarios. *Journal of Hydrology: Regional Studies*, 5(1), 149-163.

31. Pereira, D.R., Almeida, A.Q., Martinez, M.A., Rosa, D.R.Q. (2014). Impacts of deforestation on water balance components of a watershedon the Brazilian east coast. *Revista Brasileira de Ciência do Solo*, 38(4), 1350-1358.
32. Pinto, L.C., Mello, C.R., Owens, P.R, Norton, L.D., Curi, N. (2015). Role of Inceptisols in the Hydrology of Mountainous Catchments in Southeastern Brazil. *Journal of Hydrologic Engineering*, 21(2), 05015017.
33. Rodrigues, E.L., Elmiro, M.A.T., Braga, F.D.A., Jacobi, C.M., Rossi, R.D. (2015). Impact of changes in land use in the flow of the Pará River Basin, MG. *Revista Brasileira de Engenharia Agrícola e Ambiental*, 19(1), 70–76.
34. Sahin, V., Hall, M.J. (1996). The effects o f afforestation and deforestation on water yields. *Journal of Hydrology*, 178(1-4), 293–309.
35. Serpa, D., Nunes, J.P., Santos, J., Sampaio, E., Jacinto, R., Veiga, S.et al. (2015). Impacts of climate and land use changes on the hydrological and erosion processes of two contrasting Mediterranean catchments. *Science of the Total Environment*. 538(1), 64–77.
36. Srinivasan, R., Zhang, Z., Arnold, J.G. (2010). SWAT ungauged: hydrological budget and crop yield predictions in the upper Mississippi river basin. *Transactions of ASABE*, 53(5), 1533–1546.
37. Srinivasan, R., Ranabarayanan, T. S., Arnold, J.G., Bednarz, S. T. (1998). Large area hydrologic modeling and assessment part II: Model application. *Journal of the American Water Resources Association*, 34(1), 91-101.
38. Van Liew, M.W., Veith, T.L., Bosch, D.D., Arnold, J.G. (2007). Suitability of SWAT for the Conservation Effects Assessment Project : Comparison on USDA Agricultural Research Service Watersheds Project : Comparison on USDA Agricultural Research. *Journal of Hydrological Engineering*, 12(2), 173–189.
39. Viola, M.R., Mello, C.R., Beskow, S., Norton, L.D. (2014). Impacts of Land-use Changes on the Hydrology of the Grande River Basin Headwaters, Southeastern Brazil. *Water Resources Management*, 28(13), 4537–4550.
40. Viola, M.R., Mello, C.R. De, Beskow, S., Norton, L.D. (2013). Applicability of the LASH Model for Hydrological Simulation of the Grande River Basin , Brazil. *Journal of Hydrological Engineering*, 18(12),

1639–1652.

41. Wiekenkamp, I., Huisman, J.A., Bogena, H.R, Lin, H.S., Vereecken, H. (2016). Spatial and temporal occurrence of preferential flow in a forested headwater catchment, *Journal of Hydrology*, 534(1), 139-149.
42. Xue, C., Chen, B., Wu, H. (2014). Parameter uncertainty analysis of surface flow and sediment yield in the Huolin Basin, China. *Journal of Hydrological Engineering*, 19(6), 1224–1236.
43. Ye, L., Cai, Q., Liu, R., Cao, M. (2009). The influence of topography and land use on water quality of Xiangxi River in Three Gorges Reservoir region. *Environmental Geology*, 58(5), 937–942.
44. Zhao, A., Zhu, X., Liu, X., Pan, Y., Zuo, D. (2016). Impacts of land use change and climate variability on green and blue water resources in the Weihe River Basin of northwest China, *Catena*, 137(1), 318-327.

ARTIGO 2 – ASSESSMENT OF THE IMPACTS OF CLIMATE CHANGE ON STREAMFLOW AND HYDROPOWER POTENTIAL IN THE HEADWATER REGION OF THE GRANDE RIVER BASIN, SOUTHEASTERN BRAZIL

Artigo submetido ao periódico International Journal of Climatology – ISSN: 1097-0088, sendo apresentado segundo normas de publicação do mesmo

[1]Vinícius Augusto de Oliveira, [1]Carlos Rogério de Mello, [1]Marcelo Ribeiro Viola, [2]Raghavan Srinivasan

[1] Department of Engineering, Federal University of Lavras, 37200-000, Lavras, MG, Brazil

[2] Department of Ecosystem Science and Management, Texas A&M University, 77840, College Station, TX, United States of America

ABSTRACT: Maintaining water availability and electric energy production are the major concerns for the future in countries like Brazil, which are extremely dependent on their water resources. The objective of this study was to assess the impacts of climate change on streamflow and therefore on hydropower potential at two headwaters within the Grande river basin. For this purpose, the SWAT model was used to simulate the hydrological behavior of the headwaters under the Representative Concentration Pathways (RCPs) 4.5 and 8.5 scenarios, obtained from the Regional Climate Models (RCMs) Eta-HadGEM-ES and Eta-MIROC5 between the years 2007 and 2099. Through power duration curves (PDCs) we were able to estimate the hypothetical average annual energy production at three hydropower plants installed in cascade in the region, being, from upstream to downstream, Camargos, Itutinga and Funil, which account for a potential of 277 MW. SWAT was able to calibrate the streamflow of the Grande river basin headwaters and, therefore, was able to reproduce the observed monthly streamflow from the baseline period (1961-2005) reasonably well for all three hydropower plants. In general, the results indicated significant streamflow reduction and therefore reductions in runoff during all time periods and all radiative forcing analyzed, when compared to the baseline period. Thus, these results led to reductions on hydropower potential and therefore, decreases of the annual energy production varying from 6.1% to 58.6% throughout the XXI Century.

Keywords: Hydrological simulation; SWAT model; Eta-HadGEM-ES; Eta-MIROC5; Hydropower potential; Headwater basin

1. Introduction

According to the 5th Assessment Report (AR5) of the International Panel on Climate Change (IPCC, 2013), climate change is a well-documented and acknowledged phenomenon which may cause human health problems, water supply shortages, damage to biodiversity and ecosystems, as well as other economic an environmental problems (Lubini and Adamowski, 2013).

Changes in temperature, precipitation and sea level due to the increase of greenhouse gases emission has been investigated for the past 3 decades through simulations performed by General Circulation Models (GCMs). However, the study of the hydrological impacts caused by climate change has been widely applied at the regional scale using GCM simulations (e.g. Ouyang et al., 2015; Kopytkovskiy et al., 2015; Ho et al., 2016), which are too coarse (usually 1-degree grid) for hydrological simulation at watershed scale level simulation and do not capture many important orographic effects (Deb et al., 2014).

According to (Chou et al., 2014a), the assessment of the impacts of climate change at the regional scale requires more detailed data since the impacts and vulnerabilities of a given region are linked to local issues. Thus, Regional Climate Models (RCMs) might be effective to improve GCM outputs, since RCMs downscale global climate simulations into refined data, taking into account the local climate features linked to the coastlines, mountains, lakes and vegetation that has a strong influence on the regional climate (Rajib and Rahman, 2012). These refined data can enhance effectiveness of the regional water

resources management and planning as well as reduce losses caused by floods and droughts (Ouyang et al., 2015).

Thus, the assessment of the hydrological impacts due to climate change is a very important tool to support water resources management. This is especially true for countries like Brazil, where almost 78% of its electric energy is produced by hydropower plants (EPE, 2016), making the country strongly dependent on rainfall and hydrological regimes, and thus, on climate change effects.

The Grande River is one of the main tributaries of the Paraná River, which is a main tributary of La Plata River Basin, one of the major river basins in South America. With an area of approximately 145,000 km^2, the Grande River Basin (GRB) is located in Southeastern Brazil and is one of the most important river basins in the country regarding water availability and electric power generation (Nóbrega et al., 2011; Viola et al., 2014).

In its headwaters, it is installed a cascade of three hydropower plants, being Camargos, Itutinga and Funil, accounting for 15,409 km^2 of drainage area, in which the total hydropower potential designed for these facilities is 277 MW. Together, they are very important to the maintenance of the electric energy supply for the entire south Minas Gerais state and also, for water supplying Furnas hydropower plant, which is the subsequent downstream plant that has one of the most important reservoirs in the Grande River Basin, which allows the water regulation in the entire GRB.

Thus, as the most of GCMs/RCMs have simulated a negative impact on the rainfall pattern in the studied region (Chou et al., 2014), the studies related to the impacts of

climate change over the hydrology of the GRB's headwaters are fundamental to analyze the possible reductions or even the disruption of the hydropower production over the entire electric energy generation in the GRB, as the system is entirely connected having in Furnas hydropower plant the main support.

Several studies evaluating the impacts of climate change on hydrology using hydrological models like SWAT driven by RCM/GCM outputs have been performed around the world (Kay et al., 2008; Jung et al., 2012; Huang et al., 2014; Ouyang et al., 2015, Ramos & Martínez-Casasnovas, 2015; Uniyal et al., 2015) as well as in Brazil (Collischonn et al., 2005; Siqueira Júnior et al., 2015; Ho et al., 2016).

Also, this approach have been performed in the GRB. (Nóbrega et al., 2011) evaluated the uncertainties in climate change impacts on hydrology for the entire GRB, forcing HadCM3 simulations through MGB-IPH model and comparing the results to multimodel runs using six different GCMs in order to evaluate the uncertainties related to GCM structures. (Viola et al., 2014) used simulations from the RCM Eta-HadCM3 forced through the LASH model to assess the climate change impacts on the hydrology of four headwaters in the GRB.

However, none of the studies mentioned above investigated the impacts of climate change on the hydropower potential within GRB. This issue has been widely investigated worldwide. (van Vliet et al., 2016) investigated the impacts of climate change on potential hydropower and thermoelectric power in a global scale using 5 different GCMs under the Representative Concentration Pathways (RCPs) 2.6 and 8.5. According to their study, most

of the hydropower plants (61% for RCP 2.6 and 74% for RCP 8.5) are located in regions where significant declines in streamflow are projected, resulting in mean global reductions in hydropower usable capacity.

Similar studies can be found around the world in continental and regional scale. (Lehner et al., 2005) used three different GCMs to evaluate the impacts on hydropower potential in Europe. The study projected a decreasing trend of the annual hydropower potential of more than 25% in southern and parts of east-central Europe, especially in Spain, Turkey, Bulgaria and Ukraine. On the other hand, projections show an increasing trend of more than 25% in northern Europe, mainly in Norway, Finland, Sweden and Russia.

(Minville et al., 2009) evaluated the impacts of climate change in the Peribonka River water resource system exploited for hydropower in Canada. The results show a decrease in annual hydropower of 1.8% for the period 2010-2039 and then increase of 9.3% and 18.3% during the periods 2040–2069 and 2070–2099, respectively.

(Siqueira Júnior et al., 2015) assessed the impacts of climate change on hydropower potential at Madeira River basin, one of the main Amazon River tributaries, from 2011 to 2099, using eight different climate projections. The authors found that there was no consensus among the models, which some of them presented reductions in hydropower potential of up to 45% and some presented increases of up to 38%,from 2071 to 2099.

Given the importance of GRB regarding hydropower production and due to the lack of investigation on the impacts of climate in this regard, the objective of this study was to

evaluate the impacts of climate change on hydrology and on hydropower potential in the GRB's headwater region. This approach is relevant since the total installed capacity of the GRB is about 7,600 MW, which corresponds to approximately 8.7% of the whole country (Aneel, 2015) and hydrological impacts on its headwater region can generate shortcomings throughout the system, compromising energy supply for Minas Gerais state as well as for southeastern Brazil..

Also, since the GRB hydropower production system is interconnected, changes on streamflow due to the varying climate might disrupt the system of the entire basin. The upstream reservoirs are mainly used to store water to supply the downstream hydropower plants in the dry period, which is the case of Camargos and Funil hydropower plants supplying Furnas, evidencing the strategic importance of the GRB's headwater region and its hydropower plant for the electric energy production.

For this purpose, the Soil and Water Assessment Tool (SWAT) was used to calibrate and validate, at a monthly basis, the streamflow of the cascade of hydropower plants – Camargos, Itutinga and Funil. Then, maximum and minimum temperatures and precipitation data sets under RCP's 4.5 and 8.5 from the RCMs Eta-HadGEM2-ES and MIROC5 were used as input into SWAT to simulate future hydrological projections and then to analyze the potential impacts on the hydropower potential and possible disruptions on these plants in the future.

This paper is organized as follows: Section 2 presents the study area, input data and describes the hydrological model, climate projections and calibration/validation

methodologies; the results of calibration/validation of streamflow, evaluation of the climate projections, assessment of the projected impacts on streamflow, runoff and hydropower potential are presented in Section 3. Conclusions are drawn in Section 4.

2. Material and Methods

2.1. Study area

The study was carried out in the headwater region of Grande River Basin (GRB), located in south and southeast Minas Gerais state, Southeastern Brazil. Figure 1 shows the study area and the location of Camargos, Itutinga and Funil hydropower plants.

Figure 1

According to (Mello et al., 2012) and (Viola et al., 2014), the climate of the region is classified as Cwa and Cwb, according to the Köppen climate classification. In both climates, the summers are wet and mild and the winters are dry and cool, which allows characterizing a well-defined hydrological year between October of one year and September of the following year. The climate in the headwaters is strongly influenced by mountainous regions like the Mantiqueira Range, where springs of the Grande, Aiuruoca and Mortes rivers are located. With elevations above sea level greater than 2,300 m, the range has mountainous and strong undulated relief.

The total annual precipitation is about 1,500mm, 80% of which occurs between November and March. The mean annual temperature is about 18°C with mean minimum

and maximum temperatures ranging from 8°C to 24°C, respectively. The drainage area of the headwaters region was delimited from Funil hydropower plant, account for 15,409 km^2, whereas the contributing area for Camargos and Itutinga hydropower plants account for 6,137 km^2 and 6,250 km^2, respectively.

The water availability of this region is extremely important, since it plays an important role in regulating the streamflow of other downstream reservoir, highlighting Furnas hydropower plant. In addition, the available water of this region is the main source for irrigation and water supply for at least 66 municipalities in the south Minas Gerais state.

2.2. The SWAT model

The Soil and Water Assessment Tool (SWAT) is a large-scale model which was developed to predict the impact of land management practices on water, sediment and agricultural chemical yields in large complex watersheds with varying soils, land use and management conditions over long periods of time (Neitsch et al., 2005).It is a continuous-time, long-term, distributed-parameter, physically based hydrological model that divides the basin into subbasins connected by a stream network. Each subbasin is further delineated into hydrological response units (HRUs) which consist of unique combinations of land cover, slope and soil type and are non-spatially distributed (Arnold et al., 1998; Srinivasan et al., 2010).

SWAT simulations are based on water balance and are achieved through hydrological routines that calculate the water cycle components such as surface and subsurface flows, evapotranspiration, infiltration, percolation, lateral flows, evaporation and plant uptake. Equation 1 describes the water balance adopted by the SWAT model.

$$SW_t = SW_0 + \sum_{i=1}^{t}\left(P_{day} - Q_{surf} - E_a - w_{seep} - Q_{gw}\right) \quad (1)$$

Where SW_t is the final soil water content (mm), SW_0 is the initial soil water content on day i (mm), t is the time (days), P_{day} is the amount of precipitation on day i (mm H2O), Qsurf is the amount of surface runoff on day i (mm), E_a is the amount of evapotranspiration on day i (mm), w_{seep} is the amount of water entering the vadose zone from the soil profile on day i (mm), and Q_{gw} is the amount of base flow on day i (mm).

When running the model in a monthly time step, SWAT summarizes the daily data into monthly data. That means the model runs in a daily time step in the background, then calculates and prints the monthly data.

The model requires topography, soil, land use and weather data as input to predict the surface and subsurface flow, sediment, and nutrient and pesticides loadings throughout the watershed. For this study, only the components regarding the runoff process will be analyzed. A more detailed description of the SWAT model can be found in (Arnold et al., 1998), (Srinivasan et al., 1998) and (Neitsch et al., 2005).

2.3. Model inputs for GRB headwaters

To calibrate SWAT model, daily values of maximum and minimum temperatures, humidity, solar radiation and wind speed data are required. These data were obtained from weather stations of the Brazilian National Institute of Meteorology (INMET) to calculate the evapotranspiration. In addition, precipitation gauges were obtained from the Brazilian National Water Agency (ANA-Hidroweb) and the naturalized streamflow data from each hydropower plant was obtained from the National Electric System Operator (ONS), which is responsible to coordinate and control the generation and transmission of electric energy in the country.

The naturalized streamflows are those that would occur, in a stream, without any anthropogenic activities, such as reservoir operations upstream and withdrawal of water for consumptive uses, such as irrigation and human supply (Guilhon et al. 2007).

To obtain the natural streamflow, ONS uses a system which integrates 96 stochastic models to forecast the streamflows in each hydropower plant, which are the basis for the short and medium-term hydropower production planning by the National Interconnected System (SIN) (ONS, 2008).

The meteorological variables data were obtained from 1990 to 2012. The percentage of missing data for the meteorological variables is about 10% while the streamflow data is less than 2%. In order to fill in the gaps, SWAT uses a weather generator in which the daily

values for weather are generated from average monthly values. For this purpose, the generator uses a number of methods, such as the first order Markov chain, for precipitation, continuity equations, for air temperature and radiation, exponential equation, for wind speed and a triangular distribution, for relative humidity (Neitsch et al., 2005)

Figure 2a shows the hydrologic, pluviometric and weather stations used in this study, as well as the RCMs grid points.

Figures 2b and 2c show the land use and soil maps, respectively. The land use map of the GRB's headwaters was produced from Landsat 8 images from 2013 with the aid of supervised classification through the maximum likelihood classifier. Pasture is the predominant land use, followed by forests and agriculture, which cover 70.74%, 15.65% and 10.35% of the area, respectively.

Figure 2

The soil map was derived from the Minas Gerais State Environmental Foundation (FEAM, 2010) in a scale of 1:650,000. The headwater region presents the soil types Argisol, Cambisol (Inceptsol), Latosol (Oxisol), Litholic Neosol and Fluvic Neosol with predominance of the Cambisol, which covers 47% of the area. Latosol, Argisols, Litholic Neosol and Fluvic Neosol represents 33.4, 9.5, 4.4 and 0.7%, respectively.

2.4. Calibration, validation and model performance evaluation

The calibration and uncertainty analyses for SWAT are carried out in SWAT-CUP, which is a stand-alone program that links to SWAT's output text file sets and integrates different optimization algorithms. Among them, the Sequential Uncertainty Fitting (SUFI-2) algorithm stands out due to its capability to account for all sources of uncertainty on the parameter ranges such as uncertainty in driving variables (e.g., rainfall), conceptual model, parameters, and measured data (Abbaspour et al., 2007).

The algorithm tries to capture most of the measure data within the 95% prediction uncertainty (95PPU) calculated at the 2.5% and 97.5% levels of the cumulative distribution of an output variable obtained through Latin hypercube sampling (Abbaspour et al., 2004; Abbaspour et al., 2007).

Automatic calibration through SUFI-2 was performed using monthly naturalized streamflow data from Camargos, Itutinga and Funil hydropower plants. For Camargos and Itutinga, it was used data sets from 1995 to 2005, with a warm-up period from 1990 to 1994. For Funil, it was used data sets from 2003 to 2008, with a warm-up period from 2001 to 2002. The validation was performed updating the SWAT model with the calibrated parameters achieved in the calibration period from 2006 to 2012 for Camargos and Itutinga and from 2009 to 2012, for Funil.

To evaluate the goodness of fit of the calibration and validation periods, the Nash-Sutcliffe Efficiency (NSE) (Nash and Sutcliffe, 1970) and the percent bias (PBIAS) were used and are represented as follows:

$$NSE = 1 - \left[\frac{\sum_{i=1}^{n} (Q_{obs_i} - Q_{sim_i})^2}{\sum_{i=1}^{n} (Q_{obs_i} - Q_{mean_i})^2} \right] \quad (2)$$

$$PBIAS = \left[\frac{\sum_{i=1}^{n} (Q_{obs_i} - Q_{sim_i})}{\sum_{i=1}^{n} (Q_{obs_i})} \right] \times 100 \quad (3)$$

where Q_{obs}, Q_{sim} and Q_{mean} are the observed, simulated and mean streamflow, respectively.

2.5. Climate change simulations

In order to predict the potential future impacts on hydrology due to climate change in the GRB headwaters, simulations from the GCMs HadGEM2-ES and MIROC5, both dynamically downscaled by the RCM Eta (Chou et al., 2014b), were used.

The HadGEM2-ES is a general circulation model of the earth system developed by the Hadley Centre (Collins et al., 2011; Martin et al., 2011) with a resolution of 1.875 degrees in longitude and 1.275 degrees in latitude. The MIROC5 (Watanabe et al., 2010) is a Japanese cooperatively developed coupled ocean-atmosphere model with resolution of about 150 km in horizontal and 40 levels in vertical. The Eta regional model has been

adapted by the Brazilian National Institute of Spatial Research (INPE/CPTEC) to run for long-term integrations over Central and South America and has been applied for impacts and vulnerability studies (Chou et al., 2011; Marengo et al., 2011; Pesquero et al., 2009).

The Eta-HadGEM2-ES and Eta-MIROC5 were simulated based on two different Representative Concentration Pathways (RCPs), RCP 4.5 and RCP 8.5. These RCPs are based on the anthropogenic and non-anthropogenic radiative forcings by the end of the 21st century that represent forcings of 4.5 and 8.5 W m^{-2}. They represent the change in the balance between incoming and out- going radiation to the atmosphere caused by changes in atmospheric constituents, such as carbon dioxide (Moss et al., 2010).

The RCP 8.5 corresponds to a global average warming ranging from 2.6 to 4.8°C by the end of the 21st century, whereas RCP 4.5 represents a global average warming ranging from 1.1 to 2.6°C (IPCC, 2013).

The downscaling method provided simulations for Central and South America with resolution of 20 km covering the following periods: 1961-2005 (baseline); 2007-2040; 2041-2070; and 2071-2099. The variables simulated by both RCMs used to assess the potential hydrological impacts in the GRB headwater region were daily precipitation and daily maximum and minimum temperatures.

Climate variables outputs from RCMs - such as precipitation and temperatures - are often subjected to systematic errors (biases) and when forced directly into a hydrological model can generate considerable deviations in the simulated streamflow compared to the

observed ones. Thus, bias correction of the RCM outputs for hydrologic impact assessment is recommended (Graham et al., 2007; Teutschbein & Seibert, 2010).

This study adopted the method of linear scaling of precipitation and temperature. This method operates with monthly correction values based on the differences between observed and historical simulated values. This method is described by the equations below:

$$P^*_{contr}(d) = P_{contr}(D)\left[\frac{\mu_m(P_{obs}(d)}{\mu_m(P_{contr}(d)}\right] \quad (4)$$

$$P^*_{scen}(d) = P_{scen}(D)\left[\frac{\mu_m(P_{obs}(d)}{\mu_m(P_{contr}(d)}\right] \quad (5)$$

$$T^*_{contr}(d) = T_{contr}(d) + \mu_m(T_{obs}(d)) - \mu_m(T_{contr}(d)) \quad (6)$$

$$T^*_{scen}(d) = T_{scen}(d) + \mu_m(T_{obs}(d)) - \mu_m(T_{contr}(d)) \quad (7)$$

Where P (d) and T (d) are daily precipitation and temperatures, respectively; μ_m is the mean of the variable within the month; and “contr”, “scen” and “obs” refer to the control (baseline period), scenarios and observed data, respectively.

By definition, bias corrected RCM simulations will agree in their monthly mean values with the observations. Precipitation and temperature are corrected with a factor based on the ratio of long-term monthly mean observed and control run data. These factors are assumed to remain unvaried even for future conditions (Lenderink et al., 2007;

Teutschbein & Seibert, 2012). Other applications of this method can be found in studies like (Fiseha et al., 2014) and (Teutschbein & Seibert, 2012).

After performing the bias correction, to assess the hydrological impacts in Camargos, Itutinga and Funil, monthly streamflow simulations from the baseline period (1961-2005) were compared to the three future time periods (2011-2040; 2041-2070; 2071-2099).

2.6. Assessment of impacts on hydropower production

The impacts on the gross hydropower potential due to climate change were evaluated for Camargos, Itutinga and Funil hydropower plants, which present installed capacities of 45, 52 and 180 MW, respectively. Itutinga is a run-of-the-river hydropower plant with an average head fall of 25 m. Camargos and Funil are conventional hydropower plants with reservoir areas of 73.35 and 42.65 km^2 and an average head fall of 25 and 40 m, respectively (Chachapuz, 2006).

The hydropower potential is defined as the maximum amount of power that can be generated based on the total plant efficiency, streamflow, and hydraulic head, as shown in Equation 6.

$$N_P = Q \cdot H \cdot \rho_w \cdot g \cdot \eta \quad (8)$$

Where N_P is the hydropower potential (W); Q is the streamflow ($m^3\ s^{-1}$); H is the hydraulic head (m); ρ_w is the water density ($kg\ m^{-3}$); g is the gravitational acceleration ($m\ s^{-2}$); and n is the total plant efficiency.

(Sampaio et al., 2005) analyzed the total plant efficiency of 71 hydropower plants in Brazil with installed capacity greater than 50 MW. The authors found that 68.2% of the plants presented total plant efficiency between 80% and 100% within the Paraná River basin, which Camargos, Itutinga and Funil hydropower plants are installed. Therefore, to calculate the hydropower potential for each hydropower plant studied, we considered a plant efficiency of 80%.

Through the Equation 6, baseline and the future streamflow projections were used to estimate the future hydropower potential. The hydropower potential of the baseline and future scenarios were then converted into power duration curves (PDC), and compared to one another in order to assess the impacts of climate change. Also, the PDCs were used to estimate the hypothetical average annual energy.

Similarly to the flow duration curves, the PDC is a graphic representation of the percent of time that a given hydropower potential was equaled or exceeded and are mainly used for studies of hydropower feasibility. It illustrates the relationship between the frequency and magnitude of the hydropower potential. The integration of the area below the PDC constrained by the installed and minimum capacities represents the hypothetical average annual energy production, in MWh/year (Vogel and Fenessey, 1995).

Also, observed data of actual hydropower generation from Camargos, Itutinga and Funil hydropower plants were obtained from the Minas Gerais State Electric Company (Cemig) in a daily time step from 2006 to 2012 with about 3.9% of missing data.

The minimum actual hydropower of 6 MW, 9.7 MW and 25 MW generated in Camargos, Itutinga and Funil hydropower plants, respectively, was recorded in 2014, when the southeast of Brazil experienced a major austral summer drought ever recorded. According to (Coelho et al., 2016), this drought led to a number of impacts in water availability for human consumption, agricultural irrigation and hydropower production, heavily affecting water resources, food and energy production in Brazil's most populated region.

Therefore, the most critical situation experienced by these plants in terms of actual generation (6 MW, 9.7 MW and 25 MW) was considered to evaluate if the plant would experience similar or worst situation considering the future climate projections. In addition, the installed capacities (45MW, 52 MW and 180 MW) and the mean hydropower generation (20 MW, 28 MW and 89 MW) of Camargos, Itutinga and Funil respectively, obtained from the observed data provided by the Minas Gerais State Electric Company (Cemig), were used to evaluate the hydropower feasibility of the future predictions.

The application of the methods mentioned above can be found in a number of studies such as (van Vliet et al., 2016), (Lobanova et al., 2016), (Majone et al., 2016), (Siqueira Júnior et al., 2015) (Mohor et al., 2015), (Lehner et al., 2005), (Buttle et al., 2004), among others.

3. Results and Discussion

3.1. SWAT calibration and validation

As a first step to assess the hydrological impacts of climate change, calibration of the naturalized streamflows from Camargos, Itutinga and Funil hydropower plants were performed at a monthly time step. For this purpose, 14 parameters regarding the behavior of surface and subsurface runoff were used. After calibration, these parameters were updated in SWAT with the values of the best simulation achieved by the calibration phase. Then, the model performed the simulations with the new parameter's values for the respective validation periods. Table 1 shows the parameters' descriptions, initial ranges and the final calibrated values of the best simulation during calibration for each hydropower plant.

Table 1

Table 2 shows that SWAT was able to predict adequately the monthly streamflow of Camargos, Itutinga and Funil hydropower plants, since both calibration and validation periods presented values of model performance greater than 0.5 for NSE and PBIAS within the range of ±25 for all hydropower plants.

Table 2

According to (Moriasi et al., 2007), these results show that SWAT had "good" and "satisfactory" performances predicting the monthly naturalized streamflow from Camargos, Itutinga and Funil, which are in agreement with the graphical results presented in Figure 3.

Figure 3

However, in general, the simulated naturalized streamflow was slightly underestimated, especially in the validation periods, for all three hydropower plants, which is acceptable from the hydrological model point of view.

The use of naturalized streamflow as input for hydrological modeling has been used in a number of studies around the world, such as (Matheussen et al., 2000), (Weedon et al., 2015) and (Foy et al., 2016). In Brazil, (Nóbrega et al., 2011) used monthly naturalized streamflow data as input for the MGB-IPH model in order to assess the hydrological impacts of climate change of 10 hydropower plants in GRB. The authors found satisfactory results during calibration and validation periods, with NSE varying from 0.85 to 0.94.(Lucena et al., 2009) analyzed the vulnerability of renewable energy to climate change in Brazil. In order to assess the vulnerability of the hydropower system, the authors used stochastic modeling and monthly natural streamflow series from 148 hydropower facilities. According to the authors, the parameters of the fitted linear equations presented statistical significance for 70% of the hydropower plants analyzed.

3.2. Climate model projections

Figure 4 shows the climate change projections for both scenarios and hydropower plants of the RCMs Eta-HadGEM2-ES and Eta-MIROC5. After bias correction, the results showed an increase in both mean maximum and minimum temperatures for all time

periods, both radiative forcing and RCMs. When considering Eta-HadGEM2-ES, the RCP 4.5 showed an average increase of 3.1°C and 0.5°C for maximum and minimum temperatures, respectively, while RCP 8.5 showed an average increase of 5.4°C and 1.7°C, respectively.

Figure 4

Regarding the RCM Eta-MIROC5, the mean maximum and minimum temperatures also increased, but lesser than the Eta-HadGEM2-ES. The results showed an average increase of 1.4ºC and 1.2ºC for maximum and minimum temperatures for RCP 4.5 and 2.2°C for both maximum and minimum temperatures for RCP 8.5 in relation to the baseline period.

According to (Chou et al., 2014a) the Eta-HadGEM2-ES is more sensitive to the increase of greenhouse gases in comparison to the Eta-MIROC5 simulations, where major warming tended to occur in Central and Southeast Brazil, which is a highly dense populated area. Also, greater warming was simulated when RCP8.5 was considered, as expected in higher equivalent CO_2 concentrations. The Eta-HadGEM has produced warming values larger than Eta-MIROC5 across the Brazilian territory for all time periods.

On the other hand, considering the Eta-HadGEM2-ES, both scenarios presented a decrease in the mean annual precipitation of -22.2% and -28.1% for RCPs 4.5 and 8.5, respectively. Regarding the Eta-MIROC5, the results showed a decrease in the precipitation, in relation to the baseline period, of -7.5% and -1.2%, under the RCP 4.5 and RCP 8.5, respectively. These results showed to be somewhat consistent with those of

(Siqueira Júnior et al., 2015) when comparing reductions in temperature and precipitation for RCMs after bias corrections.

The annual cycle of precipitation shows that the Eta simulations driven by MIROC5 produces more precipitation than the Eta-HadGEM2-ES during the rainy season, and generally less during the dry season (Chou et al., 2014a). This could explain the lesser reductions on the annual precipitation of Eta-MIROC5 in relation to ETA-HadGEM2-ES, and therefore, possible lesser impacts on streamflow.

These differences are not unusual, especially considering many sources of uncertainty in climate change simulations, which GCM/RCM structures stands out as the most significant source of uncertainties in climate impact studies, as reported by many authors (Kay et al., 2009; Prudhomme and Davies, 2009; Fiseha et al., 2014). As stated by (Chou et al., 2014a), the mixed signals in the precipitation change in the Southeast Brazil reveal large uncertainty in these climate simulations.

3.3. Naturalized streamflow simulations

Mean monthly observed and simulated naturalized streamflow for the baseline and future time periods for Camargos, Itutinga and Funil hydropower plants are shown in Figure 5.

Figure 5

For Camargos, the mean naturalized streamflow showed an overestimation in the low flows. The mean errors were about 37% and 41% for Eta-HadGEM2-ES and Eta-MIROC5, respectively. Regarding Itutinga, the results also showed an overestimation in the low flow, but lesser than Camargos. The simulations presented mean errors of 21.2% and 24.4%, for Eta-HadGEM2-ES and Eta-MIROC5, respectively. Regarding Funil, the results showed an underestimation of the peak flows and overestimation of the low flows. The results presented mean errors of 7.6% and 8.2% for Eta-HadGEM2-ES and Eta-MIROC5, respectively.

The results presented for Itutinga and Funil are somewhat similar with those presented by Viola et al. (2014), which found mean errors of 21.6% and 12% for two headwaters within the study area – Grande and Aiuruoca rivers - respectively, using the hydrological model LASH driven by the RCM Eta-HadCM3, under the influence of SRES A1B emission scenario, with spatial resolution of 40 km.

Although the above cited authors used a coarser spatial resolution data, their baseline simulations outperformed the ones presented in this study. This can be justified by the use of different hydrological models, which have different formulation as well as different spatial resolution of the hydrologic units, possibly affecting the streamflow frequency and magnitude. Also, the use of different RCMs with different forcing inputs might generate differences between the simulations. In addition, the authors analyzed only a small portion of the study area of the present study (around 25% of the total area) and did not use the naturalized streamflow.

The differences between the mean monthly observed and simulated streamflows from Camargos and Itutinga can be considered acceptable (Teutschbein & Seibert, 2010). According to above-cited authors, these differences are not unusual since the use of the RCMs data as input is generally not able to reproduce observed long-term seasonal streamflow in a satisfactory way, presenting deviations in timing and magnitude.

The uncertainties related to GCM/RCM model structures, radiative forcing, parameterization and downscaling should be considered. Prudhomme and Davies (2009), for example, cited that GCMs are the largest source of uncertainty when reproducing the observed streamflows.

In addition to these sources of uncertainties, other ones related to the hydrologic models can also be source of differences between observed and simulated mean monthly flows. In this study, we calibrated the contributing area of the hydropower plants with naturalized streamflows, as they are the only reliable data for this kind of study in most basins in Brazil. The determination of the naturalized streamflows is achieved through a system that incorporates 96 stochastic models, therefore, it might generate errors that can be propagated through the hydrological simulation.

Analyzing the simulations, in general, the results from Eta-HadGEM2-ES under the RCP 4.5 indicate serious changes in the hydrological behavior throughout the present century, considering both Representative Concentration Pathways. Camargos, Itutinga and Funil hydropower plants presented similar behaviors, with greater reductions during the first time period (2007-2040) when compared to the baseline, especially from May to

December, with changes varying from 41.3 to 48.1% in Camargos, 50 to 54.7% in Itutinga and 51.7 to 56.3% in Funil, for both RCP 4.5 and 8.5. Also, the results show an increase by the end of the second (2041-2070) and third (2071-2099) time periods in relation to the first period.

On the other hand, the simulations under the RCP 8.5 indicated greater reductions of mean monthly streamflow by the end of the century for all three hydropower plants, with reductions from 49.6 to 69.4%

Regarding the simulations of the Eta-MIROC5, the simulated mean monthly streamflow showed a different behavior in relation to the Eta-HadGEM2-ES. In general, under RCP 4.5, Itutinga and Funil showed the same decreasing trends, with greater reductions during the first (2007-2040) and third (2071-2099) time periods from 24.2 to 37%. Regarding Camargos, the results show greater reductions during the third time period (2071-2099), which varied from 21.9 to 36.3%.

Considering RCP 8.5, all hydropower plants presented similar trends, which indicates a decrease in the first time period, varying from 14.6 to 29%, followed by an increase of the streamflow in the subsequent time periods, especially in the rainy season (October to January), ranging from 3.8 to 22.6% at Funil. These simulations follow the same trends as those presented by (Nóbrega et al., 2011) and (Viola et al., 2014) in studies performed in the Grande river basin, which results suggested a general increase in the annual streamflow by the end of the century, with significant variations throughout the century.

The reduction of the low flows may lead to extreme and prolonged droughts, which may impact negatively, among others, the energy production of the region compromising the electric energy system operation in south Minas Gerais state along with southeast Brazil.

Table 3 presents the mean annual runoff simulated by SWAT forced by the RCMs Eta-HadGEM2-ES and Eta-MIROC5 for the baseline period and future time periods for Camargos, Itutinga and Funil hydropower plants. As a reflex of the streamflow, the results showed the same trends than the streamflow simulations for both scenarios and all three hydropower plants.

Table 3

Considering the simulations from Eta-HadGEM2-ES, the results showed greater reductions of the mean annual runoff for Itutinga, especially during the third time period (2071-2099) under RCP 8.5, with a decrease of more than 62% from the baseline period whereas Camargos and Funil showed a reduction of 58.4%.

Regarding the Eta-MIROC5, under RCP 4.5, greater changes in the mean annual runoff were observed in Itutinga, which varied from -18 to -30.1%, considering the entire period,while under the RCP 8.5 Funil showed greater reductions of mean annual runoff from -1.9 to -22.6%, with a slight increase of 0.9% during the.second time period (2041-2070).

In the study performed by (Viola et al., 2014), the authors found variations in the mean annual runoff ranged from -1.6% to +14.4% for the Upper Grande River Basin (2090

km^2) and -3.6% to +30.4% for Aiuruoca River Basin (2100 km^2), with higher increases by the end of the century.

As above explained, this inconsistency in the hydrological behavior between the RCMs can occur due to various uncertainties that exist in climate simulations, especially when comparing different GCM/RCM data as an input in hydrological models. (Fiseha et al., 2014) investigated the impacts of climate change on the hydrology of the Upper Tiber Basin in central Italy, using three different RCMs (RegCM, RCAO, and PROMES) under two different IPCC SRES emission scenarios (A2 and B2) forced thought SWAT. The results showed differences in the hydrological behavior between the models, scenarios and time periods.

Similar behaviors were also observed by (Saurral, 2010), who assessed the hydrological cycle of the La Plata Basin using the Variable Infiltration Capacity (VIC) hydrological model driven by different GCMs (CNRM-CM3, MPI-OM, GFDL CM2.0, CCCma/CGCM3-T47, GISS-AOM) under the emission scenarios A1B, A2 and B1.

The results of the present study indicate that these reductions on streamflow and, therefore, on runoff may alter significantly the water availability in the GRB headwater region and, therefore, an important threat to disrupt the electric energy production in southeast Brazil.

3.4. Impacts on hydropower production

Through power duration curves (PDC), we evaluated the potential impacts of climate change on hydropower potential at Camargos, Itutinga and Funil hydropower plant. For this purpose, the installed capacities (45, 52 and 180 MW), the mean (20, 28 and 89 MW) and minimum (6, 9.7 and 25 MW) observed hydropower generation were used to evaluate the hydropower feasibility of the future predictions.

Figure 6 shows the PDCs for the baseline period for both RCMs compared to the PDC based on the naturalized streamflow series from Camargos, Itutinga and Funil. The simulated PDCs from Camargos and Itutinga showed overestimations in the hydropower potential, while in Funil the simulations presented a better agreement between the observed and simulated PDCs for both RCMs, with a slight overestimation of the low flows and slight underestimation of the peak flows in Eta-MIROC5

Figure 6

The PDC for Funil obtained from Eta-HadGEM2-ES showed a better agreement for the minimum and mean hydropower generation as well as for the installed capacity. For the installed capacity (180 MW) the observed hydropower potential is equaled or exceed 8% of the time whereas for both Eta-HadGEM2-ES and Eta-MIROC5 models this percentage is 7% and 4%, respectively.

For the mean hydropower generation (89 MW), the observed hydropower potential is equaled or exceeded 36% of the time, whereas for bothEta-HadGEM2-ES and Eta-MIROC5 it was 45%. For the minimum hydropower generation (25 MW) the observed hydropower potential is equaled or exceeded 90.6% of the time whereas in Eta-HadGEM2-

ES and Eta-MIROC5 this value is exceeded 91.3% and 98% of the time. Figure 7 shows the PDCs for the baseline and future scenarios for both RCMs and all three hydropower plants.

Figure 7

Figure 8 shows the results of the time of exceedance for Camargos, Itutinga and Funil for both RCMs, RCPs and time periods, extracted from the PDCs.

Figure 8

Regarding Camargos, the results suggest that the time of exceedance of the minimum hydropower generation would be reduced from 97.2% to 72.3% of the time between 2071 and 2099, projected by Eta-HadGEM2-ES under RCP 8.5. Also, under the same projections, the time of exceedance of the mean hydropower generation would be reduced from 77.8% to 17.8% by the end of the century and the installed capacity would decrease from 15.1% to 4.6%. Considering the Eta-MIROC5 projections for Ca, the minimum hydropower generation would be maintained throughout the century for both RCPs. Regarding the mean hydropower generation, the most critical projection is expected by the end of the century (2071-2099) under RCP 4.5, with reductions on the time of exceedance from 91.5% to 63.7% in the minimum generation.

The results for Itutinga shows the same trends as Camargos, which suggest that the most critical scenario is expected during the third time period under projections made by Eta-HadGEM2-ES under the RCP 8.5, with reductions in the time of exceedance from 89% to 30.9% for the minimum generation, from 51.1% to 8.3% for the mean generation and from 4.7% to 1.5% for the installed capacity. These results suggest that Itutinga

hydropower plant would not be able to operate in about 69% of the time during 2071 and 2099.

For Funil, the results indicate that the most critical projection is expected from Eta-HadGEM2-ES simulations under RCP 8.5 between 2071 and 2099, with reductions in the time of exceedance from 6.7% to only 2.1% of the installed capacity, from 44.8% to 7.6% for the mean hydropower generation and from 91.3% to 50% for the minimum observed hydropower generation. These results indicate that the plant should not be operating in 50% of the time because the minimum hydropower generation should not be reached.

The most critical projections for the Eta-MIROC5 indicate that during the third time period, Funil would not be able to operate in just 5.3% of the time, under the RCP 4.5, because the minimum observed value of hydropower generation (25 MW) should not be reached. Also, the percent of time that the mean hydropower generation (89 MW) will be equaled or exceeded will be reduced from 44.8% to 23.2% in the third time period (2071-2099). The installed capacity would not be reached during the first time period, but a slight increase of the time of exceedance (from 2.1% to 2.9%) is expected for the subsequent time periods.

(Mohor et al., 2015) assessed the climate change impacts on hydropower at Teles Pires hydropower plant, in the Tapajós River Basin at the Amazon region. Coupling the MDH-INPE hydrological model with eight different GCMs, the authors found that the most critical projection indicated that the Teles Pires hydropower plant should not be operating

in 59% of the time between 2041 and 2070 because the minimum capacity should not be reached.

Table 4 presents the percentage differences of the hypothetical average annual energy production of the future projections in relation to the baseline at Camargos, Itutinga and Funil hydropower plants. Simulations from both RCMs indicate that the most critical situation regarding energy production is expected by the end of the century, especially under RCP 8.5.

Table 4

The Eta-HadGEM2-ES simulations suggest reductions on the hypothetical production of 57.2%, 66.1% and 38.2% for Camargos, Itutinga and Funil, respectively, between 2071 and 2099. The results obtained from Eta-MIROC5 simulations also showed reductions in the hypothetical energy production, but less critical than Eta-HadGEM2-ES. The results, also, indicate decreases at Funil hydropower plant of 30.7% and 11.3% during the third time period under RCPs 4.5 and 8.5, respectively.

(Mohor et al., 2015) reported a decrease of 82% on the hypothetical energy production at Teles Pires hydropower plant considering the most critical scenario. (Majone et al., 2016), using four different RCMs to evaluate the impacts of climate change on the hypothetical energy production of five hydropower plants located at the Noce catchment, in the Southeastern Alps, Italy. The authors found that the magnitude of changes in both runoff and hydropower potential is location-dependent and in general larger at higher

elevations as a consequence of the spatially nonuniform increase of precipitation. The changes in hypothetical energy productions varied from -12.4% to +213.4%.

(Lobanova et al., 2016), assessed the impacts of climate change on the hydropower production in three hydropower plants in Targus River Basin – in Spain and Portugal – using different projections from the RCM ISI-MIP driven by the scenarios RCP 4.5 and RCP 8.5 considering two future periods: 2021-2050 and 2071-2100. Similar to the findings presented in this study, their results showed that the average annual reduction of hydropower production in both future periods is between 10% and 50% under the RCP 4.5, whereas under the RCP 8.5 the projected decreases varied from 40% to 60%.

The results presented in this study suggest a possible reduction in hydropower generation in GRB headwaters, with implications to the entire GRB hydropower generation as the Brazilian Electric Energy system is interconnected and has in Furnas the main reservoir for regulating water for the basin as a whole and almost 50% of water storage in this plant depends on GRB headwaters flows. Besides, this shortcoming in the system could increase the electricity prices, as the risk of an disruption would increase, especially considering the projection of increasingly human pressure on the water resources in Minas Gerais state by 2030 (Minas Gerais, 2014).

Since there are many factors affecting the price of electricity such as market demand, planned plant outages (according to expected demand), unplanned outages, location of supply, among others, demand is not responsive to the real price of electricity. When water is scarce, the energy sector is forced to produce electricity through other

sources such as thermal plants – which can strongly influence the climate change and variability, since it burns fossil fuel – and renewable energy sources (Buttle et al., 2004); (Coelho et al., 2016). Unfortunately, in Brazil the thermal generation has been the alternative most used by the government.

It is important to mention that this study did not consider the possible future technological developments that can optimize the hydropower production, such as increasing the total efficiency or the increasing of energy production through different renewable sources such as biomass, biofuel, solar and wind energy, which could attenuate the pressure on water resources.

4. Conclusions

This research investigated the impacts of climate change on the hydrological behavior of the headwater region of the Grande River Basin, southeast Brazil, along with impacts over the potential of hydropower generation from three facilities installed in cascade within the region.

The SWAT model, driven by the RCMs Eta-HadGEM2-ES and Eta-MIROC5, simulated the hydrology of this region under the influence of RCP 4.5 and RCP 8.5. In addition, we evaluated these impacts on the hydropower production of Camargos, Itutinga and Funil hydropower plants by means of the development of power duration curves (PDCs). It is important to highlight that the flows from this hydrological region is fundamental to feed Furnas hydropower plant reservoir installed downstream and is one of

the most important Brazilian plant for both electric energy generation and for water regulating in Grande river basin as a whole.

Besides all uncertainties involved, SWAT was able to calibrate and validate the naturalized streamflows from Camargos, Itutinga and Funil satisfactorily and therefore reproduce the baseline period (1961-2005). The climate projections from the Eta-HadGEM2-ES showed large reductions of mean monthly streamflow for all time periods under both RCP 4.5 and 8.5 scenarios, impacting negatively the runoff and showing a great vulnerability of the region regarding water uses in the future.

The results showed significant reduction on the mean monthly streamflow during the first time period (2007-2040) under RCP 4.5 for all three hydropower plants and for both RCMs, while the biggest reductions were observed during the third time period (2071-2099) under RCP 8.5 simulated by Eta-HadGEM2-ES.

The projections from the Eta-MIROC5 varied in behavior between the RCPs and the studied hydropower plants, showing greater reductions on the mean monthly streamflow in Camargos hydropower plant during the third time period under the RCP 4.5. Importantly, this hydropower plant is located in the most upstream position in GRB and is responsible for water supplying the others downstream (Itutinga and Funil) mainly in the dry period. Thus, this reservoir is highlighted as strategic to guarantee the hydropower potential of the GRB headwaters. Regarding the simulations under the influence of the RCP 8.5, the results suggested an slight increase of the peak flows in the wet period and decrease of the low flows on the dry period for all hydropower plants after the middle of the century.

Due to decreased streamflow and runoff, reduced hydropower potential is also expected. The results were consistent with the streamflow simulations showing the same reduction trends throughout the century.

The results also indicate that the most critical projection is expected from Eta-HadGEM2-ES simulations under RCP 8.5 between 2071 and 2099 for Itutinga hydropower plant, which the time of exceedance of the hydropower potential could be reduced from 89% to 30.9% at the minimum hydropower generation (9.7 MW), which suggest that the plant should not be operating in 69.1% of the time. Regarding the Eta-MIROC5, the most critical projection showed that the plant should not be operating in 10.5% of the time between 2071 and 2099, under the RCP 4.5.

In terms of hypothetical average annual energy production, the most critical situation was the one simulated by Eta-HadGEM2-ES at Itutinga hydropower plant, which suggested reductions in relation to the baseline period of 66.1% between 2071 and 2099, under the scenario RCP 8.5. Simulations from Eta-MIROC5 suggest a smaller impact than Eta-HadGEM2-ES, but also showed significant reductions on hypothetical energy production. The most critical scenario showed a decrease on hypothetical energy production at Funil hydropower plant under RCP 4.5 and during 2071-2099 of 30.7%.

These results predict serious water availability problems for the region in the future, with implications not only for the region but also for entire GRB hydropower system generation. Therefore, if these reduction trends remain the same for the entire basin, the

effects may be critical and the current hydropower production of the GRB may be significantly reduced.

It is important to mention that although there are uncertainties and systematic errors associated with many sources (model structure, RCM/GCM, input data, parametrization, among others), this study has provided valuable information to subsidize the impacts in the future hydrological behavior of the GRB's headwater region.

However, the projected changes presented in this study diverged, both in behavior and magnitude, from previous studies performed in the region. Thus, these studies, including this one, may be analyzed as a tool to assist with future methodological developments as well as model structure developments in order to reduce the uncertainties associated with climate change simulations and their applications.

Acknowledgments

This work was conducted during the "Sandwich Doctorate Program" (process number 9530/2014-02) at Texas A&M University with scholarship granted to the first author, Vinícius A. de Oliveira, financed by CAPES – Brazilian Federal Agency for Support and Evaluation of Graduate Education within the Ministry of Education of Brazil.

The authors would like to thank the Minas Gerais State Electric Company (CEMIG) for providing the observed hydropower production data set and FAPEMIG PPM 00415-16 for sponsored this research. We would also like to thank Dr. Sin Chan Chou on behalf of

the National Institute for Space Research – Center for Weather Forecasting and Climate Research (INPE – CPTEC) for providing the climate change projections data.

References

Abbaspour KC, Johnson CA, Van Genuchten MT. 2004. Estimating Uncertain Flow and Transport Parameters Using a Sequential Uncertainty Fitting Procedure. *Vadose Zone Journal* **3**(4): 1340–1352. doi:10.2136/vzj2004.1340

Abbaspour KC, Yang J, Maximov I, Siber R, Bogner K, Mieleitner J, Zobrist J, Srinivasan R. 2007. Modelling hydrology and water quality in the pre-alpine/alpine Thur watershed using SWAT. *Journal of Hydrology* **333**(2-4): 413–430. doi: 10.1016/j.jhydrol.2006.09.014.

Agência Nacional de Energia Elétrica. *Boletim mensal de monitoramento do sistema elétrico brasileiro: Dezembro-2015*. Ministério de Minas e Energia: Brasília, Brasil. Available at: http://www.mme.gov.br/web/guest/secretarias/energia-eletrica/publicacoes/boletim-de-monitoramento-do-sistema-eletrico. Accessed February 8, 2016.

Arnold JG, Srinivasan R, Muttiah RS, Williams JR. 1998. Large area hydrologic modeling

and assessment part I: model development. *Journal of the American Water Resources Association* **34**(1): 73–89. doi: 10.1111/j.1752-1688.1998.tb05961.x

Buttle J, Muir T, Frain J. 2004. Economic impacts of climate change on the Canadian Great Lakes hydro–electric power producers: A supply analysis. *Canadian Water Resource Journal* **29**(2): 89-110. doi: http://dx.doi.org/10.4296/cwrj089.

Chachapuz PBB. 2006. *Usinas da Cemig: 1952-2005*. Centro da memória da eletricidade no Brasil: Rio de Janeiro, Brasil. Available at: https://www.cemig.com.br/pt-br/a_cemig/nossos_negocios/usinas/Documents/livro_usinas.pdf. Accessed August 30, 2016.

Chou SC, Lyra A, Mourão C, Dereczynski C, Pilotto I, Gomes J, Bustamante J, Tavares P, Silva A, Rodrigues D, Campos D, Chagas D, Sueiro G, Siqueira G, Marengo J. 2014a. Assessment of Climate Change over South America under RCP 4.5 and 8.5 Downscaling Scenarios. *American Journal of Climate Change* **3**(5): 512–525. doi: 10.4236/ajcc.2014.35043

Chou SC, Lyra A, Mourão C, Dereczynski C, Pilotto I, Gomes J, Bustamante J, Tavares P, Silva A, Rodrigues D, Campos D, Chagas D, Sueiro G, Siqueira G, Nobre P, Marengo JA. 2014b. Evaluation of the Eta Simulations Nested in Three Global Climate Models.

American Journal of Climate Change **3**(5): 438–454. doi: 10.4236/ajcc.2014.35039

Chou SC, Marengo JA, Lyra AA, Sueiro G, Pesquero JF, Alves LM, Kay G, Betts R, Chagas DJ, Gomes JL, Bustamante JF, Tavares P. 2011. Downscaling of South America present climate driven by 4-member HadCM3 runs. *Climate Dynamics* **38**(3-4): 635–653. DOI: 10.1007/s00382-011-1002-8. doi: 10.1007/s00382-011-1002-8

Coelho CAS, de Oliveira CP. Ambrizzi T, Reboita MS, Carpenedo CB, Campos JLPS, Tomaziello ACN, Pampuch LA, Custódio MS, Dutra LMM, da Rocha RP, Rehbein A. 2016. The 2014 southeast Brazil austral summer drought: regional scale mechanisms and teleconnections. *Climate Dynamics* **46**(11):3737–3752.

Collins WJ, Bellouin N, Doutriaux-Boucher M, Gedney N, Halloran P, Hinton T, Hughes J, Jones CD, Joshi M, Liddicoat S, Martin G, O'Connor F, Rae J, Senior C, Sitch S, Totterdell I, Wiltshire A, Woodward S. 2011. Development and evaluation of an Earth-System model – HadGEM2. *Geoscientific Model Development* **4**(4): 1051–1075. doi: 10.5194/gmd-4-1051-2011.

Collischonn W, Haas R, Andreolli I, Tucci CEM. 2005. Forecasting River Uruguay flow using rainfall forecasts from a regional weather-prediction model. *Journal of Hydrology* **305**(1-4): 87–98. doi: 10.1016/j.jhydrol.2004.08.028.

Lucena AFR, Szklo AS, Schaeffer R, Souza RR, Borba BSMC, Costa, IVL, Júnior AOP, Cunha SHF. 2009. The vulnerability of renewable energy to climate change in Brazil. *Energy Policy* **37**(3): 879-889. doi: 10.1016/j.enpol.2008.10.029

Deb D, Butcher J, Srinivasan R. 2014. Projected Hydrologic Changes Under Mid-21st Century Climatic Conditions in a Sub-arctic Watershed. *Water Resources Management* **29**(5): 1467–1487. doi: 10.1007/s11269-014-0887-5.

Empresa de Pesquisa Energética (EPE). 2016. *Balanço Energético Nacional 2016: Relatório síntese - Ano base 2015*. Ministério de Minas e Energia: Brasília, Brasil. Available at: https://ben.epe.gov.br/downloads/S%C3%ADntese%20do%20Relat%C3%B3rio%20Final_2016_Web.pdf. Acessed: August 30, 2016.

Fiseha BM, Setegn SG, Melesse AM, Volpi E, Fiori A. 2014. Impact of Climate Change on the Hydrology of Upper Tiber River Basin Using Bias Corrected Regional Climate Model. *Water Resources Management* **28**: 1327–1343. doi: 10.1007/s11269-014-0546-x.

Foy C, Arabi M, Yen H, Gironás J. 2015. Multisite Assessment of Hydrologic Processes in Snow-Dominated Mountainous River Basins in Colorado Using a Watershed Model.

Journal of Hydrologic Engineering **20**(10):. doi: http://dx.doi.org/10.1061/(ASCE)HE.1943-5584.0001130

Guilhon LGF, Rocha VF, Moreira JC. 2007. Comparação de métodos de previsão de vazões naturais a aproveitamentos hidroelétricos. *Revista Brasileira de Recursos Hídricos* **12**(3): 13-20.

Graham LP, Andréasson J, Carlsson B. 2007. Assessing climate change impacts on hydrology from an ensemble of regional climate models, model scales and linking methods – a case study on the Lule River basin. *Climatic Change* **81**(S1): 293–307. doi: 10.1007/s10584-006-9215-2.

Ho JT, Thompson JR, Brierley C. 2016. Projections of hydrology in the Tocantins-Araguaia Basin, Brazil: uncertainty assessment using the CMIP5 ensemble. *Hydrological Sciences Journal* **61**(): 1-17. doi: 10.1080/02626667.2015.1057513.

Huang S, Krysanova V, Hattermann F. 2014. Projections of climate change impacts on floods and droughts in Germany using an ensemble of climate change scenarios. *Regional Environmental Change* **15**(3): 461–473. doi: 10.1007/s10113-014-0606-z.

Intergovernmental Panel on Climate Change. Syntesis Report. 2013. *Climate change 2013:*

The physical science basis. Cambridge University Press: Cambridge, UK. Available at: http://www.ipcc.ch/report/ar5/wg1/. Accessed February 8, 2016.

Jung I-W, Moradkhani H, Chang H. 2012. Uncertainty assessment of climate change impacts for hydrologically distinct river basins. *Journal of Hydrology* **466-467**: 73–87. doi: 10.1016/j.jhydrol.2012.08.002.

Kay AL, Davies HN, Bell VA., Jones RG. 2009. Comparison of uncertainty sources for climate change impacts: flood frequency in England. *Climatic Change* **92**(1-2): 41–63. doi: 10.1007/s10584-008-9471-4.

Kopytkovskiy M, Geza M, McCray J. E. 2015. Climate-change impacts on water resources and hydropower potential in the Upper Colorado River Basin. *Journal of Hydrology: Regional Studies* **3**:473-493. doi: http://dx.doi.org/10.1016/j.ejrh.2015.02.014

Lehner B, Czisch G, Vassolo S. 2005. The impact of global change on the hydropower potential of Europe: A model-based analysis. *Energy Policy* **33**(7): 839-855. doi: 10.1016/j.enpol.2003.10.018.

Lenderink G, Buishand A, Deursen W Van. 2007. Estimates of future discharges of the river Rhine using two scenario methodologies : direct versus delta approach. *Hydrology*

and Earth System Sciences **11**(3): 1145–1159. doi: 10.5194/hess-11-1145-2007.

Lobanova A, Koch H, Liersch S, Hattermann FF, Krysanova V. 2016. Impacts of changing climate on the hydrology and hydropower production of the Tagus River basin. *Hydrological Processes*. doi: 10.1002/hyp.10966.

Lubini A, Adamowski J. 2013. Assessing the Potential Impacts of Four Climate Change Scenarios on the Discharge of the Simiyu River, Tanzania Using the SWAT Model. *International Journal of Water Sciences* **2**(1): 1–12. doi: 10.5772/56453.

Majone B, Villa F, Deidda R, Bellin A. 2016. Impact of climate change and water use policies on hydropower potential in the south-eastern Alpine region. *Science of the Total Environment* **543**(B): 965-980. doi: http://dx.doi.org/10.1016/j.scitotenv.2015.05.009.

Marengo JA, Chou SC, Kay G, Alves LM, Pesquero JF, Soares WR, Santos DC, Lyra AA, Sueiro G, Betts R, Chagas DJ, Gomes JL, Bustamante JF, Tavares P. 2011. Development of regional future climate change scenarios in South America using the Eta CPTEC/HadCM3 climate change projections: climatology and regional analyses for the Amazon, São Francisco and the Paraná River basins. *Climate Dynamics* **38**(9-10): 1829–1848. doi: 10.1007/s00382-011-1155-5.

Martin GM, Bellouin N, Collins WJ, Culverwell ID, Halloran PR, Hardiman SC, Hinton

TJ, Jones CD, McDonald RE, McLaren AJ, O'Connor FM, Roberts MJ, Rodriguez JM, Woodward S, Best MJ, Brooks ME, Brown AR, Butchart N, Dearden C, Derbyshire SH, Dharssi I, Doutriaux-Boucher M, Edwards JM, Falloon PD, Gedney N, Gray LJ, Hewitt HT, Hobson M, Huddleston MR, Hughes J, Ineson S, Ingram WJ, James PM, Johns TC, Johnson CE, Jones A, Jones CP, Joshi MM, Keen AB, Liddicoat S, Lock AP, Maidens AV, Manners JC, Milton SF, Rae JGL, Ridley JK, Sellar A, Senior CA, Totterdell IJ, Verhoef A, Vidale PL, Wiltshire A. 2011. The HadGEM2 family of Met Office Unified Model climate configurations. *Geoscientific Model Development* **4**(3): 723–757. doi: 10.5194/gmd-4-723-2011.

Matheussen B, Kirschbaum RL, Goodman IA, Donnell GMO, Lettenmaier DP. 2000. Efects of land cover change on streamflow in the interior Columbia River Basin (USA and Canada). *Hydrological Processes* **14**(5): 867-885. doi: 10.1002/(SICI)1099-1085(20000415)14:5<867::AID-HYP975>3.0.CO;2-5

Mello CR De, Norton LD, Curi N, Yanagi SNM. 2012. Sea Surface Temperature (SST) and rainfall erosivity in the Upper Grande River Basin, Southeast Brazil. *Ciência & Agrotecnologia* **36**(1): 53–59. doi: http://dx.doi.org/10.1590/S1413-70542012000100007

Minas Gerais. 2014. *Plano Diretor de Recursos Hídricos e Enquadramento de Corpos de Água da Bacia Hidrográfica do Alto Rio Grande - GD1*. Governo do Estado de Minas

Gerais: Belo Horizonte, Brazil. 280 p.

Mohor GS, Rodriguez DA, Tomasella J, Siqueira Júnior JL. 2015. Exploratory analyses for the assessment of climate change impacts on the energy production in an Amazon run-of-river hydropower plant. *Journal of Hydrology: Regional Studies* **4**(B): 41-59. doi: http://dx.doi.org/10.1016/j.ejrh.2015.04.003.

Moriasi DN, Arnold JG, Van Liew MW, Bingner RL, Harmel RD, Veith TL. 2007. Model evaluation guidelines for systematic quantification of accuracy in watershed simulations. *Transactions of the ASABE* **50**(3): 885–900.

Moss RH, Edmonds, JA, Hibbard KA, Manning MR, Rose SK, van Vuuren DP, Carter TR, Emori S, Kainuma M, Kram T, Meehl GA, Mitchell JFB, Nakicenovic N, Riahi K, Smith SJ, Stouffer RJ, Thomson AM, Weyant JP, Wilbanks TJ .2010. The next generation of scenarios for climate change research and assessment. Nature 463:747-756. doi: jdoi:10.1038/nature08823.

Nash JE, Sutcliffe JV. 1970. River flow forecasting through conceptual models part I: a discussion of principles. *Journal of Hydrology* **10**(3): 282–290. doi: 10.1016/0022-1694(70)90255-6

Neitsch SL, Arnold JG, Kiniry JR, Williams JR. 2005. *Soil and Water Assessment Tool theoretical documentation*. Available at: http://swat.tamu.edu/media/1292/swat2005theory.pdf. Access February 8, 2016.

Nóbrega MT, Collischonn W, Tucci CEM, Paz AR. 2011. Uncertainty in climate change impacts on water resources in the Rio Grande Basin, Brazil. *Hydrology and Earth System Sciences* **15**(2): 585–595. doi: 10.5194/hess-15-585-2011.

Operador Nacional do Sistema Elétrico (ONS). 2008. Metodologia para a previsão de vazões uma semana à frente na bacia do alto/médio rio Grande. ONS: Rio de Janeiro, Brazil.

Ouyang F, Zhu Y, Fu G, Lü H, Zhang A, Yu Z, Chen X. 2015. Impacts of climate change under CMIP5 RCP scenarios on streamflow in the Huangnizhuang catchment. *Stochastic Environmental Research and Risk Assessment*. Springer Berlin Heidelberg **29**(7): 1781–1795. doi: 10.1007/s00477-014-1018-9.

Pesquero JF, Chou SC, Nobre CA, Marengo JA. 2009. Climate downscaling over South America for 1961–1970 using the Eta Model. *Theoretical and Applied Climatology* **99**(1-2): 75–93. doi: 10.1007/s00704-009-0123-z.

Prudhomme C, Davies H. 2009. Assessing uncertainties in climate change impact analyses on the river flow regimes in the UK. Part 2: future climate. *Climatic Change* **93**(1-2): 197-222. doi: 10.1007/s10584-008-9461-6.

Rajib M, Rahman M. 2012. A Comprehensive Modeling Study on Regional Climate Model (RCM) Application — Regional Warming Projections in Monthly Resolutions under IPCC A1B Scenario. *Atmosphere* **3**(4): 557–572. doi: 10.3390/atmos3040557.

Ramos MC, Martínez-Casasnovas JA. 2015. Climate change influence on runoff and soil losses in a rainfed basin with Mediterranean climate. *Natural Hazards* **78**(2): 1065–1089. doi: 10.1007/s11069-015-1759-x.

Sampaio LMB, Ramos FS, Sampaio Y. 2005. Privatização e eficiência das usinas hidrelétricas brasileiras. Economia Aplicada **9**(3): 465-480. doi: http://dx.doi.org/10.1590/S1413-80502005000300007

Saurral RI. 2010. The Hydrologic Cycle of the La Plata Basin in in the WCRP-CMIP3 Multimodel Dataset. *Journal of Hydrometeorology* **11**: 1083–1101. doi: 10.1175/1525-7541(2002)003<0630:THCOTL>2.0.CO;2.

Schaeffer R, Szklo AS, de Lucena AFP, Borba BSMC, Nogueira LPP, Fleming FP,

Troccoli A, Harrison M, Boulahya MS. 2012. Energy sector vulnerability to climate change: A review. *Energy* **38**(1): 1-12. doi: http://dx.doi.org/10.1016/j.energy.2011.11.056.

Siqueira Júnior JL, Tomasella J, Rodriguez DA. 2015. Impacts of future climatic and land cover changes on the hydrological regime of the Madeira River basin. *Climatic Change* **129**(1-2): 117–129. doi: 10.1007/s10584-015-1338-x.

Srinivasan R, Ranabarayanan TS, Arnold JG, Bednarz ST. 1998. Large area hydrologic modeling and assessment part II: Model application. *Journal of the American Water Resources Association* **34**(1): 91–101. doi: 10.1111/j.1752-1688.1998.tb05962.x.

Srinivasan R, Zhang Z, Arnold JG. 2010. SWAT ungauged: hydrological budget and crop yield predictions in the upper Mississippi river basin. *Transactions of the ASABE* **53**(5): 1533–1546.

Teutschbein C, Seibert J. 2010. Regional Climate Models for Hydrological Impact Studies at the Catchment Scale : A Review of Recent Modeling Strategies. *Geography Compass* **4**(7): 834–860. doi: 10.1111/j.1749-8198.2010.00357.x.

Teutschbein C, Seibert J. 2012. Bias correction of regional climate model simulations for hydrological climate-change impact studies: Review and evaluation of different methods.

Journal of Hydrology. **456-457**(3): 12–29. doi: 10.1016/j.jhydrol.2012.05.052.

Uniyal B, Jha MK, Verma AK. 2015. Assessing Climate Change Impact on Water Balance Components of a River Basin Using SWAT Model. *Water Resources Management* **29**(13): 4767–4785. doi: 10.1007/s11269-015-1089-5.

van Vliet MTH, Wiberg D, Leduc S, Riahi K. 2016. Power-generation system vulnerability and adaptation to changes in climate and water resources. *Nature Climate Change* **6**(4): 375-381. doi: 10.1038/NCLIMATE2903.

Viola MR, de Mello CR, Chou SC, Yanagi SN, Gomes JL. 2015. Assessing climate change impacts on Upper Grande River Basin hydrology, Southeast Brazil. *International Journal of Climatology* **35**(6): 1054–1068. doi: 10.1002/joc.4038.

Vogel RM , Fenessey NM. 1995. Flow–duration curves II: review of applications in water resources planning. *Water Resources Bulletin* **31**(6): 1029–1039. doi: 10.1111/j.1752-1688.1995.tb03419.x.

Watanabe M, Suziki T, O'ishi R, Komuro Y, Watanabe S, Emori S, Takemura T, Chikira M, Ogura T, Sekiguchi M, Takata K, Yamazaki D, Yokohata T, Nozawa T, Hasumi H, Tatebe H, Kimoto M. 2010. Improved Climate Simulation by MIROC5: Mean States,

Variability, and Climate Sensitivity. *Journal of Climate* **23**(23): 6312-6335. doi: http://dx.doi.org/10.1175/2010JCLI3679.1.

Weedon GP, Prudhomme C, Crooks S, Ellis RJ, Folwell SS, Best MJ. 2015. Evaluating the Performance of Hydrological Models via Cross-Spectral Analysis : Case Study of the Thames Basin , United Kingdom. *Journal of Hydrometeorology* **16**(1): 214-231.

Tables

TABLE 1. Parameters used to calibrate Camargos, Itutinga and Funil hydropower plants as well as their ranges and fitted values. The prefixes "v", "r" and "a" correspond to the operations "replace", "relative" and "add", respectively.

Parameter	Parameter description	Initial range		Final Value		
		Min	Max	Camargos	Itutinga	Funil
v_ESCO	Soil evaporation compensation coefficient	0.5	0.95	0.72	0.734	0.672
r_CN2	Initial SCS runoff curve number for moisture condition II	-0.1	0.1	-0.059	-0.071	-0.082
v_ALPHA_BF	The baseflow recession constant	0.005	0.015	0.006	0.006	0.006
a_GW_DELAY (days)	Groundwater delay time	-30	60	39.15	53.61	-27.16

a_GWQMN (mm)	Threshold depth of water in the shallow aquifer required for return flow to occur	-1000	1000	38.3	386	879.5
v_CANMX (mm)	Maximum canopy storage	0	30	0.825	20.37	13.78
v_CH_K2 (mm h^{-1})	Effective hydraulic conductivity in main channel	0	10	8.62	9.87	7.04
v_CH_N2	Manning's "n" value for the main channel	-0.01	0.2	0.146	0.144	0.195
v_EPCO	Plant uptake compensation factor	0.01	1	0.339	0.866	0.458
v_GW_REVAP	Groundwater "revap" coefficient	0.02	0.2	0.116	0.059	0.142
a_REVAPMN (mm)	Threshold depth of water in the shallow aquifer for “revap” or percolation to the deep aquifer to occur	-1000	1000	328	-162	234
r_SOL_AWC (mm mm^{-1})	Soil available water capacity	-0.05	0.05	0.037	-0.037	0.02
r_SOL_K (mm h^{-1})	Saturated hydraulic conductivity	-0.05	0.05	-0.02	-0.024	0.004
v_SURLAG	Surface runoff lag coefficient	0.01	24	12.8	1.5	13.6

TABLE 2. Model performance indices for Camargos, Itutinga and Funil hydropower plants, during calibration and validation.

Index	Camargos		Itutinga		Funil	
	Calibration	Validation	Calibration	Validation	Calibration	Validation
NSE	0.62	0.56	0.62	0.53	0.74	0.54
PBIAS (%)	2.30	0.63	0.90	16.69	3.20	23.4

TABLE 3. Mean annual runoff (D, in mm yr^{-1}) for the baseline period (1961-2005) and changes (ΔD, in mm yr^{-1} and %) from future scenarios (2007-2040; 2041-2070; 2071-2099) simulated through SWAT and forced by the RCMs Eta-HadGEM2-ES and Eta-MIROC5.

Watershed	RCP	Baseline	2007-2040		2041-2070		2071-2099	
		D (mm yr^{-1})	ΔD (mm yr^{-1})	%	ΔD (mm yr^{-1})	%	ΔD (mm yr^{-1})	%
Eta-HadGEM2-ES								
Camargos	4.5	838.9	-370.5	-44.2	-281.9	-33.6	-273.5	-32.6
	8.5		-334.8	-39.9	-337.3	-40.2	-490.1	-58.4
Itutinga	4.5	733.8	-362.3	-49.4	-260.4	-35.5	-268.5	-36.6
	8.5		-317	-43.2	-320.7	-43.7	-457.3	-62.3
Funil	4.5	592.7	-314.3	-42.8	-224.6	-30.6	-233.4	-31.8
	8.5		-275.9	-46.5	-274	-46.2	-346.3	-58.4
Eta-MIROC5								
Camargos	4.5	856.3	-232.9	-27.2	-148.3	-17.3	-230.7	-26.9
	8.5		-169.6	-19.8	-27.4	-3.2	-41	-4.8
Itutinga	4.5	754.3	-227	-30.1	-135.4	-18	-224.4	-29.7
	8.5		-163.5	-21.7	-18	-2.4	-33.4	-4.4
Funil	4.5	593.8	-139.4	-18.5	-45.1	-6	-161.3	-21.4
	8.5		-134.2	-22.6	5.6	0.9	-11.5	-1.9

TABLE 4. Changes (%) in the hypothetical average annual energy production at Camargos, Itutinga and Funil hydropower plants simulated from Eta-HadGEM2-ES and Eta-MIROC5 under the scenarios RCP 4.5 and RCP 8.5.

Hypotetical average annual energy (x 10^5 MWh/ano)							
RCM	Time period	Camargos		Itutinga		Funil	
		RCP 4.5	RCP 8.5	RCP 4.5	RCP 8.5	RCP 4.5	RCP 8.5
Eta-HadGEM2-ES	Baseline	5.9		4.5		14.3	
	2007-2040	-44.4	-34.2	-29.7	-30.2	-32.5	-16.9
	2041-2070	-37	-37.9	-21.2	-39.4	-10	-17
	2071-2099	-36.6	-57.2	-28	-66.1	-12.2	-38.2
Eta-MIROC5	Baseline	5.2		4.7		22.3	
	2007-2040	-19.1	-6.9	-29.4	-21.8	-26.9	-16.5
	2041-2070	-8.8	-2.3	-10.3	-3.6	-14.3	-7.9
	2071-2099	-17.4	-2.1	-23.1	-3.7	-30.7	-11.3

Figures list and captions

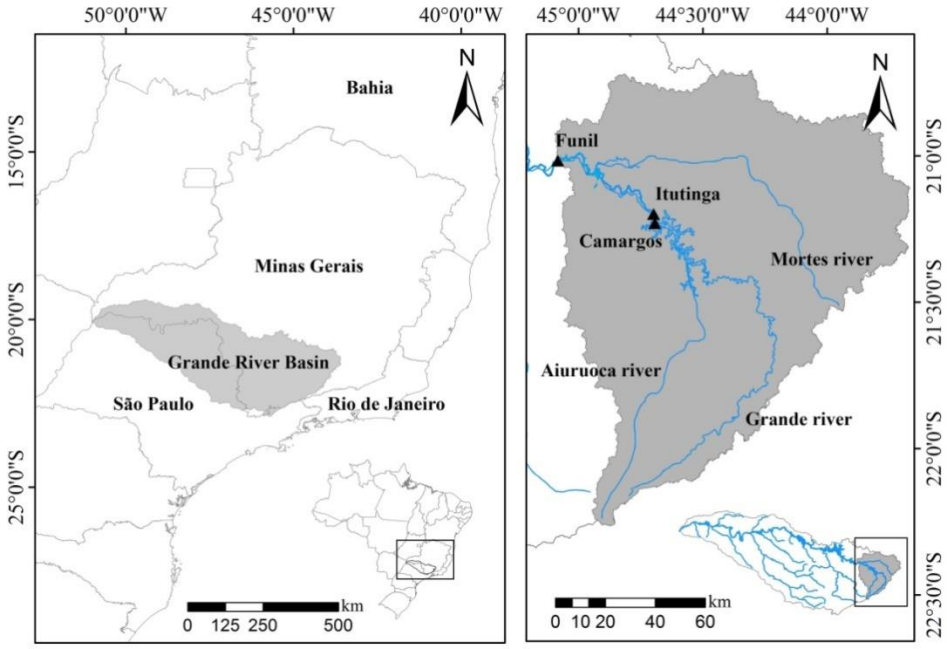

FIGURE 1. Geographical location of the headwater region of Grande River Basin, as well as Camargos, Itutinga and Funil hydropower plants.

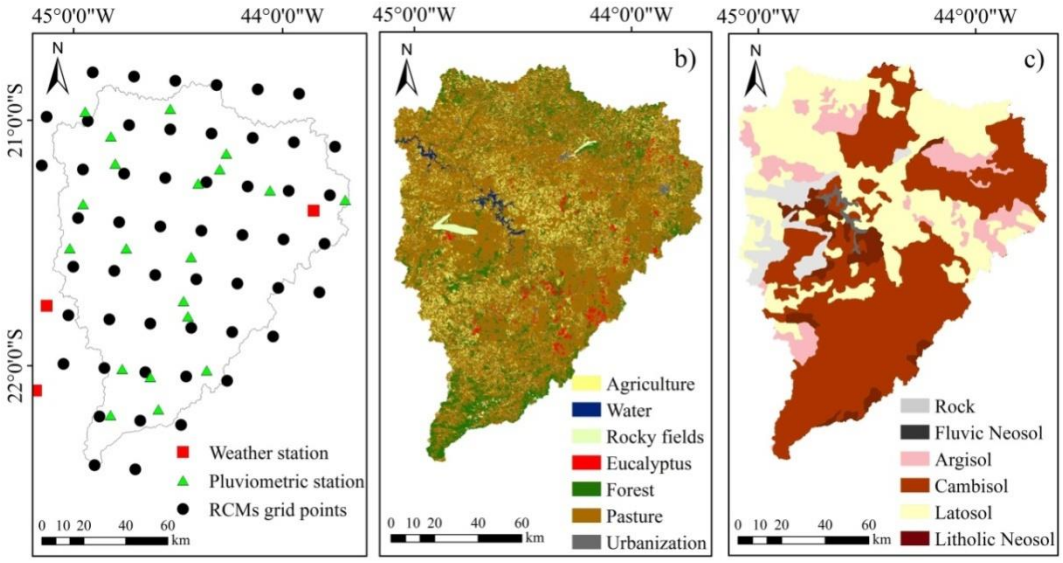

FIGURE 2. Hydrologic, pluviometric, weather stations and RCMs grid point (a), land use (b) and soil (c) maps of the study area.

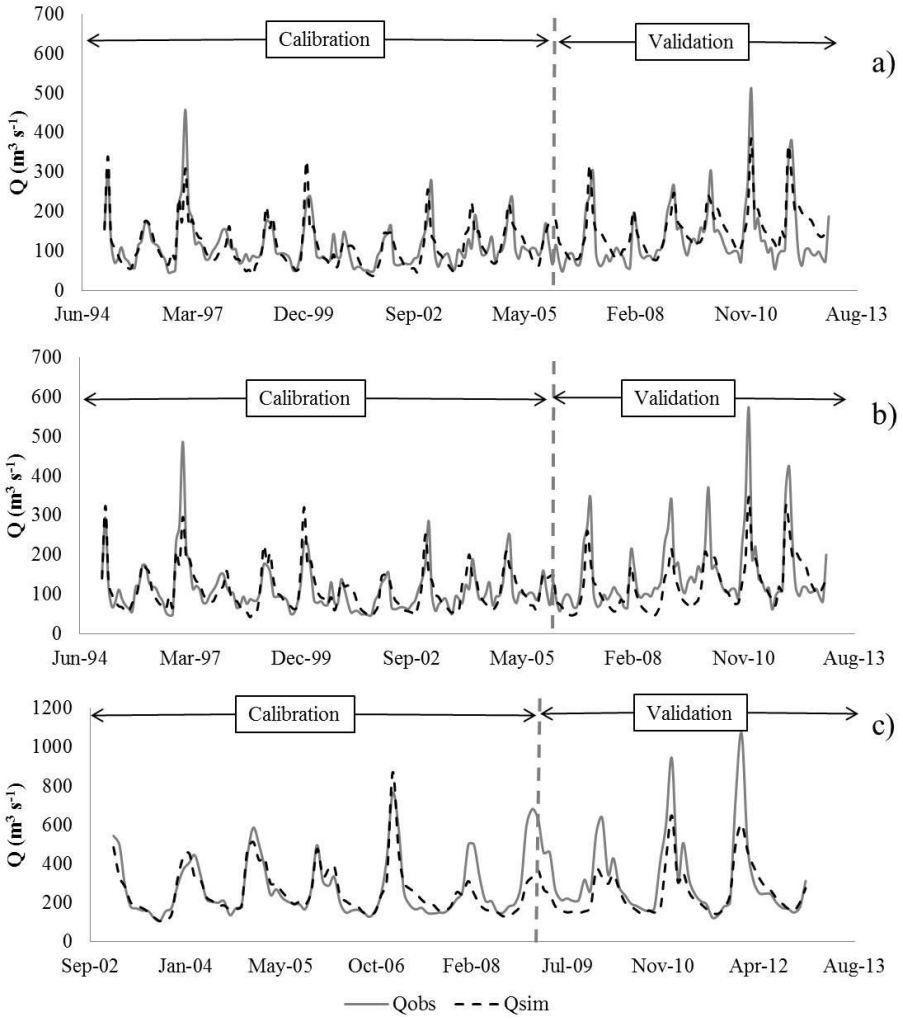

FIGURE 3. Observed and simulated naturalized streamflow from Camargos (a), Itutinga (b) and Funil (c) hydropower plants.

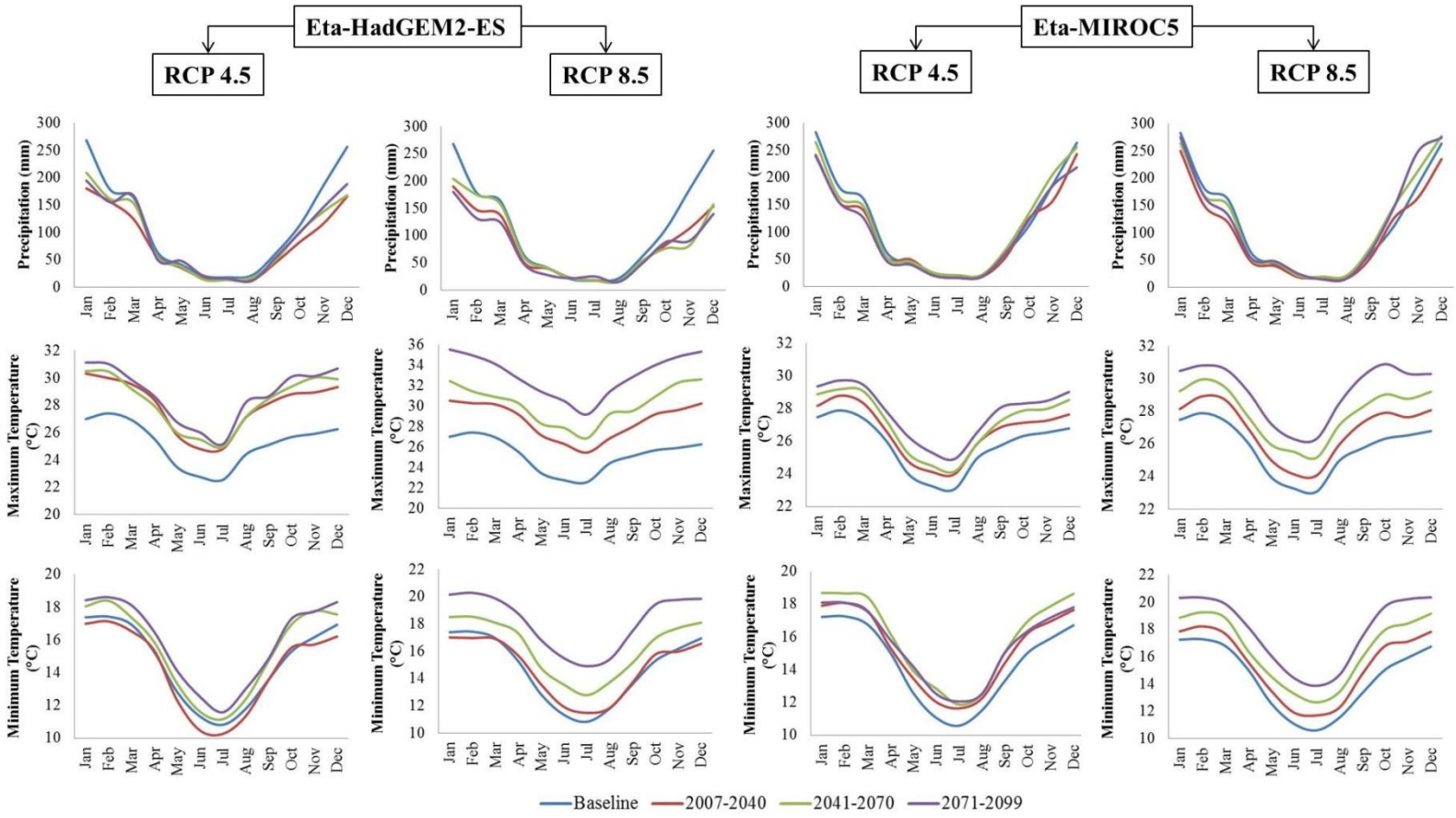

FIGURE 4. Mean monthly climate change projections (precipitation and maximum and minimum temperatures) from Eta-HadGEM2-ES and Eta-MIROC5 for the study area under RCP 4.5 and RCP 8.5 scenarios.

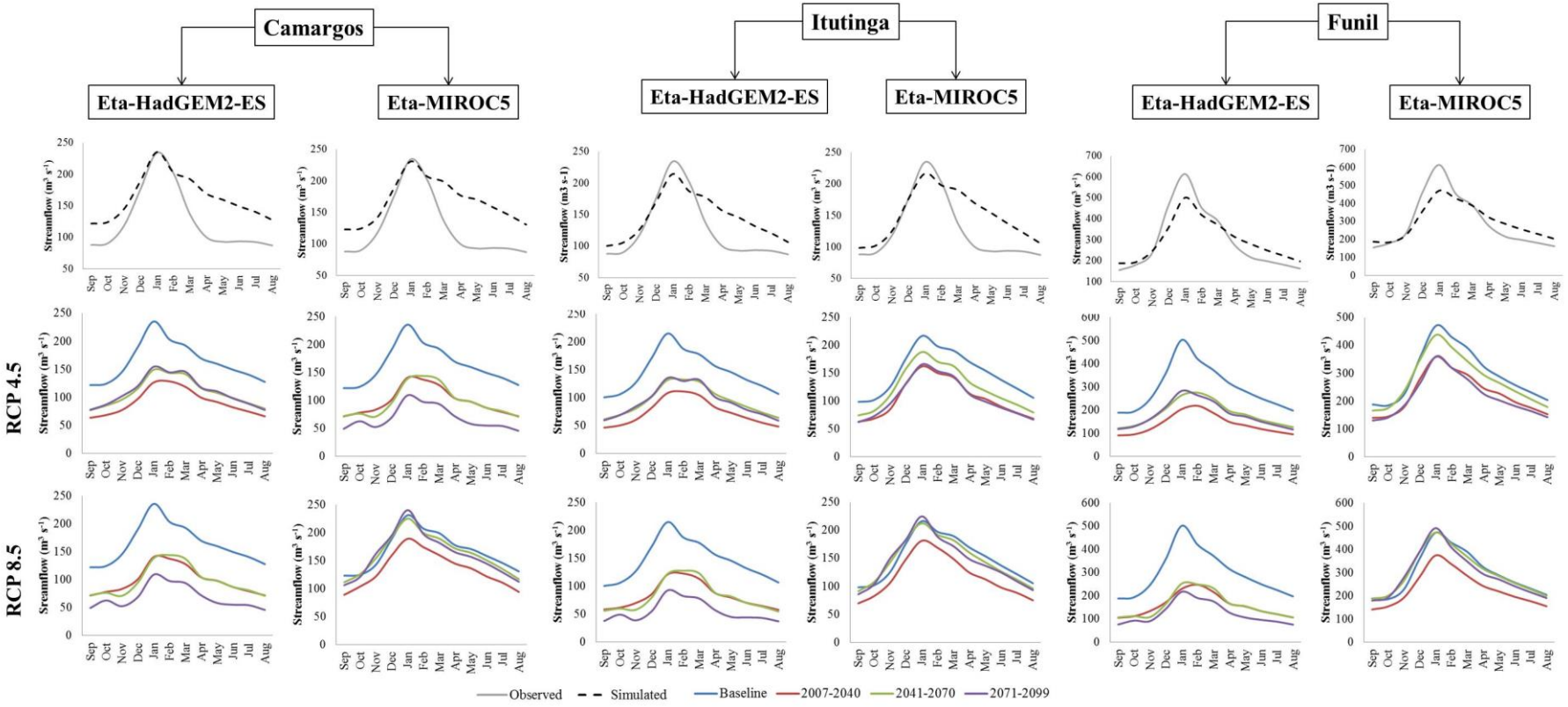

FIGURE 5. Mean monthly streamflow simulations from Eta-HadGEM2-ES and Eta-MIROC5 for Camargos, Itutinga and Funil hydropower plants

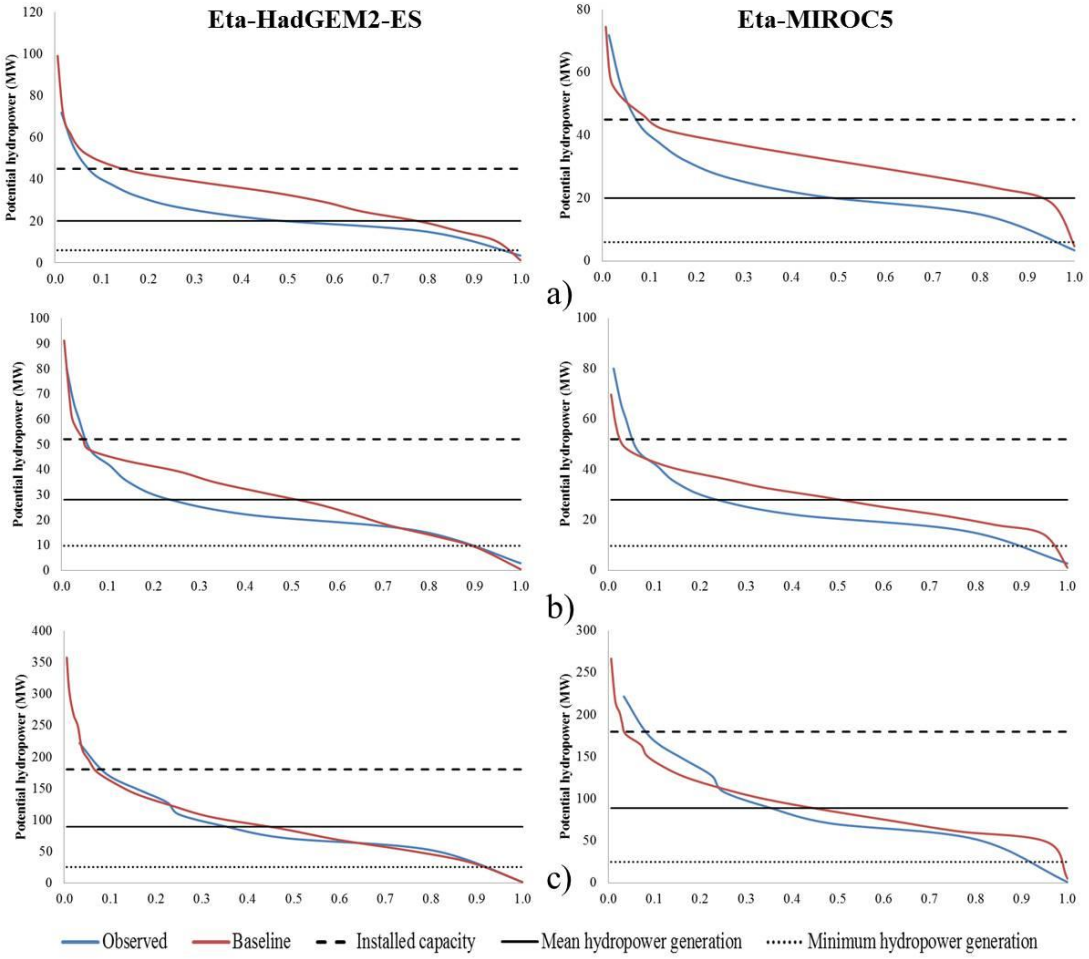

FIGURE 6. Power duration curves (PDCs) derived from the naturalized streamflow series and the baseline obtained from the RCMs Eta-HadGEM2-ES and Eta-MIROC5 at Camargos (a), Itutinga (b) and Funil (c) hydropower plants.

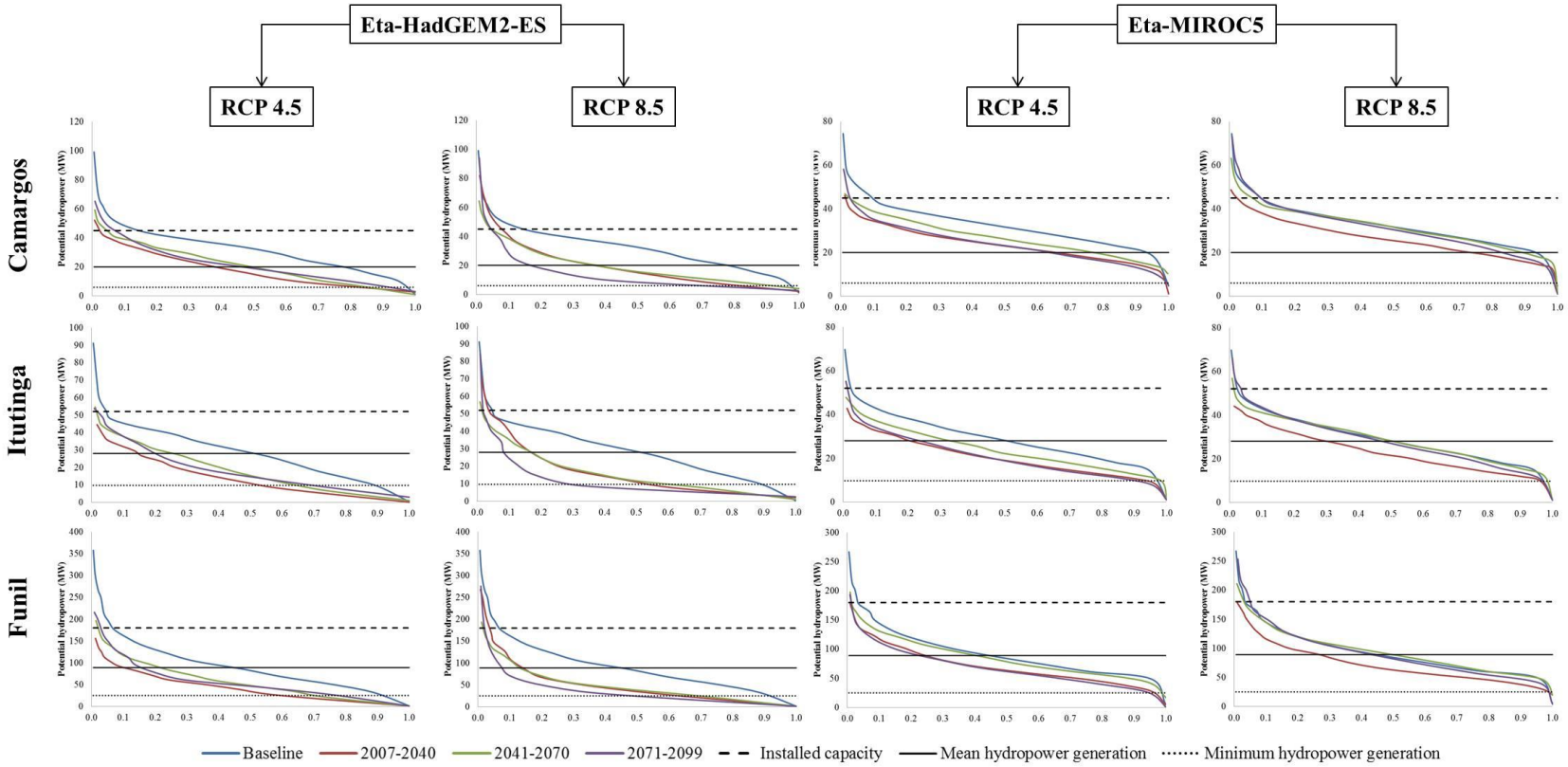

FIGURE 7. Power duration Curves (PDCs) derived from the baseline (1961-2005) and the three future time periods (2007-2040; 2041-2070; and 2071-2099) obtained from the RCMs Eta-HadGEM2-ES and Eta-MIROC5 under RCPs 4.5 and 8.5, at Camargos, Itutinga and Funil hydropower plants.

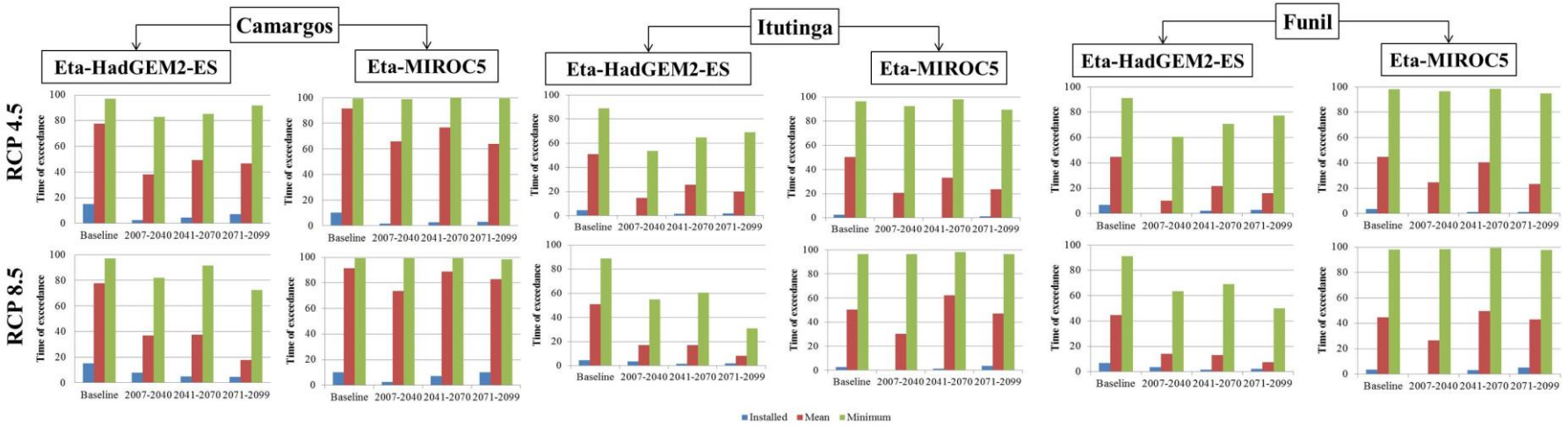

FIGURE 8. Time of exceedance for Camargos, Itutinga and Funil obtained from Power Duration Curves (PDC) generated from the RCMs Eta-HadGEM2-ES and Eta-MIROC5 under RCPs 4.5 and 8.5.

ANEXOS

ANEXO A – SWAT

1 *Soil and Water Assessment Tool*

De acordo com Neitsch et al. (2005), o modelo é subdividido em sete componentes: hidrologia, clima, sedimentos, crescimento vegetal, manejo agrícola, nutrientes e pesticidas. Assim, somente serão descritos os componentes hidrologia e clima, que são as estruturas responsáveis pelo balanço hídrico, abordados neste trabalho. Maiores detalhes sobre o modelo podem ser encontrados em Arnold et al. (1998), Srinivasan et al. (1999) and Neitsch et al. (2005).

1.1 Fase terrestre do ciclo hidrológico

O ciclo hidrológico simulado pelo SWAT baseia-se na seguinte equação de balanço hídrico:

$$SW_t = SW_0 + \sum_{i=1}^{t}\left(P_{day} - Q_{surf} - E_a - w_{seep} - Q_{gw}\right) \quad (1)$$

Em que:

SW_t: conteúdo final de água no solo (mm);
SW_0: conteúdo inicial de água no solo (mm);
P_{day}: precipitação (mm);
Q_{surf}: escoamento superficial (mm);
E_a: evapotranspiração (mm);

W_{seep}: percolação (mm);

Q_{gw}: fluxo de base (mm).

Parte da água precipitada pode ser interceptada pela vegetação e outra parte atinge a superfície do solo. Da parte interceptada, a água pode ser retornada para a atmosfera pelo processo de evaporação, enquanto parte da parcela que atingiu a superfície pode ser infiltrada e parte pode escoar superficialmente. Da parcela infiltrada, a água pode retornar à atmosfera pelo processo de evapotranspiração ou promover a recarga dos aquíferos.

O escoamento superficial ocorre quando a quantidade de água que atinge a superfície do solo excede a capacidade de infiltração de água do solo. Além disso, o escoamento superficial está condicionado à umidade antecedente do solo. O modelo SWAT apresenta dois métodos para a estimativa do escoamento superficial: o método da Curva-Número (SOIL CONSERVATION SERVICE - SCS, 1972) e o método de infiltração de Green-Ampt. Neste trabalho, o método da Curva-Número foi empregado:

$$Q_{surf} = \frac{\left(R_{day} - 0,2S\right)^2}{\left(R_{day} + 0.8S\right)} \qquad (2)$$

Em que Q_{surf} é escoamento superficial diário(mm), R_{day} é precipitação diária (mm) e S é o armazenamento potencial do solo. O escoamento só irá ocorrer se $R_{day} > 0,2S$.

O parâmetro de retenção de água no solo (S) varia de acordo com mudanças no solo, uso do solo, manejo, declividade e conteúdo de água no solo.

$$S = 254\left(\frac{100}{CN} - 1\right) \quad (3)$$

Em que CN é o valor da Curva-Número.

O valor de CN é definido em função da permeabilidade do solo, separando os tipos de solo em grupos hidrológicos, além do uso e manejo do solo e da umidade antecedente. O CN varia de 1 (extremamente permeável) a 100 (extremamente impermeável) e são representados por três condições de umidade:

- CN_1: Curva-Número para solos com baixa umidade;
- CN_2: Curva-Número para solos com umidade próxima à capacidade de campo;
- CN_3: Curva-Número para solos com umidade acima da capacidade de campo.

O CN para condições de solos secos ou úmidos é calculado em função do CN2:

$$CN_1 = CN_2 - \frac{20 * (100 - CN_2)}{\left(100 - CN_2 + \exp\left[2,533 - 0,0636 * (100 - CN_2)\right]\right)} \quad (4)$$

$$CN_3 = CN_2 * \exp\left[0,00673 * (100 - CN_2)\right] \quad (5)$$

Após o cálculo do escoamento, a quantidade de escoamento superficial que é liberada para o canal principal é calculada pela Equação 6:

$$Qsurf = \left(Q'_{surf} + Q_{stor,i-1}\right) \cdot \left(1 - \exp \cdot \left[\frac{-surlag}{t_{conc}}\right]\right) \quad (6)$$

Em que:

Q_{surf}: escoamento superficial descarregado no canal principal em um dado dia (mm);

Q'_{surf}: escoamento superficial gerado em uma sub-bacia em um dado dia (mm);

$Q_{stor,i-1}$: volume escoado superficialmente armazenado no dia anterior (mm);

surlag: coeficiente de retardamento do escoamento superficial (h);

t_{conc}: tempo de concentração da bacia (h).

A vazão de pico é calculada pelo método racional. Este método é baseado na suposição de que, se uma chuva com intensidade i comece no tempo t = 0 e continua indefinidamente, a taxa de escoamento irá aumentar até o tempo de concentração t = tconc, quando toda a área da sub-bacia estiver contribuindo com o fluxo na seção de controle.

$$q_{peak} = \frac{C.i.A}{3,6} \quad (7)$$

Em que q_{peak} é a vazão de pico ($m^3\ s^{-1}$), C é o coeficiente de escoamento superficial (adimensional), i é a intensidade da chuva (mm h^{-1}) e A é a área da bacia (km^2).

A percolação é calculada para cada camada de solo do perfil. A água percola no solo se de água no solo exceder a capacidade de campo daquela

camada de solo e se a camada abaixo não estiver saturada. Ao percolar abaixo da zona radicular a água é armazenada como água subterrânea ou retorna como escoamento à jusante do ponto considerado. O volume de água disponível para percolação em uma camada de solo é dada pelas Equações 8 e 9.

$$SW_{ly,excess} = SW_{ly} - FC_{ly} \quad \text{se} \quad SW_{ly} > FC_{ly} \tag{8}$$

$$SW_{ly,excess} = 0 \quad \text{se} \quad SW_{ly} \leq FC_{ly} \tag{9}$$

A quantidade de água percolada é calculada pela seguinte equação:

$$w_{perc,ly} = SW_{ly,excess} \cdot \left(1 - \exp\left[\frac{-\Delta t}{TT_{perc}}\right]\right) \tag{8}$$

Em que,

$w_{perc,ly}$: quantidade de água percolada para a próxima camada de solo (mm);

$SW_{ly,excesso}$: volume drenável de água da camada de solo (mm);

Δt: duração do passo de tempo (h);

TT_{perc}: tempo de propagação através da camada i (h);

FCly: conteúdo de água na capacidade de campo para a camada i (mm).

O tempo de propagação através de uma dada camada de solo é dada por:

$$TT_{perc} = \frac{SAT_{ly} - FC_{ly}}{K_{sat}} \tag{11}$$

Em que SAT_{ly} é o conteúdo de água no solo quando a camada está completamente saturada (mm) e K_{sat} é a condutividade hidráulica saturada (mm h^{-1}).

O modelo SWAT incorpora um modelo de onda cinemática desenvolvido por Sloan e Moore (1984), no qual simula o escoamento subsuperficial com base na equação de continuidade de massa onde o segmento do declive é usado como volume de controle, calculando, assim, o escoamento subsuperficial para cada camada de solo, representado pela Equação 12.

$$Q_{lat} = 0,024 \cdot \left(\frac{2 \cdot SW_{ly,excess} \cdot K_{sat} \cdot slp}{\phi_d \cdot L_{hill}} \right) \quad (12)$$

em que,

Q_{lat}: escoamento subsuperficial (mm);

slp: declividade média da sub-bacia (m m^{-1});

ϕ_d: porosidade drenável da camada de solo (mm mm^{-1});

L_{hill}: comprimento do declive (m).

O escoamento subterrâneo é calculado considerando o aquífero raso e o profundo. O aquífero raso contribui para os fluxos de base no canal principal ou em trechos na sub-bacia. Por outro lado, o aquífero profundo não contribui para a vazão na bacia. A água armazenada no aquífero subterrâneo até a recarga é dada pela seguinte equação:

$$Q_{gw} = \frac{8000 \cdot K_{sat}}{L_{gw}^{2}} \cdot h_{wtbl} \qquad (13)$$

Em que Q_{gw} é o escoamento subterrâneo do canal principal no dia i (mm), K_{sat} é a condutividade hidráulica saturada do aquífero (mm h^{-1}), L_{gw}^{2} é a distância do divisor da bacia do sistema subterrâneo para o canal principal (m) e h_{wtbl} é a altura do lençol freático (m).

O escoamento subterrâneo somente entra no trecho do canal se a quantidade de água armazenada no aquífero exceder um valor limite especificado pelo usuário ($aq_{shtrh,q}$). Ocorrendo a recarga do aquífero raso o escoamento subterrâneo poderá ser calculado por:

$$Q_{gw,i} = Q_{gw,i-1} \cdot \exp\left[-\alpha_{gw} \cdot \Delta t\right] + w_{rchrg,sh} \cdot \left(1 - \exp\left[-\alpha_{gw} \cdot \Delta t\right]\right) \qquad \text{se } aq_{sh} > aq_{shthr,q} \qquad (14)$$

$$Q_{gw,i} = 0 \qquad \text{se } aq_{sh} \geq aq_{shthr,q} \qquad (15)$$

onde,

$Q_{gw,i}$: escoamento subterrâneo no canal principal no dia i (mm);

$Q^{gw,i-1}$: escoamento subterrâneo no canal principal no dia anterior (mm);

α_{gw}: constante de recessão de escoamento subterrâneo;

Δ_t: passo de tempo (1 dia);

$w_{rchrg,sh}$: quantidade de água de recarga entrando no aquífero raso no dia i (mm);

aq_{sh}: quantidade de água inicial armazenada no aquífero raso no dia i (mm);

$aq_{shthr,q}$: nível limite de água no aquífero raso para que ocorra a contribuição da água subterrânea para o canal principal (mm).

Quando não há recarga no aquífero raso, a Equação 13 é simplificada para:

$$Q_{gw} = Q_{gw,0} \cdot \exp\left[-\alpha_{gw} \cdot t\right] \qquad \text{se } aq_{sh} > aq_{shthr,q} \qquad (16)$$

$$Q_{gw} = 0 \qquad \text{se } aq_{sh} \leq aq_{shthr,q} \qquad (17)$$

Em que,

Q_{gw}: escoamento subterrâneo no canal principal no tempo t (mm);

$Q_{gw,0}$: escoamento subterrâneo no canal principal no início da recessão (t=0) (mm);

t: tempo passado desde o início da recessão.

A constante de recessão do escoamento subterrâneo pode ser calculada diretamente analisando séries de vazões observadas em períodos que não ocorrem recarga na bacia. A constante de recessão é calculada pelo SWAT por meio da Equação 17:

$$\alpha_{gw} = \frac{1}{N} \cdot \ln\left[\frac{Q_{gw,N}}{Q_{gw,0}}\right] = \frac{1}{BFD} \cdot \ln\left[10\right] = \frac{2.3}{BFD} \qquad (18)$$

Em que $Q_{gw,N}$ é o escoamento subterrâneo no canal principal no tempo N (mm) e BFD é o número de dias com o escoamento em recessão na bacia hidrográfica.

1.2 Clima

Para o cálculo da evapotranspiração potencial, o modelo SWAT disponibiliza-se de 3 métodos: Penman-Montheith, Priestley-Taylor e Hargreaves. Neste trabalho, adotou-se o método de Penman-Montheith por ser considerado o método padrão de para estimativa da evapotranspiração potencial preconizado pela FAO (*Food and Agriculture Organization*). Este método é representado pela seguinte equação:

$$\lambda E = \frac{\Delta \cdot (Rn - G) + \frac{\rho_{ar} \cdot c_p \cdot \Delta e}{r_a}}{\Delta + \gamma \cdot \left(1 + \frac{r_c}{r_a}\right)} \qquad (19)$$

Em que:

λE: densidade do fluxo de calor latente de evaporação ($MJ.m^{-2}\ dia^{-1}$);

Δ: declividade da curva de saturação de vapor d'água ($kPa.^oC^{-1}$);

Rn: radiação líquida ($MJ.m^{-2}\ dia^{-1}$);

G: fluxo de calor no solo ($MJ.m^{-2}.dia^{-1}$);

ρ_{ar}: densidade do ar ($kg.m^{-3}$);

c_p: calor específico do ar ($MJ.kg^{-1}.^oC^{-1}$);

Δe: déficit de pressão de vapor d'água (kPa);

γ: coeficiente psicométrico ($kPa.^oC^{-1}$);

rc: resistência da cultura à difusão do vapor d'água ($s.m^{-1}$);

ra: resistência aerodinâmica à difusão do vapor d'água ($s.m^{-1}$).

Uma vez calculada a evapotranspiração potencial, o modelo calcula a evaporação real, primeiramente evaporando a água interceptada pela cobertura vegetal e, depois, a quantidade máxima de transpiração e a quantidade máxima de evaporação do solo.

Se a evapotranspiração potencial (E_0) for menor que a quantidade de água livre retida no dossel (R_{int}), utiliza-se a Equação 19. Se a evapotranspiração potencial (E_0) for maior que a quantidade de água livre mantida no dossel (R_{int}) é utilizada a Equação 20.

$$E_a = E_{can} = E_0 \rightarrow R_{INT(f)} = R_{INT(i)} - E_{can} \quad (20)$$

$$E_{can} = R_{INT(i)} \rightarrow R_{INT(f)} = 0 \quad (21)$$

Onde,

E_a: quantidade de evapotranspiração real que ocorre numa bacia hidrográfica (mm.dia-1);

E_{can}: quantidade de evaporação de água livre no dossel ($mm.dia^{-1}$);

E_0: evapotranspiração potencial ($mm.dia^{-1}$);

$R_{INT(i)}$ a quantidade inicial de água livre mantida no dossel ($mm.dia^{-1}$);

$R_{INT(f)}$ a quantidade final de água livre mantida no dossel ($mm.dia^{-1}$).

A evaporação de água no solo é determinada pela utilização de funções exponenciais conforme a profundidade do solo e a quantidade de água. A distribuição da profundidade utilizada para determinar a quantidade máxima de água que pode ser evaporada é calculada por:

$$E_{soil,z} = E_s'' \cdot \frac{z}{z + \exp\left(2,374 - 0,00713 \cdot z\right)} \quad (22)$$

Em que,

$E_{soil,z}$: demanda de evaporação na profundidade z (mm);

E''_z: evaporação máxima da água no solo (mm dia^{-1});

z a profundidade da camada do solo a partir da superfície (mm).

A quantidade de demanda evaporativa para uma dada camada de solo é determinada pela diferença entre as demandas evaporativas calculadas nos limites superior e inferior da camada de solo:

$$E_{soil,ly} = E_{soil,zl} - E_{soil,zu} \quad (23)$$

Em que,

$E_{soil,ly}$: demanda evaporativa para a camada ly (mm);

$E_{soil,zl}$: demanda evaporativa na camada inferior do solo (mm);

$E_{soil,zu}$: demanda evaporativa na camada superior do solo (mm).

O coeficiente de compensação denominado *esco* foi incorporado na Equação 22 para permitir que o usuário modifique a distribuição em profundidade usada para atender a demanda evaporativa do solo.

$$E_{soil,ly} = E_{soil,zl} - E_{soil,zu} \cdot esco \quad (24)$$

À medida que o valor de *esco* é reduzido, o modelo é capaz de extrair uma maior quantidade de água pela demanda evaporativa nas camadas inferiores.

Quando o conteúdo de água de uma camada de solo for menor do que a capacidade de campo, a demanda evaporativa para essa camada será reduzida de acordo com a Equação 24:

$$E'_{soil,ly} = E_{soil,ly} \cdot \exp\left(\frac{2,5\left(SW_{ly} - FC_{ly}\right)}{FC_{ly} - WP_{ly}}\right) \text{ quando } SW_{ly} < FC_{ly} \quad (25)$$

$$E'_{soil,ly} = E_{soil,ly} \qquad \text{quando} \quad SW_{ly} \geq FC_{ly} \qquad (26)$$

Em que $E'_{soil,ly}$ é a demanda evaporativa para a camada ly ajustada ao conteúdo de água (mm), SW_{ly} é o conteúdo de água na camada ly (mm), FC_{ly} é o conteúdo de água da camada ly na capacidade de campo (mm) e WP_{ly} é o conteúdo de água da camada ly no ponto de murcha permanente.

Além de limitar a quantidade de água removida pela evaporação em condições secas, o SWAT define um valor máximo de água que pode ser removido do solo, considerado como 80% da água disponível para as plantas.

$$E''_{soil,ly} = \min \cdot \left(E'_{soil,ly} \cdot 0,8 \cdot \left[SW_{ly} - WP_{ly}\right]\right) \qquad (27)$$

Em que $E''_{soil,ly}$ é a quantidade de água removida da camada ly pela evaporação (mm).